PALACKÝ UNIVERSITY OLOMOUC

Faculty of Science

Laboratory of Growth Regulators

Synthesis and biological activity of fluorescently labelled auxin derivatives

MASTER THESIS

Author's first name and Surname: **Kristýna Bieleszová**

Study programme: N1501 Experimental biology

Study course: Experimental biology

Form of study: Full-time

Supervisor: **Dr. Asta Žukauskaitė**

The year of presentation: 2019

Bibliographical identification

Author's first name and surname	Kristýna Bieleszová
Title of thesis	Synthesis and biological activity of fluorescently labelled auxin derivatives
Type of thesis	Master
Department	Laboratory of Growth Regulators and Department of Chemical Biology and Genetics, CRH
Supervisor	Dr. Asta Žukauskaitė
The year of presentation	2019

Abstract — This master thesis aims to the synthesis and biological testing of fluorescently labelled auxin derivatives. The theoretical part summarizes the current knowledge about auxin signalling, auxin biosynthesis and polar auxin transport. In the experimental part, synthesis of fluorescently labelled auxin analogues, followed by the preliminary assessment of their biological activity is described. Further, the lead compounds **IV** and **VIII** are investigated for their effect on auxin-mediated growth and development, auxin distribution, dynamics and their activity in auxin transport machinery.

Keywords	auxins, IAA, fluorescent labelling, biological testing, *Arabidopsis thaliana*
Number of pages	77
Number of appendices	0
Language	English

Bibliografická identifikace

Jméno a příjmení autora	Kristýna Bieleszová
Název práce	Syntéza a biologická aktivita fluorescenčně značených derivátů auxinů
Typ práce	Magisterská
Pracoviště	Laboratoř růstových regulátorů a Oddělení chemické biologie a genetiky, CRH
Vedoucí práce	Dr. Asta Žukauskaitė
Rok obhajoby práce	2019

Abstrakt	Diplomová práce je zaměřena na syntézu a biologické testování fluorescenčně značených auxinových derivátů. V teoretické části byla zpracována literární rešerše zabývající se biosyntézou auxinů, jejich mechanismem působení a polárním auxinovým transportem. V experimentální části byly připraveny fluorescenčně značené analogy auxinů. Bylo provedeno předběžné posouzení biologické aktivity připravených derivátů. Dále byl zkoumán vliv vybraných látek **IV** a **VIII** na růst a vývoj rostlin zprostředkovaný auxinem, distribuci auxinu, dynamiku a aktivitu auxinového transportního mechanismu.

Klíčová slova	auxiny, IAA, fluorescenční značení, biologické testování, *Arabidopsis thaliana*

Počet stran	77
Počet příloh	0
Jazyk	Anglický

I declare that I wrote this master thesis independently, under scientific guidance of my supervisor Dr. Asta Žukauskaitė. All the used literature is thoroughly cited.

In Olomouc on

Kristýna Bieleszová

Acknowledgments

Table of Contents

Abbreviations

1-NOA	1-naphthoxyacetic acid
2-NOA	2-naphthoxyacetic acid
2,4-D	2,4-dichlorophenoxyacetic acid
2,4,5-T	2,4,5-trichlorophenoxyacetic acid
4-Cl-IAA	4-chloroindole-3-acetic acid
AAO	ALDEHYDE OXIDASE
ABC	ATP-binding cassette
Ac	acetone
AFBs	auxin F-Box proteins
ARFs	AUXIN RESPONSE FACTORs
AS	anthranilate synthase
auxinole	(α-[2,4-dimethylphenylethyl-2-oxo]-IAA)
AUX/LAX	AUXIN1/LIKE-AUX1
AVG	aminoethoxyvinylglycine
BBo	4-biphenylboronic acid
BFA	Brefeldin A
BH-IAA	*tert*-butoxycarbonylaminohexyl-IAA
br s	broad singlet
BSA	bovine serum albumin
c-CA	*cis*-cinnamic acid
CCLR	cell culture lysis reagent
ccv-TIR1	concave TIR1
CHPAA	3-chloro-4-hydroxyphenylacetic acid
cvx-IAA	convex IAA
d	doublet
DMF	*N,N*-dimethylformamide
DMSO	dimethyl sulfoxide
D-Trp	D-tryptophan
DR5	auxin responsive promoter
EDTA	ethylenediaminetetraacetic acid
equiv	equivalent
ESI-MS	electrospray ionisation mass spectrometry

EtOAc	ethyl acetate
FA	fluoresceinamine
FITC	fluorescein 5-isothiocyanate
GFP	green fluorescent protein
GUS	β-glucuronidase
HPLC/FD	high performance liquid chromatography with fluorescence detection
IAA	indole-3-acetic acid
IAAld	indole-3-acetaldehyde
IAM	indoleacetamide
IAN	indole-3-acetonitrile
IAOx	indole-3-acetaldoxime
IBA	indole-3-butyric acid
IGP	indole-3-glycerol phosphate
IGS	indole-3-glycerol phosphate synthese
iMT	indole-3-methyl tetrazole
IND	indole
INS	indole synthase
IPA	indole-3-pyruvate
J	*J* coupling constant
L-AOPP	L-aminooxyphenylpropionic acid
L-Kyn	L-kynurenine
L-Trp	L-tryptophan
LUC	luciferase
m	multiplet
MCPA	2-methyl-4-chlorophenoxyacetic acid
MDR/PGP	multi-drug-resistant/P-glycoproteins
NAA	1-naphthylacetic acid
NBD-Cl	4-chloro-7-nitrobenzofurazan
NPA	1-*N*-naphthylphthalamic acid
p	pentet
PAA	phenylacetic acid
PAT	phosphoribosylanthranilate transferase
PAT	polar auxin transport

PBA	1-pyrenoylbenzoic acid
PBS	sodium phosphate buffer
PCIB	*p*-chlorophenoxyisobutyric acid
PE	petroleum ether
PEO-IAA	*α*-(phenylethyl-2-oxo)-IAA
PFA	paraformaldehyde
PGP	P-glycoprotein
PINs	PIN-FORMED proteins
PPBo	4-phenoxyphenylboronic acid
ppm	parts per million
q	quartet
RFP	red fluorescent protein
r.t.	room temperature
s	singlet
t	triplet
TAA1	tryptophan aminotransferase
TAM	tryptamine
TBAB	tetra-*N*-butylammonium bromide
t-CA	*trans*-cinnamic acid
TCBA	2,3,5-trichlorobenzoic acid
TDC	TRYPTOPHAN DECARBOXYLASE
TFA	trifuoroacetic acid
TIBA	2,3,5-triiodobenzoic acid
TIR1	transport inhibitor response 1
Trp	tryptophan
TSA	tryptophan synthase α
TSB	tryptophan synthase β
X-Gluc	5-bromo-4-chloro-3-indolyl-β-D-glucuronide
δ	delta, chemical shift
Δ	reflux

1. Introduction

Plant hormone auxin is influencing all crucial stages of plant life cycle and numerous studies are devoted to unravel its role in a huge spectrum of physiological processes. Fluorescent labelling of plant hormones allows sensitive and specific visualization of their subcellular and tissue-specific localization and transport in plants. Despite the great potential for answering questions concerning plant growth and development, up to date only few fluorescently labelled auxins had been developed.

Recently, several IAA and NAA based fluorescently labelled auxins have been developed by Hayashi *et al*. (Hayashi, Nakamura *et al*. 2014). The two most potent derivatives, NBD-IAA and NBD-NAA, are not active for auxin signalling, but can be used to visualize auxin distribution. Also, Sokolowska *et al*. prepared FITC-IAA and RITC-IAA (Sokolowska, Kizinska *et al*. 2014) which are described as active auxin analogues, but the sufficient evidence of the structure and purity of these compounds is lacking.

Thus, this thesis is focused on the synthesis of new fluorescently labelled indole-3-acetic acid derivatives by attaching fluorophores at the *α*-position of the molecules *via* the linkers of different length. These new derivatives, in parallel with the fluorescently labelled NH-tagged auxins prepared during bachelor thesis, are then screened for their biological activity and applicability to be used as auxin tracers.

2. Theoretical part

2.1. Natural and synthetis auxins

2.1.1. Natural auxins

Indole-3-acetic acid (IAA) is the major form of auxin in higher plants and was the first plant hormone to be discovered (Murofushi, Yamane *et al.* 1999). Besides IAA other three plant auxins have been described, namely indole-3-butyric acid (IBA), 4-chloroindole-3-acetic acid (4-Cl-IAA), and phenylacetic acid (PAA) (Figure 1) (Sauer, Robert *et al.* 2013). Auxins regulate cell division, elongation and developmental processes including vascular tissue and floral meristem differentiation, leaf initiation, phyllotaxy, senescence, apical dominance, root formation and they are also essential components in tropic responses (Grossmann 2010; Swarup and Peret 2012).
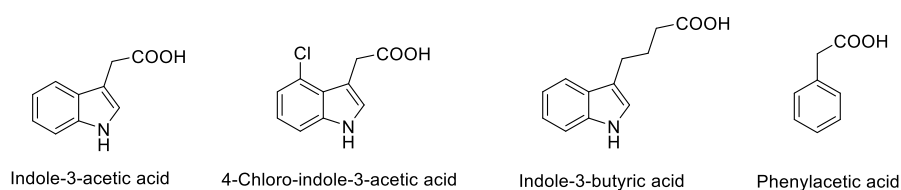
Figure 1 Naturally occuring auxins

2.1.2. Synthetic auxin analogues

The essential structural requirements for the auxin activity are a strong negative charge on the carboxyl group and a weaker positive charge on the planar aromatic ring (Grossmann 2003). Over the years, a lot of synthetic compounds with auxin-like activities have been identified (Swarup and Peret 2012), many of which had found application in agriculture as auxin-like plant growth regulators and herbicides. The most famous synthetic auxins include: dichlorophenoxyacetic acid (2,4-D), 2,4,5-trichlorophenoxyacetic acid (2,4,5-T), 2-methyl-4-chlorophenoxyacetic acid (MCPA), 1-naphthaleneacetic acid (1-NAA), 4-amino-3,5,6-trichloro-2-pyridinecarboxylic acid (picloram), 3,6-dichloro-2-methoxybenzoic acid (dicamba), quinclorac, aminocyclopyrachlor or halauxifen-methyl (Busi, Goggin *et al.* 2018; Jiang and Asami 2018) (Figure 2). The herbicide syndrome is mediated by hormone interaction in signalling between auxin, ethylene and the upregulation of abscisic acid biosynthesis (Grossmann 2010). Responses mediated by auxin herbicides include growth inhibition, senescence and tissue decay in sensitive dicots, while, quinclorac also controls grass weeds.
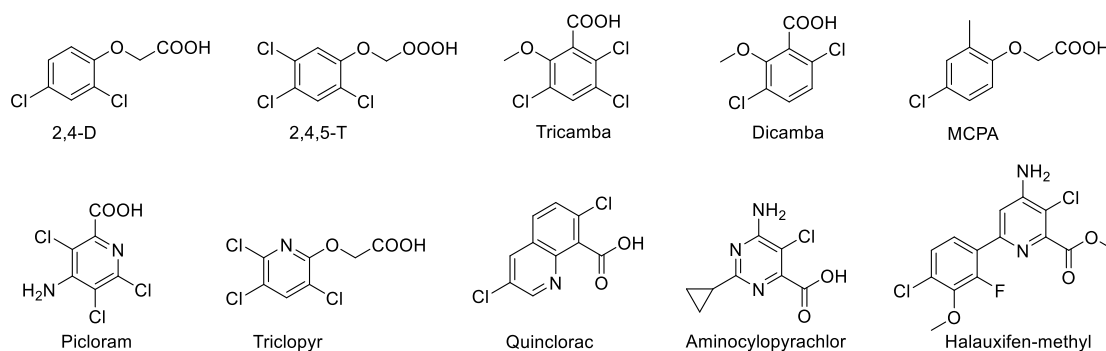
Figure 2 Synthetic auxin analogues

However, it was also noticed, that certain structural modification of the auxin-like compounds can lead to antagonistic effect. More than 50 years ago, it was suggested that *p*-chlorophenoxyisobutyric acid (PCIB) has antiauxin activity (Burstrom 1950). PCIB inhibits many auxin-induced physiological effects, for example auxin-dependent DR5::GUS expression (Oono, Ooura *et al*. 2003). Additionally, it inhibits lateral root development, gravitropic response in roots and primary root growth. These effects suggest that PCIB disrupts auxin-signalling pathway by regulating Aux/IAA protein stability, however, the mechanism of PCIB-mediated inhibition of auxin action is not clear at the molecular level (Figure 3).
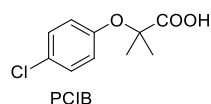
Figure 3 Synthetic anti-auxin PCIB

2.1.3. Auxin signalling

The mechanism of auxin action is coordinated through transcriptional regulation of the action of three main protein families called the Transport Inhibitor Response 1/Auxin Signalling F-box protein (TIR1/AFB) (Dharmasiri, Dharmasiri *et al*. 2005; Mockaitis and Estelle 2008), the Aux/IAA transcriptional repressors (Remington, Vision *et al*. 2004; Overvoorde, Okushima *et al*. 2005), and the family of Auxin Response Factors (ARFs) (Okushima, Overvoorde *et al*. 2005; Guilfoyle and Hagen 2007). The F-box protein TIR1 is the best studied auxin receptor (Ruegger, Dewey *et al*. 1998). The TIR1 family includes five additional AFBs in *Arabidopsis*, namely, AFB1, AFB2, AFB3, AFB4, AFB5 (Dharmasiri, Dharmasiri *et al*. 2005).

13

At low auxin concentrations, AUX/IAA transcriptional repressor proteins repress genes targeted by transcriptional activators ARFs (Santner, Calderon-Villalobos *et al.* 2009). On the other hand, at high auxin concentrations, auxin binds to TIR1 creating a high affinity surface. Auxin acts as a "molecular glue" to increase the strength of the interaction between TIR1 and the Aux/IAA protein (Tan, Calderon-Villalobos *et al.* 2007; Parry, Calderon-Villalobos *et al.* 2009), followed by SCF ubiquitin ligase catalyzed ubiquitination of the AUX/IAAs and consequent degradation in the proteasome, which results in reduction in concentrations of AUX/IAA proteins. Then, the ARFs releases, allowing transcription to commence (Figure 4).
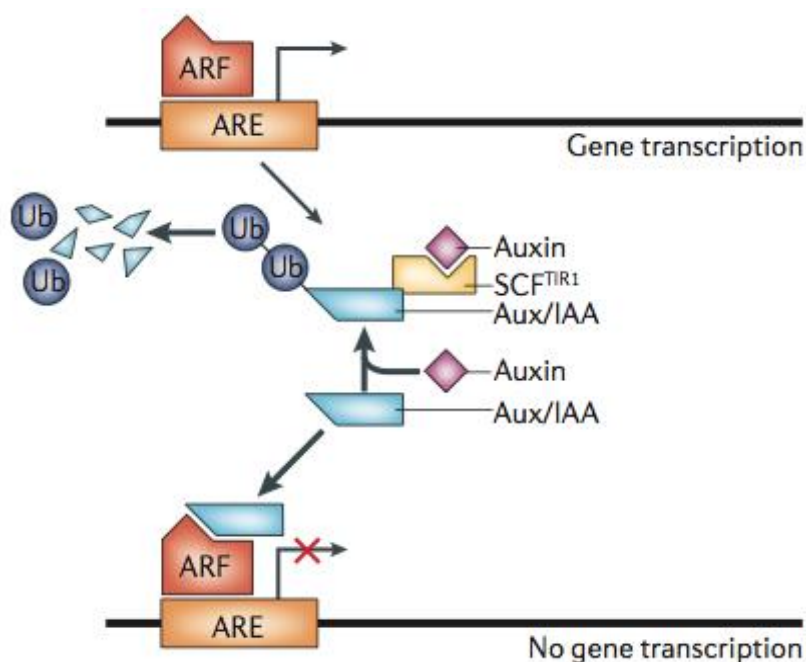
Figure 4 A model for auxin response through the TIR1 auxin receptor pathway (Teale, Paponov *et al.* 2006)

2.1.3.1. Agonists and antagonists of TIR1 receptor function

IAA binds to the TIR1 pocket *via* two important functional moieties, the side-chain carboxyl group and the indole ring (Tan, Calderon-Villalobos *et al.* 2007). Moreover, NH group of the IAA indole ring is involved in the hydrogen bonding with a carboxyl group at the backbone of TIR1. Despite having different ring structures (for example, the naphthalene ring of 1-NAA or the dichlorophenyl ring of 2,4-D) other synthetic compounds with auxin-like activities fit into TIR1. On the other hand, AFB5 has been shown to be the dominant site of action for the picolinate herbicides (Walsh, Neal *et al.* 2006; Lee, Sundaram *et al.* 2014).

Recently, Quareshy *et al.* explored the tetrazole functional group as a bioisostere of carboxylic acid group and proved that indole-3-methyl tetrazole (iMT) works as a weak

auxin (Figure 5), which selectively binds to TIR1 but not to its homologue AFB5 (Quareshy, Prusinska *et al*. 2018).
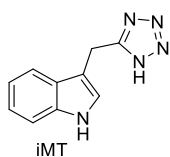
Figure 5 Tetrazole analog **-** indole-3-methyl tetrazole (iMT)

On the other hand, Hayashi *et al*. designed a series of small molecule agonists and antagonists of TIR1 receptor function (Hayashi, Tan *et al*. 2008). They showed that auxin derivatives with methyl, ethyl, and *n*-propyl groups at *α*-position of IAA molecule retained auxin activity. On the other hand, compounds with *n*-butyl or longer alkyl chains at this position showed antagonistic activity against auxin. Among prepared compounds, *α*-butoxycarbonyl aminohexyl-IAA (BH-IAA) had the strongest anti-auxin effect (Figure 6). However, BH-IAA is not a potent auxin antagonist due to its low binding affinity to TIR1 and flexibility of the long alkyl chain at the *α*-position which therefore prevents the docking of the Aux/IAA to TIR1 less efficiently. However, other derivaties with stronger antagonistic activity, namely, *α*-(phenylethyl-2-oxo)-IAA (PEO-IAA) and *α*-(2,4-dimethylphenylethyl-2-oxo)-IAA (auxinole) (Figure 6) were also developed. In comparison with BH-IAA, the tight π−π stacking between the phenyl ring of derivatives PEO-IAA and auxinole and Phe82 of TIR1 contribute to the high affinity of the derivatives to the receptor (Hayashi, Neve *et al*. 2012). These two derivatives had since been extensively studied for their effects and found application in plant sciences. Auxinole blocks auxin-induced Ca^{2+} signalling in root cells (Dindas, Scherzer *et al*. 2018) and decreases auxin-increased density of actin filaments in root epidermal cells (Scheuring, Lofke *et al*. 2016). PEO-IAA suppresses root gravitropism and enhances root phototropism (Kimura, Haga *et al*. 2018). Further, treatment of proliferating plant cells with PEO-IAA, causes chromatin loosening (Hasegawa, Sakamoto *et al*. 2018). Moreover, the agricultural potential of these derivatives had also been demonstrated, for instance PEO-IAA improved grain yield in rice (Tamaki, Reguera *et al*. 2015).
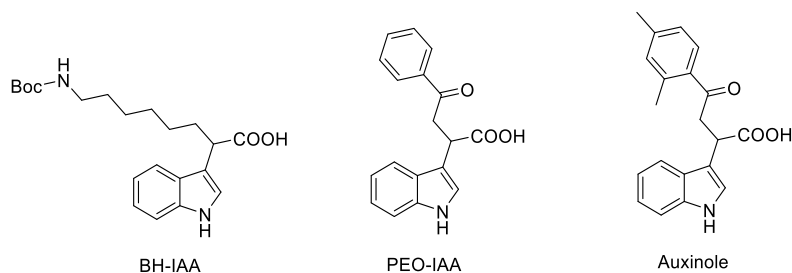
Figure 6 Rationally designed auxin antagonists

2.1.3.2. Engineered auxin–receptor pairs

Synthetic auxin analogues can activate or inhibit auxin response. However, exact inducing of auxin signalling mediated by a specific receptor in an organ, tissue or cell-type of interest up to now was not possible. To overcome such problem, bump-and-hole approach was used to engineer an orthogonal auxin–receptor pair cvxIAA-ccvTIR1 (Torii, Hagihara *et al*. 2018; Uchida, Takahashi *et al*. 2018). A bulky moiety (a"bump") was added to the IAA molecule to produce synthetic auxin analogues 5-(3-methylphenoxyl-IAA) (cvxIAA) and 5-adamantyl-IAA (pico-cvxIAA) (Figure 7) (Yamada, Murai *et al*. 2018) which are inactive auxin analogues that are not able to bind to the endogenous TIR1/AFBs, but are recognized by an engineered ccvTIR1 (Torii, Hagihara *et al*. 2018), which is a mutated TIR1 with a created cavity (or "hole"), which cannot recognize the natural auxin IAA. In the absence of cvxIAA, *Arabidopsis* plants expressing ccvTIR1 do not exhibit any auxin response. However, similarly to natural pair IAA-TIR1, cvxIAA-ccvTIR1 can recruit AUX/IAA proteins. The orthogonal cvxIAA-ccvTIR1 pair can be further elaborated to delineate auxin response in systems of interest and to elusidate the specific contributions of auxin receptors.
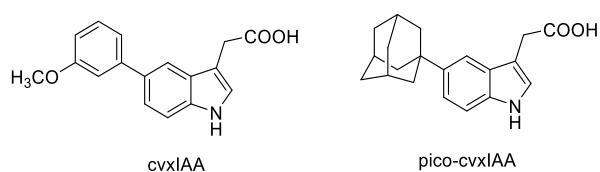
Figure 7 Convex-auxins - inactive auxin analogues recognized by an engineered ccvTIR1

2.1.4. Auxin biosynthesis in plants

Main criteria in evaluating the proposed IAA biosynthesis pathways in plants include identification of genes, characterization of enzyme activities, quantification of metabolites, determination of physiological role, and distribution in plant kingdom (Kasahara 2016).

There are two main auxin biosynthesis pathways proposed in plants, namely, tryptophan-dependent and independent pathways.

<u>Trp-dependent pathway</u>

The first step of this pathway is conversion of chorismic acid to anthranilate which is catalyzed by anthranilate synthase (AS) (Li and Last 1996). Then, the formation of indole-3-glycerol phosphate (IGP) follows through phosphoribosylanthranilate transferase (PAT), and indole-3-glycerol phosphate synthase (IGS) (Kasahara 2016). Subsequently, tryptophan synthase α (TSA) and tryptophan synthase β (TSB) form a complex and convert IGP to Trp (Miles 1991; Radwanski, Zhao *et al*. 1995; Jian, Shao *et al*. 2000). IAA biosynthetic pathway from Trp is then divided into different routes catalysed by different enzymes (Kasahara 2016) (Scheme 1).

IPA pathway

TRYPTOPHAN AMINOTRANSFERASE OF ARABIDOPSIS (TAA) and YUCCA (YUC) flavin-containing monooxygenase families produce IAA from L-tryptophan (Trp) *via* indole-3-pyruvate (IPA) in two-step reactions in *Arabidopsis* (Mashiguchi, Tanaka *et al*. 2011; Stepanova, Yun *et al*. 2011; Won, Shen *et al*. 2011). TAA and YUC families play a crucial role in IAA biosynthesis in various plant species, including *Arabidopsis*, maize, rice, and liverwort (Brumos, Alonso *et al*. 2014; Eklund, Ishizaki *et al*. 2015) (Scheme 1).

The IAOx pathway in *Arabidopsis*

In the initial step of the IAOx pathway CYP79B2 and CYP79B3 catalyze the conversion of Trp to IAOx (Hull, Vij *et al*. 2000; Mikkelsen, Hansen *et al*. 2000; Zhao, Hull *et al*. 2002). The IAOx pathway may be a species-specific pathway in Brassicaceae plants (Bender and Celenza 2009; Sugawara, Hishiyama *et al*. 2009). The underlying pathway from IAOx to IAA is not clear. However, indoleacetamide (IAM) and indole-3-acetonitrile (IAN) have been suggested as possible precursors because they show metabolic profiles similar to IAOx (Sugawara, Hishiyama *et al*. 2009). Then, the NITRILASE (NIT) family of enzymes convert IAN to IAA in *Arabidopsis* and maize (Bartel and Fink 1994; Vorwerk, Biernacki *et al*. 2001; Park, Kriechbaumer *et al*. 2003; Kriechbaumer, Park *et al*. 2007). However, IAN and NIT enzymes may play more important roles in indole glucosinolate metabolism, camalexin homeostasis, and cyanide detoxification rather than IAOx-dependent IAA biosynthesis in

Arabidopsis (Nafisi, Goregaoker *et al*. 2007; Su, Xu *et al*. 2011; Brumos, Alonso *et al*. 2014) (Scheme 1).

Other proposed pathways from Trp

Many auxin-producing bacteria have iaaM and iaaH genes, encoding TRYPTOPHAN 2-MONOOXYGENASE (iaaM) and INDOLE-3-ACETAMIDE HYDROLASE (iaaH), respectively (Patten and Glick 1996). The enzyme TRYPTOPHAN 2-MONOOXYGENASE catalyzes the conversion of Trp to indoleacetamide (IAM) and INDOLE-3-ACETAMIDE HYDROLASE converts IAM to IAA (Scheme 1).

Additionally, tryptamine (TAM) and indole-3-acetaldehyde (IAAld) have been suggested as possible precursors of IAA in plants (Woodward and Bartel 2005). TRYPTOPHAN DECARBOXYLASE (TDC) family enzymes can convert Trp to TAM (Woodward and Bartel 2005; Mano and Nemoto 2012). ALDEHYDE OXIDASE (AAO) family, which catalyzes the conversion of IAAld to IAA, has also been suggested as an IAA biosynthesis enzyme (Sekimoto, Seo *et al*. 1997; Seo, Akaba *et al*. 1998) (Scheme 1).

Trp-independent pathway

In addition, analyses of Trp biosynthetic mutants demonstrate that plants can also synthesize IAA without using a Trp intermediate (Woodward and Bartel 2005; Kasahara 2016). It has been shown that endogenous amounts of IAA were remarkably higher in Trp biosynthesis mutants *trp3-1* and *trp2-1* than in wild-type plants. These mutants are defective in Trp synthase α and β, respectively (Last, Bissinger *et al*. 1991; Radwanski, Barczak *et al*. 1996) and accumulate amide- and ester-linked IAA conjugates (Normanly, Cohen *et al*. 1993; Jian, Shao *et al*. 2000), despite containing lower Trp levels (Jian, Shao *et al*. 2000; Muller and Weiler 2000). Moreover, maize mutants fed with ^{15}N-labelled anthranilate did not synthesize tryptophan but did synthesize IAA (Murofushi, Yamane *et al*. 1999). Based on this finding, IAA is probably produced from Trp precursors, indole (IND) and indole-3-glycerol phosphate (IGP), but not from Trp. IGP was also proposed as a branch point intermediate in the Trp-independent pathway in *Arabidopsis* (Jian, Shao *et al*. 2000). In addition, cytosol-localized indole synthase (INS) functions in the Trp independent pathway in *Arabidopsis* (Wang, Chu *et al*. 2015). This study showed that INS produces IND as an initial precursor of IAA in the cytosol. However, the underlying pathway from IND to IAA is not solved. INS plays a crucial role in the establishment of the apical–basal pattern during early

embryogenesis. For this reason, Trp-dependent and Trp-independent IAA biosynthetic pathways seems to be important to regulate embryogenesis of higher plants.
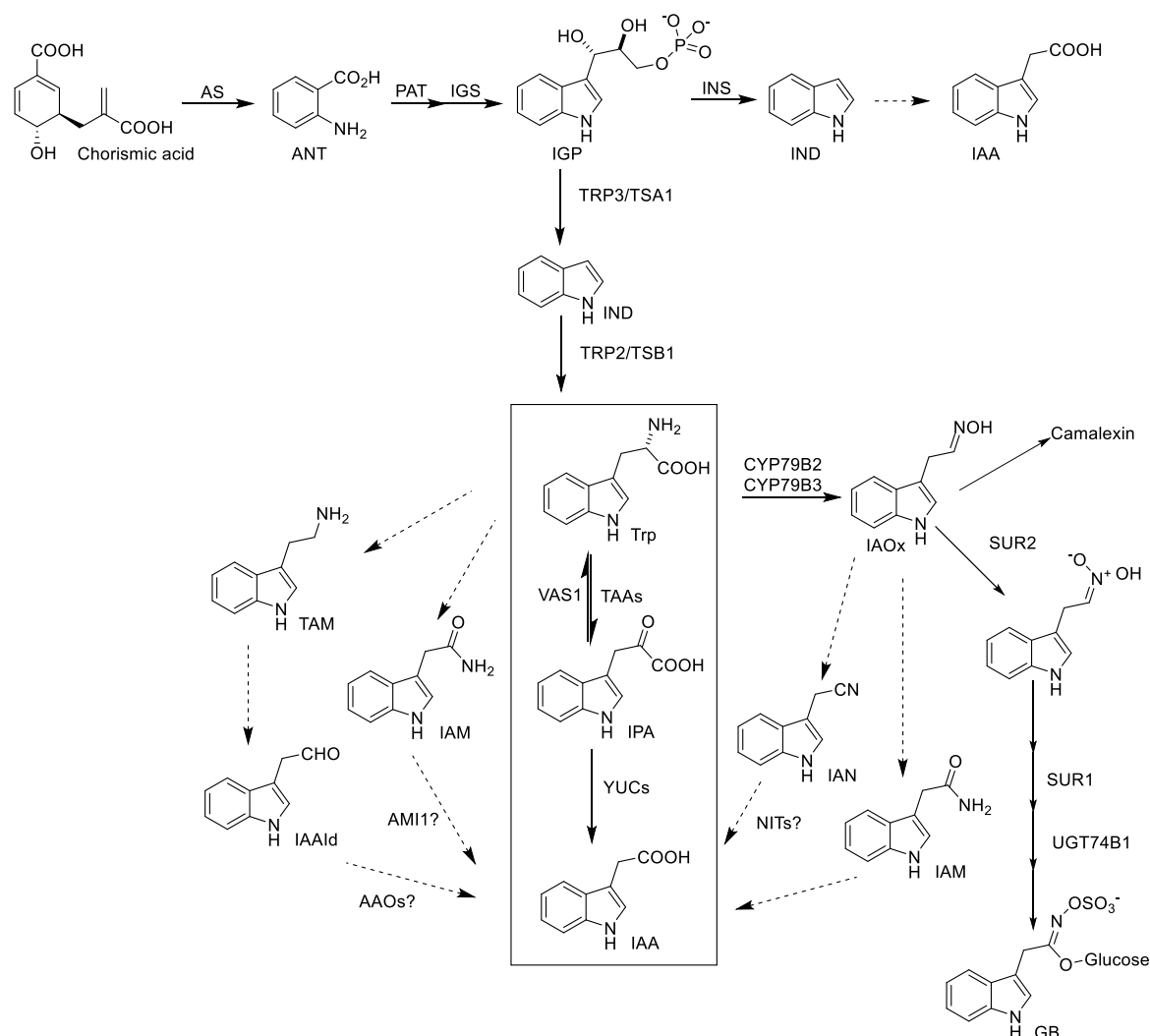
Scheme 1 A schematic model of the IAA biosynthetic pathways (Li and Last 1996; Kasahara 2016)

2.1.4.1. Auxin biosynthesis inhibitors

Few auxin biosynthesis inhibitors which target tryptophan-dependent pathway are known. Soeno *et al.* reported L-aminooxyphenylpropionic acid (L-AOPP) to reduce the endogenous levels of IAA by targeting the Trp aminotransferase. (Soeno, Goda *et al.* 2010). Then, L-kynurenine (L-Kyn), which suppresses ethylene responses in *Arabidopsis* roots was identified (He, Brumos *et al.* 2011). Further studies indicated that L-Kyn acts as a competitive substrate of tryptophan aminotransferase-related (TAA1/TAR) and thus, suppresses auxin biosynthesis. In addition, 5-(4-chlorophenyl)-4*H*-1,2,4-triazole-3-thiol (yucasin), has been reported to be a potent inhibitor of IAA biosynthesis (Nishimura,

Hayashi *et al*. 2014) by inhibiting YUC1 in a competitive manner against the substrate IPA. Moreover, Kakei *et al*. prepared few inhibitors that target YUC for example, 4-biphenylboronic acid (BBo) and 4-phenoxyphenylboronic acid (PPBo) (Kakei, Yamazaki *et al*. 2015). These inhibitors of TAA1/TAR and YUC are useful for understanding the mechanisms of tryptophan-dependent IAA biosynthesis (Jiang and Asami 2018) (Figure 8).
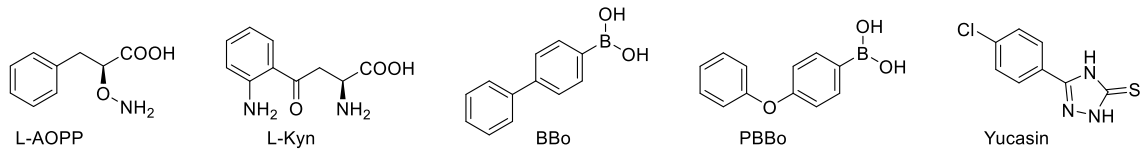
Figure 8 Inhibitors of auxin biosynthesis

2.1.5. Auxin transport

Auxin is distributed by two distinct transport systems in plants (Adamowski and Friml 2015). Among the two, nondirectional stream in the phloem along with photosynthetic assimilates is faster, while the directional cell-to-cell polar auxin transport (PAT) is slow. Auxin is distributed in a precise way by polar auxin transport which is crucially important for the formation of local auxin maxima, mainly in developing tissues, such as lateral root initiation sites in pericycle or concave side of apical hook (Parizkova, Pernisova *et al*. 2017). Chemiosmotic polar diffusion hypothesis explains the mechanism of cell-to-cell polar auxin transport (Goldsmith 1977). IAA movement is facilitated by auxin influx and efflux carriers (Swarup and Peret 2012). IAA is weak acid and in the apoplast at pH 5.5, small portion of IAA in its non-dissociated form (IAAH) can passively diffuse to the cell. However, the majority of IAA is in dissiociated form (IAA$^-$) and can be transported only actively with transporter proteins. In the cytosol at pH 7.0, all IAA remains in its polar IAA$^-$ form and needs auxin efflux carriers for transport out of the cell (Zazimalova, Murphy *et al*. 2010) (Figure 9).
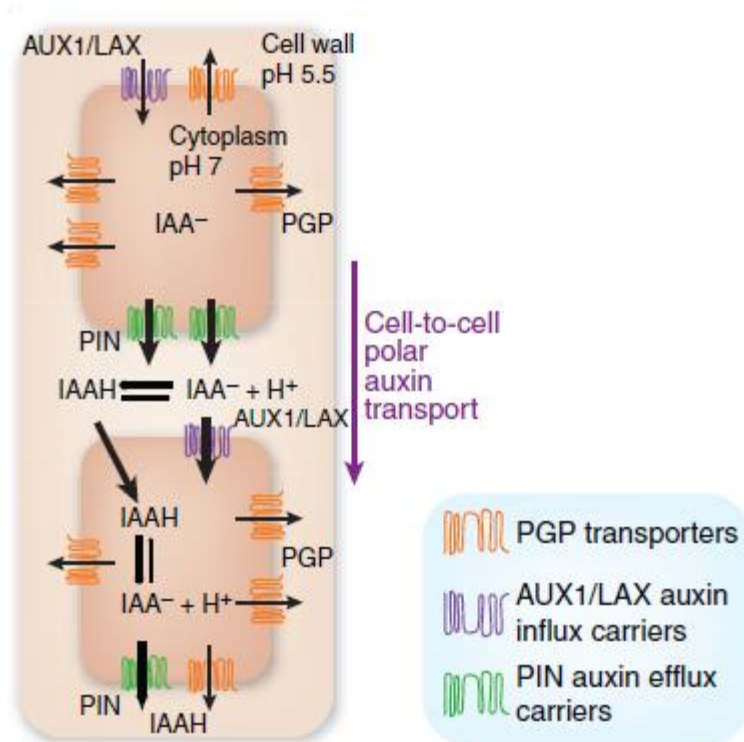
Figure 9 The chemiosmotic model for polar auxin transport. (Robert and Friml 2009)

Differential distribution of the auxin is known to mediate many fundamental processes in plant development, such as the formation of the embryogenic apical–basal axis, pattern formation, tropisms, and organogenesis (Vanneste and Friml 2009). There are proven auxin influx carriers AUXIN RESISTANT 1/LIKE AUXIN RESISTANT (AUX1/LAX) family and auxin efflux carriers PIN-FORMED (PIN) proteins as well as P-GLYCOPROTEIN (PGP) family members (Lankova, Smith *et al.* 2010). The activity of these transporters directs the distribution of auxin and formation of auxin gradients (Figure 9).

2.1.5.1. Major auxin efflux carriers

The PIN-FORMED (PIN) proteins are a plant-specific family of transmembrane proteins that transport auxin out of the cell (Krecek, Skupa *et al.* 2009). They play a role during embryogenesis, organogenesis, and vasculature formation. Moreover, they are responsible for the root gravitropic growth and regulate the activity of the root meristem (Friml, Wisniewska *et al.* 2002; Benkova, Michniewicz *et al.* 2003; Friml, Vieten *et al.* 2003; Blilou, Xu *et al.* 2005; Sieburth and Deyholos 2006). PINs are encoded by a small gene family comprising of eight members (Grunewald and Friml 2010). *Arabidopsis thaliana* was used as model plant for description and functional characterization of the first PIN family

members - PIN1, PIN2, PIN3, PIN4, and PIN7 (Krecek, Skupa *et al*. 2009). According to localization, PIN proteins can be divided into two groups. PIN 1, 2, 3, 4, and 7 are localized on the plasma membrane (Swarup and Peret 2012). On the other hand, PIN 5, 6 and 8 are localized in the endoplasmatic reticulum (Mravec, Skupa *et al*. 2009; Dal Bosco, Dovzhenko *et al*. 2012; Bender, Fekete *et al*. 2013). PIN1 is localized on the basal rootward face of vascular cells (Galweiler, Guan *et al*. 1998). This facilitates rootward movement of auxin. On the other hand, PIN2 is asymmetrically localized at the apical shootward face of lateral root cap and epidermal cells, additionally basal rootward face of cortical cells of meristem (Blilou, Xu *et al*. 2005; Wisniewska, Xu *et al*. 2006; Rahman, Takahashi *et al*. 2010). The localization of PIN2 is creating an auxin reflux loop. PIN3 localizes at the inner lateral side, while it has a symmetric localization in columella cells (Friml and Palme 2002). Further, PIN4 is distributed at the basal side of the cells in the central root meristem and with less pronounced polarity in the cells of the quiescent center (Kleine-Vehn and Friml 2008). The last one PIN7 is localized at the basal side of the stele cells and apolar in the columella cells (Figure 10). PIN5 and PIN8 have not been fully functionally characterized but they play a key part in both intercellular and intracellular auxin movement and regulation of auxin homeostasis in endoplasmatic reticulum (Mravec, Skupa *et al*. 2009).
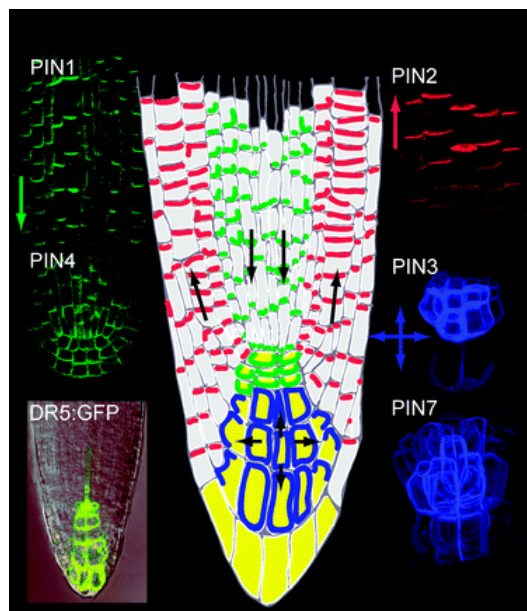
Figure 10 PIN protein and auxin distributions in the *Arabidopsis* root. The root tip-associated auxin maximum is demonstrated with the synthetic auxin response reporter (DR5::GFP) (Wabnik, Govaerts *et al*. 2011).

Three members of the multi-drug-resistant/P-glycoproteins (MDR/PGP) subfamily of ATP-binding cassette (ABC) transporters PGP1, PGP4 and PGP19 are involved in polar auxin transport (Swarup and Peret 2012). PGP1 and PGP19 are involved in auxin efflux

(Noh, Bandyopadhyay *et al*. 2003; Blakeslee, Bandyopadhyay *et al*. 2007), while PGP4 participates in the shootward (basipetal) redirection of auxin from the root apex. Different studies suggest that PGP4 can function both as an efflux and influx carrier (Terasaka, Blakeslee *et al*. 2005; Cho, Lee *et al*. 2007; Yang and Murphy 2009; Kubes, Yang *et al*. 2012). Some of PGP proteins interact with PIN proteins and probably provide stabilization of membrane transport complexes (Bandyopadhyay, Blakeslee *et al*. 2007).

2.1.5.2. Major auxin influx carriers

In *Arabidopsis*, AUXIN1/LIKE-AUX1 (AUX/LAX) family provide transport of auxin into the cell (Swarup and Peret 2012). AUX1 belongs to a small gene family including AUX1 and LIKE-AUX1 (LAX) genes, LAX1, LAX2, and LAX3. They form a plant-specific subclass within the aminoacid/auxinpermease (AAAP) superfamily (Young, Jack *et al*. 1999; Peret, Swarup *et al*. 2012). The AUX1/LAX proteins localize at the plasma membrane (Bennett, Marchant *et al*. 1996; Yang, Hammes *et al*. 2006). Each member of the AUX/LAX family is a functional auxin influx carrier and mediates auxin related developmental processes in different organs and tissues (Swarup and Peret 2012). AUX1 plays a key role in root gravitropic response, unlike any other AUX/LAX family members that are not root gravitropic response related (Péret *et al*., 2012). AUX1 also helps to maintain high auxin levels in the differentiation zone and facilitates root hair growth (Jones, Kramer *et al*. 2009), whereas LAX2 is important for vascular development in cotyledons (Péret *et al*., 2012). Further, AUX1 and LAX3 have influence in lateral root development and apical hook formation (Marchant, Bhalerao *et al*. 2002; Swarup, Benkova *et al*. 2008; Vandenbussche, Petrasek *et al*. 2010). On the other hand, AUX1 and LAX1 and possibly LAX2 are important for leaf phyllotactic patterning (Bainbridge, Guyomarc'h *et al*. 2008).

2.1.5.3. Inhibitors of auxin efflux and influx carriers

Auxin influx and efflux pathways can be physiologically recognized using auxin efflux inhibitors. Multiple auxin signal inhibitors, such as 1-*N*-naphthylphthalamic acid (NPA), 1-pyrenoylbenzoic acid (PBA), and 2,3,5-triiodobenzoic acid (TIBA), have been confirmed as polar auxin transport inhibitors (Jiang and Asami 2018) (Figure 11). Structurally, NPA is a benzoic acid *ortho*-linked with an aromatic ring system. This is a shared structural similarity with compounds possessing auxin-like activity. It has been suggested that there is some positive correlation between the structure of NPA and its activity. (Katekar and Geissler

1977). On the other hand, the known inhibitor TIBA does not share this structural pattern. Explanation of the mechanism of inhibition of NPA was supported by the existence of an NPA-binding protein forming part of the auxin efflux carrier complex (Friml and Palme 2002). The other study suggest that some of the inhibitors (TIBA and PBA) can act through actin mediated vesicle trafficking processes in eukaryotic cells (Dhonukshe, Grigoriev *et al.* 2008).

The other known auxin efflux inhibitor is *cis*-cinnamic acid (*c*-CA) (Steenackers, Klima *et al.* 2017) (Figure 11). *c*-CA is a novel endogenous inhibitor of auxin transport, which is the photo-isomerization product of the phenylpropanoid pathway intermediate *trans*-CA (*t*-CA). *c*-CA was found slightly less efficient in the auxin accumulation assay, compared to NPA, although both NPA and *c*-CA block cellular auxin efflux. The reason may come from the broader specificity of NPA, known to affect different types of auxin efflux carriers.

On the other hand, auxin influx inhibitors include 1-naphthoxyacetic acid (1-NOA), 2-naphthoxyacetic acid (2-NOA), and 3-chloro-4-hydroxyphenylacetic acid (CHPAA) (Lankova, Smith *et al.* 2010) (Figure 11). 1-NOA is the most potent inhibitor, as it blocks the activities of both auxin influx and efflux carriers, while 2-NOA and CHPAA mainly inhibit auxin influx. Activities of auxin influx inhibitors regulate overal auxin transport across the plasma membrane depending on the dynamics of particular membrane vesicles.
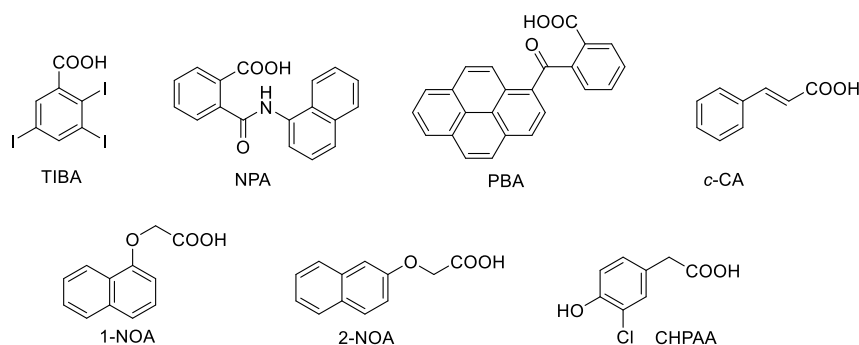
Figure 11 Inhibitors of auxin efflux and influx carriers

2.1.6. Fluorescently labelled auxins

Fluorescent labelling of plant hormones allows sensitive and specific visualization of their subcellular and tissue-specific localization and transport in plants. Thus, it is of great importance for answering questions concerning plant growth and development, however, up to date only few fluorescently labelled auxins had been developed. The first two fluorescently labelled auxins are IAA analogues with FITC and RITC fluorescent labels attached at N1 position of the molecule, fluorescein isothiocyanate coupled to IAA (FITC-

IAA) and rhodamine isothiocyanate (RITC) coupled to IAA (RITC-IAA), respectively (Sokolowska, Kizinska *et al.* 2014) (Figure 12). These substances are described as active auxin analogues, but the sufficient evidence of the structure and purity of these compounds is lacking. Also, ESI-MS analysis revealed FITC-IAA degradation, therefore potential fragmentation of analogues *in planta* should be considered.

Hayashi *et al.* developed several IAA and NAA based fluorescently labelled auxins by attaching to them number of fluorophores *via* different linkers (Hayashi, Nakamura *et al.* 2014). The two most potent compounds, 7-nitro-2,1,3-benzoxadiazole (NBD)-conjugated naphthalene-1-acetic acid (NBD-NAA) and indole-3-acetic acid (NBD-IAA), are not active for auxin signalling, but are active for auxin transport and can thus be used to visualize auxin distribution (Figure 12).

More recently, Mravec *et al.* prepared IAA conjugate with fluoresceinamine (FA) using the carboxyl group of IAA for the formation of an amide bond (Mravec, Kracun *et al.* 2017) (Figure 12). IAA-FA was proven to not bind to the cell wall, supporting the fact that carboxyl group of auxinic compounds is important for the binding to cell wall.

Figure 12 Fluorescently labelled auxins

Despite these valuable examples, the need of developing new fluorescently labelled auxins remains highly relevant.

3. Experimental part

3.1. Chemistry

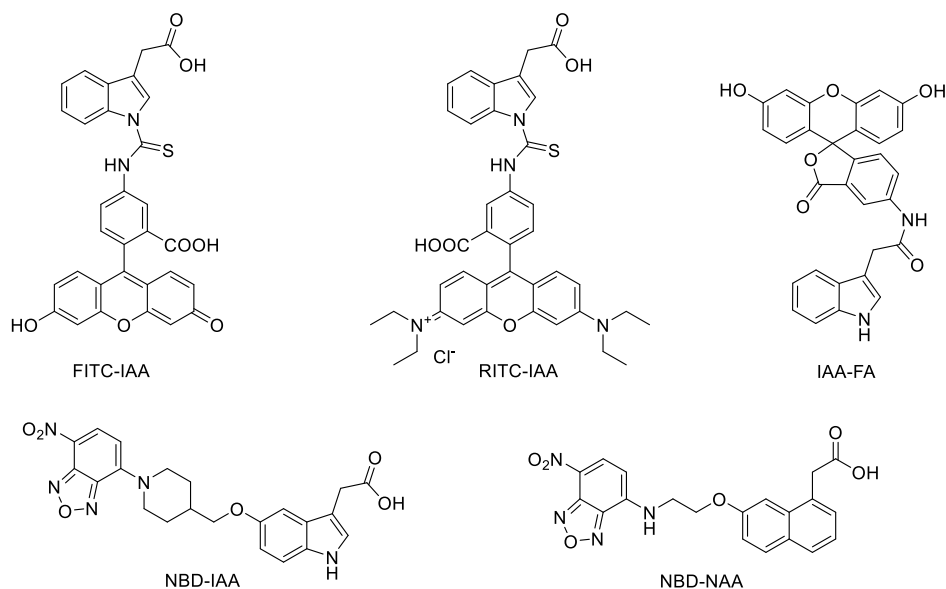### 3.1.1. Materials

3.1.1.1. Chemicals, solvents and solutions

Commercially available solvents and reagents were purchased from common chemical suppliers and were used without further purification, unless stated otherwise: acetone-d_6, DMSO-d_6, CDCl$_3$, AcCl ($\geq$99%), PPh$_3$ (99%), TFA ($\geq$98%), NBD-Cl (98%), NaH (60% in mineral oil), 4-aminobutan-1-ol (98%), 6-aminohexan-1-ol (97%), 5-aminopentan-1-ol (95%), *N*-Boc-ethanolamine (98%), 3-(Boc-amino)-1-propanol (97%), 4-(Boc-amino)-1-butanol ($\geq$98%), IAA, Boc$_2$O (99%), (Sigma-Aldrich); Na$_2$S$_2$O$_3$, NaCl, NH$_4$Cl, Celite, HCl, KHSO$_4$, Na$_2$SO$_4$ ($\geq$99%), Et$_3$N ($\geq$99.5%) (Penta); acetone, CH$_2$Cl$_2$, Et$_2$O, DMF, DMSO, EtOH, EtOAc, heptane, CHCl$_3$, MeOH, NaHCO$_3$, PE, CH$_3$CN, sucrose (Lach-Ner); I$_2$ (Merck); LiOH $\cdot$ H$_2$O ($\geq$99%), imidazole ($\geq$99.5%), TBAB ($\geq$99%) (Fluka).

Dry CH$_2$Cl$_2$ was distilled over calcium hydride. Preparation of other dry solvents (DMF, DMSO) was carried out according to Williams Lawton: the required amount of solvent (20% w/v) was added to activated molecular sieves (24 h, 300 °C) and dried under calcium chloride cap for 72 hours (Bradley, Williams *et al*. 2010).

All saturated and staining solutions were prepared as follows:

KMnO$_4$ staining solution: 1.5 g of KMnO$_4$, 10 g of K$_2$CO$_3$ and 1.25 mL of 10% NaOH were dissolved in 200 mL of water.

Vanillin staining solution: 15 g of vanillin was dissolved in 250 mL of ethanol and 2.5 mL of conc. H$_2$SO$_4$ were added.

Ninhydrin staining solution: 1.5 g of ninhydrin was dissolved in 100 mL of *n*-butanol and 3 mL of acetic acid were added.

3.1.2. Methods

3.1.2.1. General methods

To control the course of the reactions thin layer chromatography (TLC) aluminum plates coated with silica gel 60 F254 (Merck, USA) were used. Additives used in mobile phase are stated for individual substances. TLC results were visualized using a UV lamp (CAMAG,

Switzerland) and visualization reagents (vanilin, ninhydrin and KMnO$_4$ staining solutions). Prepared compounds were purified by column chromatography in glass columns filled with silica gel 40-63 micron Davisil LC60A (Grace Davison, UK). Elution composition of the mixture is given for specific substances. Purity of the compounds was determined by high performance liquid chromatography (ACQUITY UPLC® H-Class System, Waters, Milford, USA) with a column C18 symmetry (Waters, UK) with dimensions 2.1×150 mm, particle size 5 µm. The samples were dissolved in MeOH, or in DMSO diluted in MeOH to a final concentration of 10 ng/ml. Separation was carried out by gradient elution (0' - 90% A; 25' - 10% A; 35' - 10% A; 36' - 90% A; 45' - 10% A) at a flow rate 0.2 ml/min. Mobile phase A - HCOONH$_4$ 15 mM, pH 4.0, mobile phase B - MeOH. Analyte detection facilitated by UV-VIS diode array detector (PDA 2996, Waters, UK) operating in the wavelength range 210-400 nm. The molecular mass of the prepared compounds was measured on a hybrid mass spectrometer with Q-Da (Waters, UK). The eluent from the HPLC was led into the ion source (ESI), Ionization was carried out in the positive (ESI$^+$) and/or negative (ESI$^-$) mode, followed by detection in FULLSCAN mode in the range of m/z 50 to 1000. The compounds were further analyzed by nuclear magnetic resonance (NMR) spectrometer ECA-500 (JEOL, Japan) at 500 MHz (^{1}H) and 125 MHz (^{13}C) by measuring in deuterated solvents (acetone-d_6, DMSO-d_6, CDCl$_3$). Chemical shifts were calibrated to values of appropriate solvents - ^{1}H 2.50 ppm of residual DMSO-d_6 peak, 7.26 ppm of residual CDCl$_3$ peak, 2.05 ppm of residual acetone-d_6 peak and ^{13}C 39.5 ppm signal of DMSO-d_6, 77.16 ± 0.06 ppm signal of CDCl$_3$, 29.84 and 206.26 ppm signal of acetone-d_6.

3.1.2.2. Organic synthesis

Synthesis of methyl 3-(2-methoxy-2-oxoethyl)-1H-indole-1-carboxylate 3
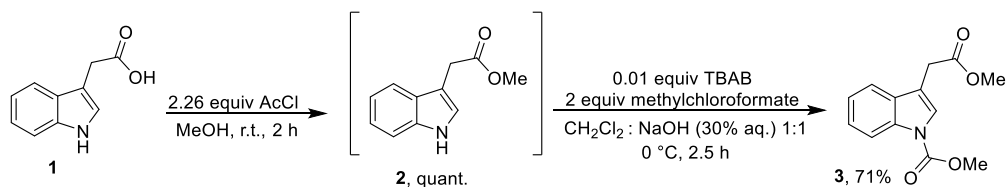
Scheme 2 Synthesis of Methyl 3-(2-methoxy-2-oxoethyl)-1H-indole-1-carboxylate **3**

The methyl 3-(2-methoxy-2-oxoethyl)-1H-indole-1-carboxylate **3** was prepared in accordance to the procedure described by Hayashi *et al.* (Hayashi, Neve *et al.* 2012) with minor modifications. To a solution of indol-3-acetic acid **1** (3396 mg, 19.38 mmol) in MeOH (85 ml), AcCl (3.12 ml, 43.71 mmol) was added dropwise at 0 °C and the reaction mixture

was stirred at room temperature for 2 hours. The solvent was evaporated under reduced pressure and crude was redissolved in EtOAc (20 ml), quenched with aqueous saturated NaHCO$_3$ solution (15 ml) and extracted with EtOAc (3 × 25 ml). The combined organic extracts were washed with brine (2 × 15 ml). Drying with Na$_2$SO$_4$, filtration and evaporation of the solvent under reduced pressure afforded crude methyl 2-(1*H*-indol-3-yl)acetate **2**, which was used as such without further purification. Crude methyl 2-(1*H*-indol-3-yl)acetate **2** (3667 mg, 19.38 mmol) was dissolved in CH$_2$Cl$_2$ (42 ml) and TBAB (62 mg, 0.19 mmol) was added. The resulting mixture was cooled down to 0 °C and NaOH solution (30% aq.) (42 ml) was added dropwise, followed by dropwise addition of methylchloroformate (2.99 ml, 38.77 mmol). The reaction mixture was stirred at 0 °C for 2.5 hours. Subsequently, the reaction mixture was acidified with 6 M HCl and 1 M HCl solutions to pH = 6 and extracted with CH$_2$Cl$_2$ (3 × 25 ml). The combined organic extracts were washed with brine (2 × 15 ml). Drying with Na$_2$SO$_4$, filtration and evaporation of the solvent under reduced pressure and the purification of the residue by flash chromatography on silica gel (PE/EtOAc 9/1.5) afforded pure compound methyl 3-(2-methoxy-2-oxoethyl)-1*H*-indole-1-carboxylate **3** in 71% yield (Scheme 2).

Synthesis of Boc-protected iodoalkylamines 6
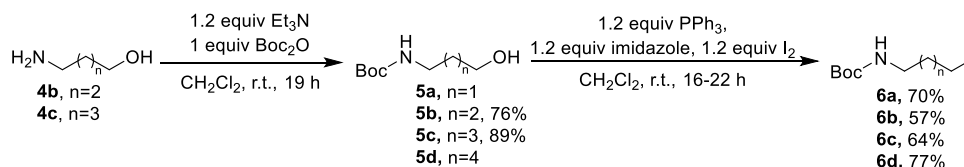
Scheme 3 Synthesis of *tert*-butyl (iodoalkyl)carbamates **6**

The Boc-protected alkanolamines **5** were prepared according to the modified procedure published by Ensch *et al.* (Ensch and Hesse 2002). Synthesis of 4-(Boc-amino)-1-butanol **5b** is representative. Reaction was performed under argon atmosphere. 4-Amino-1-butanol **4b** (707 mg, 7.94 mmol) was dissolved in CH$_3$CN (15 ml). To a resulting solution Et$_3$N (1.33 ml, 9.53 mmol) was added dropwise, followed by Boc$_2$O (1731 mg, 7.94 mmol) at 0 °C. The reaction mixture was stirred at room temperature for 19 h. Subsequently, reaction mixture was quenched with water (10 ml) and extracted with CH$_2$Cl$_2$ (3 × 20 ml). The combined organic extracts were washed with brine (2 × 10 ml). Drying with Na$_2$SO$_4$, filtration and evaporation of the solvent under reduced pressure and purification of the residue by flash chromatography on silica gel (PE/EtOAc 3/7) afforded pure compound **5c**. The Boc-

protected iodoalkylamines **6** were prepared according to the modified procedure published by Ensch *et al.* (Ensch and Hesse 2002). Synthesis of *tert*-butyl (4-iodobutyl)carbamate **6b** is representative. Reaction was performed in flame-dried glassware under argon atmosphere. To a solution of PPh$_3$ (1895 mg, 7.23 mmol) and imidazole (492 mg, 7.23 mmol) in dry CH$_2$Cl$_2$ (20 ml), I$_2$ (1837 mg, 7.23 mmol) was added at 0 °C. The reaction mixture was stirred at room temperature for 5 minutes. Subsequently, *tert*-butyl (4-hydroxybutyl)carbamate **5b** (1141 mg, 6.03 mmol), dissolved in dry CH$_2$Cl$_2$ (20 ml), was added at room temperature. The reaction mixture was stirred at room temperature for 18 h and then was filtered over Celite and the filter cake was washed with CH$_2$Cl$_2$ (3 × 5 ml). Resulting filtrate was quenched with saturated aqueous Na$_2$S$_2$O$_3$ solution (10 ml) and extracted with CH$_2$Cl$_2$ (2 × 20 ml). The combined organic extracts were washed with brine (2 × 10 ml). Drying with Na$_2$SO$_4$, filtration and evaporation of the solvent under reduced pressure and purification of the residue by flash chromatography on silica gel (PE/EtOAc 9/1) afforded pure compound **6b** (Scheme 3).

Synthesis of methyl 3-((*tert*-butoxycarbonyl)amino)-1-methoxy-1-oxoalkan-2-yl)-1*H*-indole-1-carboxylates 7
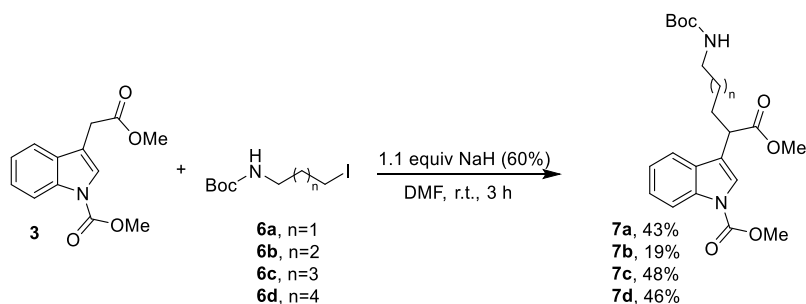
Scheme 4 Synthesis of methyl 3-((*tert*-butoxycarbonyl)amino)-1-methoxy-1-oxoalkan-2-yl)-1*H*-indole-1-carboxylates **7**

Synthesis of methyl 3-(8-((*tert*-butoxycarbonyl)amino)-1-methoxy-1-oxooctan-2-yl)-1*H*-indole-1-carboxylate **7d** is representative. To a solution of methyl 3-(2-methoxy-2-oxoethyl)-1*H*-indole-1-carboxylate **3** (200 mg, 0.81 mmol), dissolved in dry DMF (2.5 ml), solution of *tert*-butyl (6-iodohexyl)carbamate **6d** (317.62 mg, 0.97 mmol) in dry DMF (2.5 ml) was added. Then, NaH (60% in mineral oil) (35.59 mg, 0.89 mmol) was added at 0 °C and resulting reaction mixture was stirred at room temperature for 3 h. Subsequently, reaction mixture was cooled down to 0 °C, quenched with water (10 ml) and extracted with Et$_2$O (3 × 15 ml). The combined organic extracts were washed with brine (2 × 10 ml). Drying with Na$_2$SO$_4$, filtration and evaporation of the solvent under reduced pressure and

purification of the residue by flash chromatography on silica gel (PE/EtOAc 9/1.5) afforded pure compound **7d** in 46% yield (Scheme 4)**.**

Synthesis of methyl 3-(1-methoxy-(7-nitrobenzo[*c*][1,2,5]oxadiazol-4-yl)amino)-1-oxoalkan-2-yl)-1*H*-indole-1-carboxylates 9
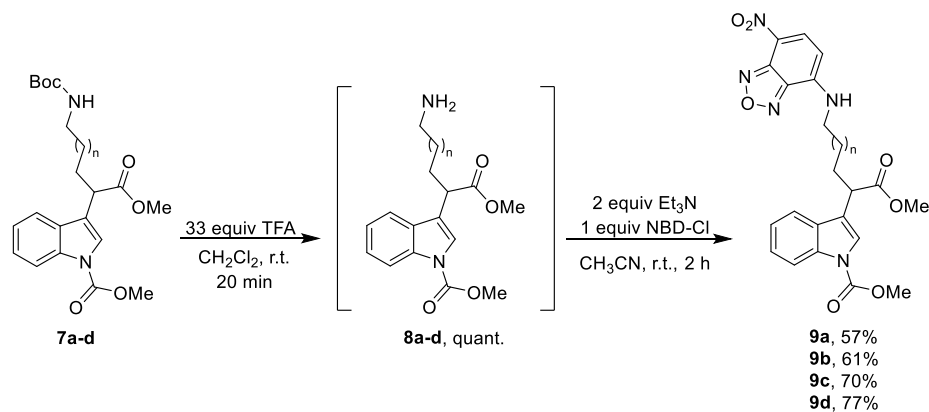
Scheme 5 Synthesis of 3-(1-methoxy-(7-nitrobenzo[*c*][1,2,5]oxadiazol-4-yl)amino)-1-oxoalkan-2-yl)-1*H*-indole-1-carboxylates **9**

Synthesis of methyl 3-(1-methoxy-8-((7-nitrobenzo[*c*][1,2,5]oxadiazol-4-yl)amino)-1-oxooctan-2-yl)-1*H*-indole-1-carboxylate **9d** is representative. Methyl 3-(8-((*tert*-butoxycarbonyl)amino)-1-methoxy-1-oxooctan-2-yl)-1*H*-indole-1-carboxylate **7d** (101 mg, 0.23 mmol) was dissolved in dry CH$_2$Cl$_2$ (4 ml) and TFA (0.52 ml) was added dropwise at 0 °C. Resulting reaction mixture was warmed up to room temperature and was stirred for 20 min. Subsequently, reaction mixture was cooled down to 0 °C, quenched by slow addition of aqueous saturated NaHCO$_3$ solution until pH = 7 and extracted with EtOAc (3 × 10 ml). The combined organic extracts were washed with brine (2 × 5 ml). Drying with Na$_2$SO$_4$, filtration and evaporation of the solvent under reduced pressure afforded crude methyl 3-(8-amino-1-methoxy-1-oxooctan-2-yl)-1*H*-indole-1-carboxylate **8d**, which was used as such without further purification. Crude methyl 3-(8-amino-1-methoxy-1-oxooctan-2-yl)-1*H*-indole-1-carboxylate **8d** (78 mg, 0.23 mmol) was dissolved in CH$_3$CN (5 ml) and cooled down to 0 °C. To the resulting solution Et$_3$N (0.06 ml, 0.45 mmol) was added dropwise, followed by addition of NBD-Cl in small portions (45 mg, 0.23 mmol). The reaction mixture was stirred at room temperature for 2 h under argon. Subsequently, reaction mixture was cooled down to 0 °C, quenched with saturated NH$_4$Cl solution (10 ml) and extracted with EtOAc (3 × 20 ml). The combined organic extracts were washed with brine (2 × 10 ml). Drying with Na$_2$SO$_4$, filtration, evaporation of the solvent under reduced pressure and purification of the residue by flash chromatography on silica gel (CH$_2$Cl$_2$/Ac 50/1) afforded

pure methyl 3-(1-methoxy-8-((7-nitrobenzo[*c*][1,2,5]oxadiazol-4-yl)amino)-1-oxooctan-2-yl)-1*H*-indole-1-carboxylate **9d** in 77 % yield (Scheme 5).

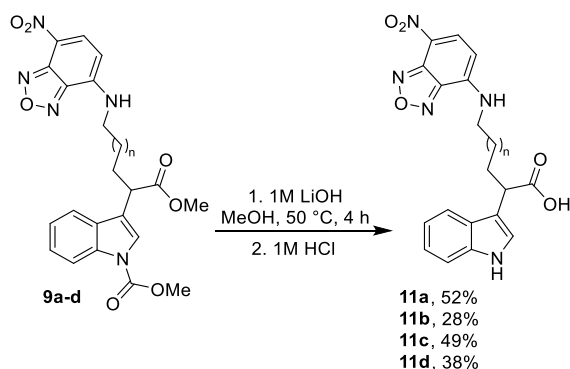## Synthesis of 2-(1*H*-indol-3-yl)-(7-nitrobenzo[*c*][1,2,5]oxadiazol-4-yl)amino)alkanoic acids 11

METHOD A
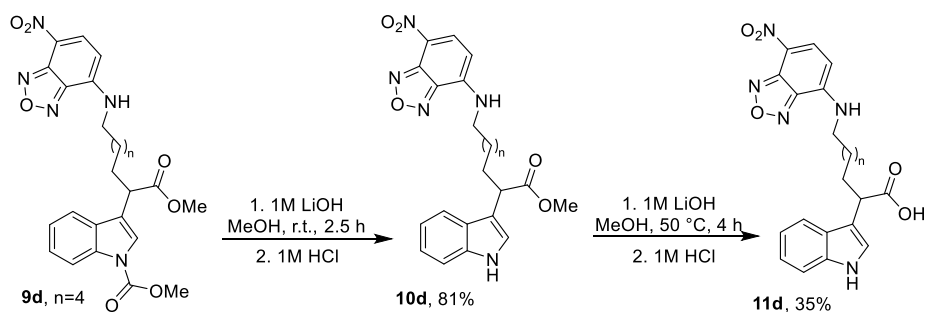
Scheme 6 Synthesis of 2-(1*H*-Indol-3-yl)-8-((7-nitrobenzo[*c*][1,2,5]oxadiazol-4-yl)amino)octanoic acid **11d**

Synthesis of 2-(1*H*-indol-3-yl)-8-((7-nitrobenzo[*c*][1,2,5]oxadiazol-4-yl)amino)octanoic acid **11d**. Methyl 3-(1-methoxy-8-((7-nitrobenzo[*c*][1,2,5]oxadiazol-4-yl)amino)-1-oxooctan-2-yl)-1*H*-indole-1-carboxylate **9d** (46 mg, 0.09 mmol) was dissolved in MeOH (4 ml) and 1 M LiOH solution (0.9 ml) was added at 0 °C. The reaction mixture was stirred at room temperature for 2.5 h. Subsequently, the reaction mixture was cooled down to 0 °C, acidified with 1 M HCl solution to pH = 6 and extracted with EtOAc (3 × 10 ml). The combined organic extracts were washed with brine (2 × 5 ml). Drying with Na_2SO_4, filtration and evaporation of the solvent under reduced pressure and the purification of the residue by flash chromatography on silica gel (CH_2Cl_2/Ac 50/1), afforded pure compound methyl 2-(1*H*-indol-3-yl)-8-((7-nitrobenzo[*c*][1,2,5]oxadiazol-4-yl)amino)octanoate **10d** in 81% yield, which was used in the further step. Compound **10d** (27 mg, 0.06 mmol) was dissolved in MeOH (2 ml) and 1 M LiOH solution (612 µl) was added at 0 °C. The reaction mixture was warmed up to 50 °C and stirred for 4 h. Subsequently, the reaction mixture was cooled down to 0 °C, acidified with 1 M $KHSO_4$ solution to pH = 6 and extracted with EtOAc (3 × 10 ml). The combined organic extracts were washed with brine (2 × 5 ml). Drying with Na_2SO_4, filtration and evaporation of the solvent under reduced pressure and the purification of the residue by flash chromatography on silica gel (CH_2Cl_2/Ac 50/1), afforded pure compound 2-(1*H*-indol-3-yl)-8-((7-nitrobenzo[*c*][1,2,5]oxadiazol-4-yl)amino)octanoic acid **11d** in 35% yield (Scheme 6).

METHOD B

Scheme 7 Synthesis of 2-(1*H*-Indol-3-yl)-(7-nitrobenzo[c][1,2,5]oxadiazol-4-yl)amino)alkanoic acids **11**

Synthesis of 2-(1*H*-indol-3-yl)-7-((7-nitrobenzo[c][1,2,5]oxadiazol-4-yl)amino)heptanoic acid **11c** is representative. Methyl 3-(1-methoxy-7-((7-nitrobenzo[*c*][1,2,5]oxadiazol-4-yl)amino)-1-oxoheptan-2-yl)-1*H*-indole-1-carboxylate **9c** (53 mg, 0.11 mmol) was dissolved in MeOH (4.5 ml) and 1 M LiOH solution (1 ml) was added at 0 °C. The reaction mixture was warmed up to 50 °C and stirred for 4 h. Subsequently, the reaction mixture was cooled down to 0 °C, acidified with 1 M $KHSO_4$ solution to pH = 6 and extracted with EtOAc (3 × 10 ml). The combined organic extracts were washed with brine (2 × 5 ml). Drying with Na_2SO_4, filtration and evaporation of the solvent under reduced pressure and the purification of the residue by flash chromatography on silica gel (CH_2Cl_2/Ac 50/1), afforded pure compound 2-(1*H*-indol-3-yl)-7-((7-nitrobenzo[*c*][1,2,5]oxadiazol-4-yl)amino)heptanoic acid **11c** in 49% yield (Scheme 7).

3.2 Biology

3.2.1. Materials

3.2.1.1. Chemicals, solvents and solutions

Murashige and Skoog medium, agar, X-Gluc (Duchefa Biochemistry B.V.), sucrose (Lach–Ner s.r.o.), Luciferase Assay Reagent II (LAR II), Stop & Glo® (S&G) Reagent, Cell Culture Lysis reagent (Promega), KOH, NAA, Driselase, BSA, Triton-X-100, NP40, BFA, paraformaldehyde (Sigma-Aldrich), EDTA, $NaH_2PO_4 \cdot H_2O$, $Na_2HPO_4 \cdot 7 H_2O$ (Merck), $K_4[Fe(CN)_6]$, $K_3[Fe(CN)_6]$ (Neolab).

½ Murashige & Skoog medium: in a one litter glass beaker with a small volume of distilled water 2.2 g of MS medium, 10 g of sucrose and 7 g of plant agar were thoroughly dissolved. The pH of the medium was adjusted to 5.6 with KOH and distilled water was added to the volume of 1 l.

Sodium phosphate buffer (PBS): 2.76 g of $NaH_2PO_4 \cdot H_2O$ were dissolved in 100 ml of distilled water to give a 0.2 M stock solution. Likewise, 5.36 g of $Na_2HPO_4 \cdot 7 H_2O$ was dissolved in 100 ml of distilled water to give a 0.2 M stock solution. Subsequently, 39 ml of $NaH_2PO_4 \cdot H_2O$ stock solution were mixed with 61 mL of $Na_2HPO_4 \cdot 7 H_2O$ to prepare PBS at pH 7.0. This volume was filled with distilled water to a total volume of 200 ml.

GUS buffer: 10 mg of X-Gluc was dissolved in 275 μl of DMSO. To the mixture 100 μl of 10% Triton X-100 stock solution and 200 μl of 0.5 M EDTA solution were added. To the solution 125 μl of 40 mM $K_4[Fe(CN)_6]$ and $K_3[Fe(CN)_6]$ stock solutions were added and the volume was filled to 10 ml with PBS buffer (i.e., 9.175 ml).

Solution for seeds sterilization: 37 ml of 95% EtOH were diluted with distilled water to the volume of 50 ml to which 50 μl of Tween 20 (0.1% Tween-20) was added.

80% acetone: 200 ml of acetone were mixed with 50 ml of distilled water.

Solutions for imunoanalysis with Intavis InsituPro VSi robot (for 10 samples):

PBS (1 × diluted in water)

Solution A: PBS + Triton (45 ml : 45 μl)

Solution B: H_2O + Triton (45 ml : 45 μl)

Solution C: H_2O (10 ml)

Solution E: PBS + 2% Drisilase (2 ml + 0.04 g)

Solution F: PBS + 10% DMSO + 3% NP40% (4 ml + 400 μl + 120 μl)

Solution G: PBS + 2% BSA (15 ml + 0.3 g)

Dilution of antibodies:

Primary antibodies: rabbit anti-PIN1 (Paciorek, Zazimalova *et al.* 2005), rabbit anti-PIN2 (Abas, Benjamins *et al.* 2006) - 1:1000 in **solution G** (PBS + 2% BSA).

Secondary antibody: anti-rabbit-Cy3 (Sigma-Aldrich) - 1:600 in **solution G** (PBS + 2% BSA).

3.2.1.2. Biological material

Arabidopsis thaliana (ecotype Columbia, Col-0) seeds.

Arabidopsis thaliana transgenic pDR5::GUS seeds (Ulmasov, Murfett *et al.* 1997).

Arabidopsis thaliana transgenic pDR5$_{rev}$::RFP seeds (Marin, Jouannet *et al.* 2010).

Arabidopsis thaliana transgenic pDR5::LUC seeds (Moreno-Risueno, Van Norman *et al.* 2010).

Arabidopsis thaliana transgenic PIN2::PIN2-mCherry seeds (Salanenka, Verstraeten *et al.* 2018).

3.2.2. Methods

3.2.2.1. General methods

Substances were dissolved in DMSO to obtain stock solutions.

Prior to use, all seeds were sterilized with 70% EtOH with 0.1% Tween-20 solution (1 ml) for 10 minutes (2×) and rinsed with 96% EtOH (1 ml) for 5 minutes.

Planting was done in a laminar flow hood under sterile conditions to reduce the risk of contamination. Seeds were kept for 2 days in the fridge (4 °C) for stratification and then were grown in a growth chamber at 22 °C with a photoperiod of 16 hours light, 8 hours dark in a vertical position for indicated time.

3.2.2.2. Root growth assay – long-term test

Arabidopsis thaliana wild-type Col-0 seedlings were germinated on sterile ½ MS medium supplemented with 0.3% DMSO as a mock, IAA as a positive control, and fluorescently labelled auxins **I-VIII** at final concentrations of 1, 5, 10 and 20 μM with or without presence of 1 μM IAA. Seeds were kept for 2 days in the fridge for stratification and then were grown in a growth chamber at 22 °C with a photoperiod of 16 hours light, 8 hours dark in a vertical position for 5 days.

3.2.2.3. Rapid root growth assay

Five-day old (5 DAG) seedlings of the *Arabidopsis thaliana* wild-type Col-0 were transfered to plates containing sterile ½ MS supplemented with 0.5% DMSO as a blank control, 500 nM IAA as a positive control or fluorescently labelled auxins **IV** and **VIII** at final concentrations of 1, 5, 10, 20 and 50 μM. Immediately, treated plates were placed on a scanner (Epson, model: V370 Photo). Samples were automatically scanned in the 8-bit grayscale and at 800 dpi every 10 min using the AutoIt program for 12 h.

3.2.2.4. The effect of compounds on lateral root formation in *Arabidopsis thaliana*

Five-day-old (5 DAG) seedlings of *Arabidopsis thaliana* (Col-0), germinated on sterile ½ MS medium, were transfered to plates containing sterile ½ MS medium supplemented with fluorescently labelled auxins **IV** and **VIII** at final concentrations of 10 and 20 µM, in the absence or presence of 100 nM IAA for 5 days. 0.3% DMSO was used as a blank control. Lateral roots were counted using ImageJ software and lateral root density was calculated.

3.2.2.5. The effect of compounds in apical hook development

Arabidopsis thaliana wild-type Col-0 seedlings were grown in plates containing sterile ½ MS medium supplemented with 0.2% DMSO as a blank control, 1 µM IAA as a positive control or fluorescently labelled auxins **IV** and **VIII** at final concentration of 20 µM. Seeds were kept for 2 days in the fridge (4 °C) for stratification, followed by 5 h in the light in a growth chambre, in a vertical position. Subsequently, seedling development was recorded at 1-hour intervals for 7 days with an infrared light source (940 nm LED; Velleman) by a spectrum-enhanced camera (Canon Rebel T2i, 550DH, EF-S 18-55 mm, IS lens kit with built-in clear filter wideband-multicoated and standard Canon accessories) and operated by the EOS utility software. Angles between the hypocotyl axes and cotyledons were measured by ImageJ software. Fifteen seedlings per one replicate with synchronized germination start were processed (Zadnikova, Petrasek *et al.* 2010).

3.2.2.6. The effect of compounds on auxin distribution in the DR5::GUS transgenic plants of *Arabidopsis thaliana*

Five-day-old (5 DAG) seedlings of the *Arabidopsis thaliana* transgenic DR5::GUS reporter line on a Col-0 background were incubated in 24-well plates containing 1 ml of ½ MS liquid media supplemented by fluorescently labelled auxins **I-VIII** at final concentrations of 5, 10, 15, 20, 25 and 50 µM. The compounds were applied for either 5 hours on their own or for 2 h on their own followed by wash-out with distilled water (10 min) and treatment with 2 µM IAA for further 3 h. Seedlings were then incubated in the presence of 500 µL of GUS staining solution (2 mM X-Gluc in GUS buffer) at 37 °C in the dark for 20 min. To stop the staining reaction, seedlings were transferred to 500 µL of 70% EtOH. Finally, GUS expression was evaluated using an inverted light microscope (Olympus IX51) with transmission light mode and phase contrast.

3.2.2.7. The effect of compounds on asymmetric auxin distribution in gravistimulated roots of transgenic plant line DR5rev::RFP

Four-day-old (4 DAG) *Arabidopsis thaliana* seedlings of transgenic plant line DR5rev::RFP were transferred to chamber slides containing sterile ½ MS medium supplemented with 0.5% DMSO as a blank control, 500 nM IAA as a positive control or fluorescently labelled auxins **IV** and **VIII** at final concentrations of 10, 20 and 50 μM. Chamber slides were left in a vertical position for 30 min, which were then rotated by 90° and kept in such position for additional 4 h. Plants were subsequently visualized by confocal microscope (ZEISSLSM 800). Experimental set up involved 20× objective. Image analysis was done on maximal intensity projection of the z-stacks of the root tip. The ratio of signal intensity in epidermis of upper/lower half of the root was calculated.

3.2.2.8. The effect of compounds on auxin signalling in the DR5::LUC transgenic plants of *Arabidopsis thaliana*

Five-day-old (5 DAG) *Arabidopsis thaliana* seedlings of transgenic plant line DR5::LUC, germinated on sterile ½ MS medium (20 seedlings per treatment), were transfered to plates containing sterile ½ MS supplemented with 0.3% DMSO as a blank control, 100 nM IAA as positive control or fluorescently labelled auxins **IV** and **VIII** at final concentration of 20 μM for 1 or 3 h. Afterwards, shoots were cut and roots were collected into a 2 ml eppendorf tubes (with 2 iron beads inside) and were immediately frozen in liquid nitrogen. Samples were ground with Retsch mill and then 700 µl of Cell Culture Lysis reagent (CCLR, $5 \times$ diluted in water) was added. Then samples were mixed, centrifugated and left for 2 min on ice. Subsequently, 100 µl of lysate were transferred on the optical plate and measured with luminometer (plattenphotometr BIOTEK, synergy H1 hybrid reader) using LAR II and S&G solution.

3.2.2.9. The effect of compounds on the subcellular localization of PIN1

Four-day-old (4 DAG) seedlings of the *Arabidopsis thaliana* wild-type Col-0 were incubated in 24-well plates containing 1 ml of ½ MS liquid media supplemented by fluorescently labelled auxins **IV** and **VIII** at final concentrations of 20 and 50 μM in the presence or absence of 10 μM NAA for 4 h. Then, fixation of samples was done with paraformaldehyde for 30 min in vacuum. An Intavis InsituPro VSi robot was used for immunostaining

according to a published protocol (Sauer, Paciorek *et al.* 2006). For digestion/permeabilization 2% driselase in PBS was used. Solution of 3% NP40 and 10% DMSO in PBS was used for better penetration of antibodies into cells. Blocking was done with 2% BSA in PBS. For analysis of PIN1 primary antibody anti-PIN1 at a dilution of 1:1000 and secondary antibody anti-Cy3 (rabbit) at a dilution of 1:600 were used. Subsequently, slides were prepared with Michifluor for stabilization of samples. Visualization was done by confocal microscope (ZEISS LSM 800). Experimental set up involved 40× objective. Image analysis was done by Image J software. Signal intensity from basal and lateral sides of the individual cells of the root in endodermis were measured and the ratio of the intensity in lateral/basal side was calculated.

3.2.2.10. The effect of compounds on the BFA body formation of PIN2

METHOD A

Five-day-old (5 DAG) *Arabidopsis thaliana* seedlings of transgenic plant line PIN2::PIN2-mCherry were incubated in 24-well plates containing 1 ml of ½ MS liquid media supplemented by fluorescently labelled auxins **IV** and **VIII** at final concentration of 50 μM or 10 μM NAA for 30 min. Then, 50 μM BFA was added to media and seedlings were incubated for additional 1 h. Plants were immediately visualized by confocal microscope (ZEISS LSM 800). Experimental set up involved 40× objective.

METHOD B

Four-day-old (4 DAG) seedlings of the *Arabidopsis thaliana* wild-type Col-0 were incubated in 24-well plates containing 1 ml of ½ MS liquid media supplemented by fluorescently labelled auxins **IV** and **VIII** at final concentration of 50 μM or 10 μM NAA for 30 min. Then, 50 μM BFA was added to the media and seedlings were incubated for additional 1 h, while control seedlings were left without BFA treatment for 1 h. Subsequently, fixation of samples was done with paraformaldehyde for 30 min in vacuum. An Intavis InsituPro VSi robot was used for immunostaining according to a published protocol (Sauer, Paciorek *et al.* 2006). For digestion/permeabilization 2% driselase in PBS was used. Solution of 3% NP40 and 10% DMSO in PBS was used for better penetration of antibodies into cells. Blocking was done with 2% BSA in PBS. For analysis of PIN2 primary antibody anti-PIN2 at a dilution of 1:1000 and secondary antibody anti-Cy3 (rabbit) at a dilution of 1:600 were used. Subsequently, slides were prepared with Michifluor for stabilization of samples.

Visualization was done by confocal microscope (ZEISS LSM 800). Experimental set up involved 40× objective.

3.2.2.11. Uptake of fluorescently labelled IAA derivatives in *Arabidopsis thaliana* wild-type Col-0 roots

Five-day-old (5 DAG) seedlings of *Arabidopsis thaliana* wild-type Col-0 were incubated in 24-well plates containing 1 ml of ½ MS liquid media supplemented with 1% sucrose and were treated with fluorescently labelled auxins **I-VIII** at final concentration of 10 µM for 10 or 25 min. Plants were subsequently visualized by confocal microscope (ZEISS LSM 800). Experimental set up involved 10× objective.

4. Results

4.1. Organic synthesis

In order to ensure selective alkylation of indole-3-acetic acid **1** at its *α*-position, first of all, carboxylic acid group and NH moiety of IAA molecule were protected as methyl esters. The carboxylic acid group of commercially available indole-3-acetic acid **1** was esterified in accordance with the procedure published by Hayashi *et al.* (Hayashi, Neve *et al.* 2012). That is, IAA **1** was treated with acetyl chloride in methanol at room temperature for 2 h, which quantitatively resulted in IAA methyl ester **2**. Then, the corresponding ester **2** was treated with tetrabutylammonium bromide and methylchloroformate in the 1:1 dichloromethane and sodium hydroxide (30% aq) mixture at 0 °C for 2.5 h, which resulted in methyl 3-(2-methoxy-2-oxoethyl)-1*H*-indole-1-carboxylate **3** in 71% yield (Scheme 2).
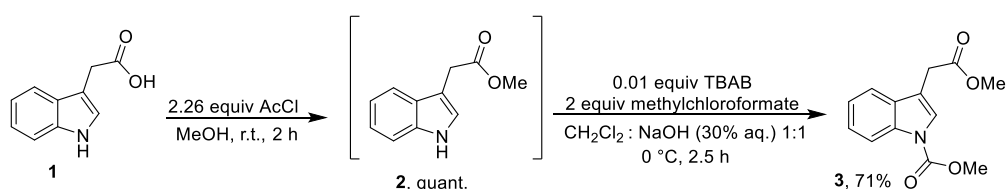

Scheme 2 Synthesis of methyl 3-(2-methoxy-2-oxoethyl)-1*H*-indole-1-carboxylate **3**

The *tert*-butyl (iodoalkyl)carbamates **6** were prepared from aliphatic amino alcohols *via* Boc-protection of amino group, followed by iodination of OH group with slight changes to the procedure published by Ensch *et al.* (Ensch and Hesse 2002). In short, in the first step amino alcohols **4b** and **4c** were treated with triethylamine and di-*tert*-butyl dicarbonate in dichloromethane at room temperature overnight and **5b** and **5c** were obtained in 76% and 89% yield, respectively. In the second step, previously prepared or commertially available (Boc-amino)alcohols **5a-d** were treated with 1.2 equiv triphenylphosphine, 1.2 equiv imidazole and 1.2 equiv iodine in dichloromethane at room temperature overnight. This led to the formation of *tert*-butyl (iodoalkyl)carbamates **6a-d** in 57-77% yield (Scheme 3).
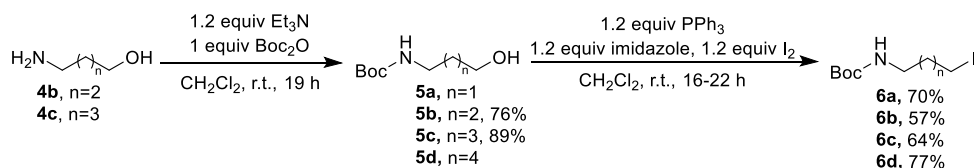
Scheme 3 Synthesis of *tert*-butyl (iodoalkyl)carbamates **6**

Subsequently, α-alkylation of IAA dimethyl ester **3** was investigated (Scheme 4, Table 1). Firstly, synthesis was tried adopting reaction conditions from Chen *et al.* (Chen, Kassenbrock *et al.* 2013). Namely, IAA dimethyl ester **3** was treated with NaH in DMF at 0 °C for 30 minutes. Then, linker **6c** was added at room temperature and the resulting mixture was stirred for 3 h, which resulted in no reaction. As the first attempt was unsuccessful, alternatively, IAA dimethyl ester **3** was treated with NaH and linker in DMF at 0°C simultaneously and the mixture was stirred at room temperature for 2-3 h resulting in **7a-d** in 43%, 19%, 48% and 46% yield, respectively.
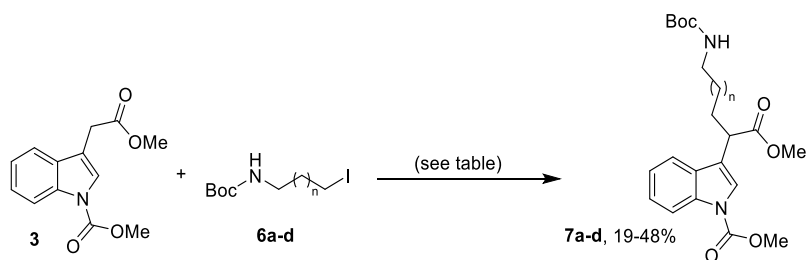

Scheme 4 Synthesis of methyl 3-((*tert*-butoxycarbonyl)amino)-1-methoxy-1-oxoalkan-2-yl)-1*H*-indole-1-carboxylates **7**

Table 1 Reaction conditions for the synthesis of **7a-d**

Entry	Reaction conditions	Result
1	1.5 equiv NaH, DMF, r.t., 0.5 h, then 1 equiv **6c**, DMF, r.t., 2.5 h	-[a]
2	1.1 equiv NaH, 1.2 equiv **6a**, DMF, r.t., 3 h	**7a**, 43%
3	1.1 equiv NaH, 1.2 equiv **6b**, DMF, r.t., 3 h	**7b**, 19%
4	1 equiv NaH, 1 equiv **6c**, DMF, r.t., 2 h	**7c**, 47%
5	1.25 equiv NaH, 1.2 equiv **6c**, DMF, r.t., 2 h	**7c**, 48%
6	1.1 equiv NaH, 1.2 equiv **6d**, DMF, r.t., 3 h	**7d**, 46%

[a] No reaction

Fluorescent labelling with 4-chloro-7-nitrobenzofurazan was performed adopting procedure published by Bieleszova *et al.* (Bieleszova, Parizkova *et al.* 2019) (Scheme 5). First of all, previously prepared linker-tagged IAA double methyl ester derivatives **7a-d** were treated with trifluoroacetic acid in dry dichloromethane at room temperature for 20 min affording free amines **8a-d**. Obtained intermediates **8a-d** were immediately treated with triethylamine and 4-chloro-7-nitrobenzofurazan in acetonitrile at room temperature for 2 h. This led to the formation of fluorescently labelled IAA methyl esters **9a-d** in 19-45% overall yield.
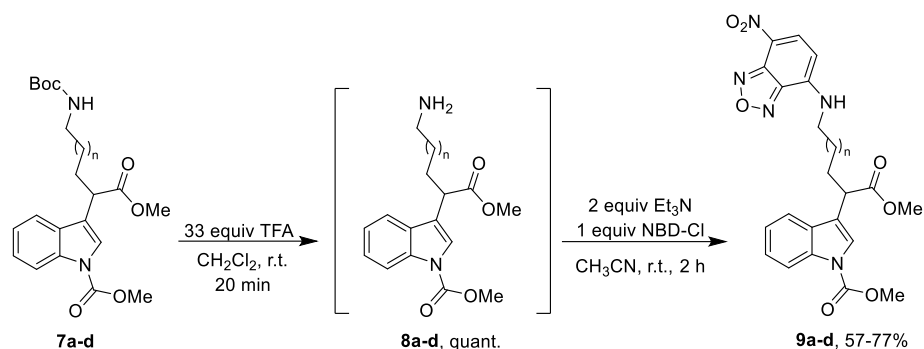
Scheme 5 Synthesis of 3-(1-methoxy-(7-nitrobenzo[*c*][1,2,5]oxadiazol-4-yl)amino)-1-oxoalkan-2-yl)-1*H*-indole-1-carboxylates **9**

Finally, the hydrolysis of labelled IAA methyl esters **9a-d** was attempted by simple alkaline hydrolysis. Interestingly, if the reaction was performed at room temperature, an intermediate methyl ester **10d** was isolated in 81% yield. Only upon raising reaction tenperature to 50 °C led to the formation of final product **11d** in 35% yield (Scheme 6).
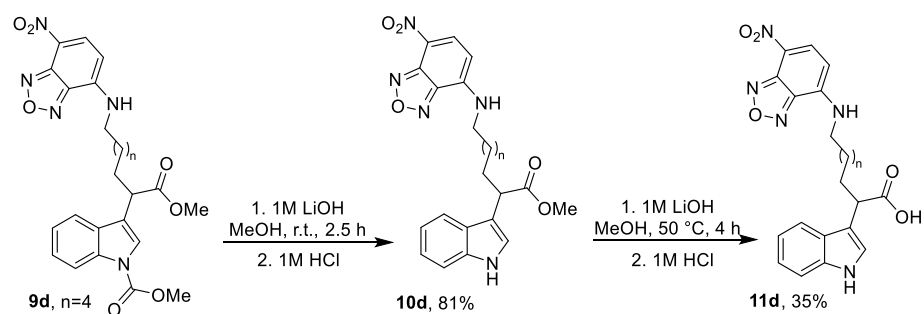
Scheme 6 Synthesis of 2-(1*H*-Indol-3-yl)-8-((7-nitrobenzo[*c*][1,2,5]oxadiazol-4-yl)amino)octanoic acid **11d**

Thus, the direct hydrolysis of labelled IAA methyl esters **9a-d** was performed similarly to the procedure published by Bieleszova *et al.* (Bieleszova, Parizkova *et al.* 2019). Methyl esters **9a-d** were dissolved in methanol, treated with 1 M lithium hydroxide solution and stirred at 50 °C for 4 h. Subsequent acidification with 1 M potassium hydrogen sulfate solution led to the formation of final products **11a-d** in 28-52% yield (Scheme 7).
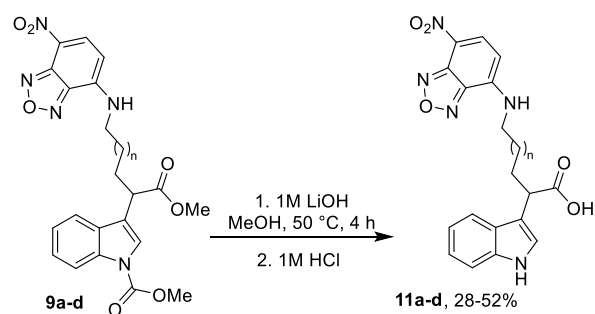
Scheme 7 Synthesis of 2-(1*H*-Indol-3-yl)-(7-nitrobenzo[*c*][1,2,5]oxadiazol-4-yl)amino)alkanoic acids **11**
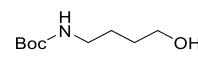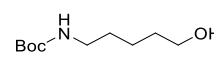
4.2. Synthesized compounds

4-(Boc-amino)-1-butanol 5b

Previously described in bachelor thesis (Bieleszova 2017). Obtained spectroscopic data matches published data. Yellow oil, yield 76%, $R_f = 0.45$ (PE/EtOAc 3/7).

5-(Boc-amino)-1-pentanol 5c

Previously described in bachelor thesis (Bieleszova 2017). Obtained spectroscopic data matches published data. Yellow oil, yield 89%, $R_f = 0.40$ (PE/EtOAc 3/7).

tert-Butyl (3-iodopropyl)carbamate 6a

Previously described in bachelor thesis (Bieleszova 2017). Obtained spectroscopic data matches published data. Yellow oil, yield 70%, $R_f = 0.58$ (PE/EtOAc 9/1).

tert-Butyl (4-iodobutyl)carbamate 6b

Previously described in bachelor thesis (Bieleszova 2017). Obtained spectroscopic data matches published data. Yellow oil, yield 57%, $R_f = 0.41$ (PE/EtOAc 9/1).

tert-Butyl (5-iodopentyl)carbamate 6c

Previously described in bachelor thesis (Bieleszova 2017). Obtained spectroscopic data matches published data. Colourless oil, yield 64%, $R_f = 0.89$ (PE/EtOAc 3/7).
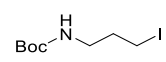
tert-Butyl (6-iodohexyl)carbamate 6d

Previously described in bachelor thesis (Bieleszova 2017). Obtained spectroscopic data matches published data. Colourless oil, yield 77%, $R_f = 0.90$ (PE/EtOAc 3/7).
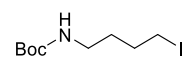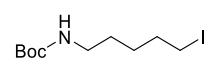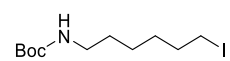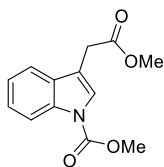
**Methyl 3-(2-methoxy-2-oxoethyl)-1*H*-indole-1-carboxylate 3**

Previously described by Hayashi *et al.* (Hayashi, Neve *et al.* 2012). Obtained spectroscopic data matches published data. White crystals, yield 71%, R$_f$ = 0.52 (PE/EtOAc 4/2). ^{1}H NMR (500 MHz, CDCl$_3$): δ 3.71 (5H, d, *J* = 2.8 Hz, CH$_2$, OCH$_3$), 4.02 (3H, s, OCH$_3$), 7.25-7.28 (1H, m, CH), 7.35 (1H, t, *J* = 7.2 Hz, CH), 7.53 (1H, d, *J* = 7.6 Hz, CH), 7.59 (1H, s, CH), 7.97-8.38 (1H, s, CH). ^{13}C NMR (126 MHz, CDCl$_3$): δ 31.0 (CH$_2$), 52.2 (OCH$_3$), 53.9 (OCH$_3$), 114.1 (C), 115.6 (CH), 119.3 (CH), 123.2 (CH), 124.1 (CH), 125.1 (CH), 130.2 (C), 135.5 (C), 151.6 (C=O), 171.5 (C=O). MS (ES, pos. mode): *m/z* (%): 248.10 (M + H$^+$, 100), purity: 100%.

Methyl 3-(5-((*tert*-butoxycarbonyl)amino)-1-methoxy-1-oxopentan-2-yl)-1*H*-indole-1-carboxylate 7a
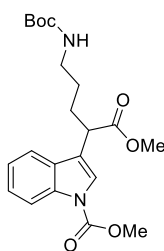
Colourless oil, yield 43.5%, R$_f$ = 0.23 (PE/EtOAc 4/1). ^{1}H NMR (500 MHz, CDCl$_3$): δ 1.41 (9H, s, (CH$_3$)$_3$), 1.48-1.54 (2H, m, CH$_2$), 1.88-1.97 and 2.10-2.17 (2H, m, CH$_2$), 3.00-3.20 (2H, m, CH$_2$), 3.66 (3H, s, OCH$_3$), 3.82 (1H, t, *J* = 7.5 Hz, CH), 4.01 (3H, s, OCH$_3$) 4.40-4.63 (1H, br s, NH), 7.23-7.27 (1H, m, CH), 7.33 (1H, t, *J* = 7.8 Hz, CH), 7.55 (1H, s, CH), 7.60 (1H, d, *J* = 7.9, CH), 8.16 (1H, s, CH). ^{13}C NMR (126 MHz, CDCl$_3$): δ 28.2 (CH$_2$), 28.5 ((CH$_3$)$_3$), 29.4 (CH$_2$), 40.2 (CH$_2$), 42.4 (CH), 52.1 (OCH$_3$), 53.9 (OCH$_3$), 79.3 (C), 115.1 (C), 115.4 (CH), 119.1 (CH), 119.4 (CH), 123.2 (CH), 124.9 (CH), 129.2 (C), 135.6 (C), 151.4 (C=O), 156.0 (C=O), 173.9 (C=O). MS (ES, pos. mode): *m/z* (%): 305.19 (M + H$^+$ - Boc, 100), purity: 100%.

Methyl 3-(6-((*tert*-butoxycarbonyl)amino)-1-methoxy-1-oxohexan-2-yl)-1*H*-indole-1-carboxylate 7b
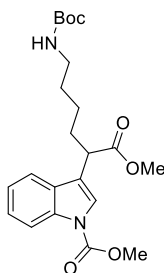
Colourless oil, yield 19%, R$_f$ = 0.30 (PE/EtOAc 4/1). ^{1}H NMR (500 MHz, CDCl$_3$): δ 1.32-1.40 (11H, m, CH$_2$, (CH$_3$)$_3$), 1.47-1.55 (2H, m, CH$_2$), 1.88-1.95 and 2.10-2.16 (2H, m, CH$_2$), 3.02-3.13 (2H, m, CH$_2$), 3.67 (3H, s, OCH$_3$), 3.79 (1H, t, *J* = 7.6 Hz, CH), 4.02 (3H, s, OCH$_3$) 4.40-4.56 (1H, br s, NH), 7.24-7.27 (1H, m, CH), 7.32-7.35 (1H, m, CH), 7.55 (1H, s, CH), 7.60 (1H, d, *J* = 7.6, CH), 8.17 (1H, s, CH). ^{13}C NMR (126 MHz, CDCl$_3$): δ 25.0 (CH$_2$), 28.6 ((CH$_3$)$_3$), 29.9 (CH$_2$), 31.9 (CH$_2$), 40.4 (CH$_2$), 42.6 (CH), 52.1 (OCH$_3$), 53.9 (OCH$_3$), 79.1 (C), 115.1 (C),115.4 (CH) 119.3 (CH), 119.4 (CH), 122.9 (CH), 124.9 (CH),

129.5 (C), 135.6 (C), 151.4 (C=O), 156.0 (C=O), 174.1 (C=O). MS (ES, pos. mode): m/z (%):319.26 (M + H$^+$ - Boc, 100), purity: 91%.

Methyl 3-(7-((*tert*-butoxycarbonyl)amino)-1-methoxy-1-oxoheptan-2-yl)-1*H*-indole-1-carboxylate 7c
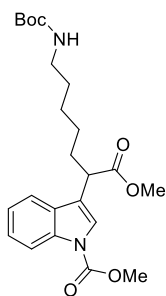
Colourless oil, METHOD A yield 47%, METHOD C yield 48%, R$_f$ = 0.20 (PE/EtOAc 4/1). ^{1}H NMR (500 MHz, CDCl$_3$): δ 1.29-1.35 (4H, m, 2 × CH$_2$), 1.42-1.45 (11H, m, CH$_2$, (CH$_3$)$_3$), 1.87-1.91 and 2.09-2.15 (2H, m, CH$_2$), 3.06 (2H, t, J = 7.0 Hz, CH$_2$), 3.66 (3H, s, OCH$_3$), 3.78 (1H, t, J = 7.6 Hz, CH), 4.01 (3H, s, OCH$_3$) 4.31-4.68 (1H, br s, NH), 7.22-7.27 (1H, m, CH), 7.32 (1H, t, J = 7.8 Hz, CH), 7.54 (1H, s, CH), 7.59 (1H, d, J = 7.9, CH), 8.16 (1H, s, CH). ^{13}C NMR (126 MHz, CDCl$_3$): δ 26.6 (CH$_2$), 27.4 (CH$_2$), 28.5 ((CH$_3$)$_3$), 29.9 (CH$_2$), 32.2 (CH$_2$), 40.6 (CH$_2$), 42.6 (CH), 52.2 (OCH$_3$), 53.8 (OCH$_3$), 79.2 (C), 114.6 (C), 115.4 (CH), 119.4 (CH), 122.8 (CH), 123.1 (CH), 124.9 (CH), 129.5 (C), 135.6 (C), 151.2 (C=O), 156.1 (C=O), 174.2 (C=O). MS (ES, pos. mode): m/z (%): 333.26 (M + H$^+$ - Boc, 100), purity: 97%.

Methyl 3-(8-((*tert*-butoxycarbonyl)amino)-1-methoxy-1-oxooctan-2-yl)-1*H*-indole-1-carboxylate 7d
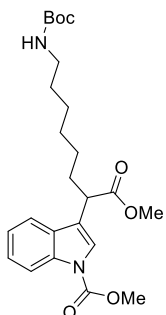
Previously described by Hayashi *et al.* (Hayashi, Neve *et al.* 2012). Obtained spectroscopic data matches published data. Colourless oil, METHOD B yield 46%, R$_f$ =0.19 (PE/EtOAc 4/1). MS (ES, pos. mode): m/z (%): 347.26 (M + H$^+$ - Boc, 100), purity: 100%.

Methyl 3-(1-methoxy-5-((7-nitrobenzo[*c*][1,2,5]oxadiazol-4-yl)amino)-1-oxopentan-2-yl)-1*H*-indole-1-carboxylate 9a
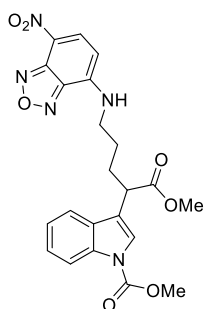
Red oil, yield 57%, R$_f$ = 0.56 (PE/EtOAc 1/1). ^{1}H NMR (500 MHz, CDCl$_3$): δ 1.78-1.91 (2H, m, CH$_2$), 2.05-2.14 and 2.23-2.38 (2H, m, CH$_2$), 3.49-3.53 (2H, m, CH$_2$), 3.68 (3H, s, OCH$_3$), 3.87 (1H, t, J = 7.5 Hz, CH), 4.01 (3H, s, OCH$_3$) 6.05 (1H, d, J = 8.6 Hz, CH), 6.48-6.62 (1H, br s, NH), 7.21 (1H, t, J = 7.6 Hz, CH), 7.31 (1H, t, J = 7.8 Hz, CH), 7.52-7.59 (2H, m, 2 × CH), 8.11 (1H, s, CH), 8.38 (1H, d, J = 8.6 Hz, CH). ^{13}C NMR (126

MHz, CDCl$_3$): δ 26.4 (CH$_2$), 29.2 (CH$_2$), 42.2 (CH), 43.7 (CH$_2$), 52.5 (OCH$_3$), 54.0 (OCH$_3$), 98.7 (CH), 115.4 (CH), 118.5 (C), 119.2 (CH), 123.2 (C), 123.4 (CH), 123.7 (CH), 125.1 (CH), 129.1 (C), 135.5 (C), 136.6 (CH), 143.7 (C), 143.9 (C), 144.2 (C), 151.3 (C=O), 173.6 (C=O). MS (ES, pos. mode): *m/z* (%): 468.24 (M + H$^+$, 100), purity: 100%.

Methyl 3-(1-methoxy-6-((7-nitrobenzo[*c*][1,2,5]oxadiazol-4-yl)amino)-1-oxohexan-2-yl)-1*H*-indole-1-carboxylate 9b
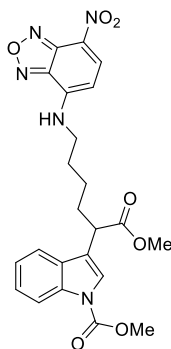
Red oil, yield 61%, R$_f$ = 0.66 (PE/EtOAc 1/1). ^{1}H NMR (500 MHz, CDCl$_3$): δ 1.48-1.54 (2H, m, CH$_2$), 1.81-1.87 (2H, m, CH$_2$), 1.97-2.04 and 2.17-2.25 (2H, m, CH$_2$), 3.41-3.52 (2H, m, CH$_2$), 3.68 (3H, s, OCH$_3$), 3.83 (1H, t, *J* = 7.6 Hz, CH), 4.02 (3H, s, OCH$_3$) 6.09 (1H, d, *J* = 8.4 Hz, CH), 6.23-6.34 (1H, br s, NH), 7.23 (1H, t, *J* = 7.6 Hz, CH), 7.32 (1H, t, *J* = 7.8 Hz, CH), 7.51-7.59 (2H, m, 2 × CH), 8.13 (1H, s, CH), 8.43 (1H, d, *J* = 10.1 Hz, CH). ^{13}C NMR (126 MHz, CDCl$_3$): δ 25.0 (CH$_2$), 28.2 (CH$_2$), 31.5 (CH$_2$), 42.5 (CH$_2$), 43.6 (CH), 52.4 (OCH$_3$), 54.0 (OCH$_3$), 98.6 (CH), 115.4 (CH), 118.8 (C), 119.3 (CH), 123.1 (C), 123.3 (CH), 124.0 (CH), 125.1 (CH), 129.3 (C), 135.5 (C), 136.6 (CH), 143.8 (C), 143.9 (C), 144.3 (C), 151.4 (C=O), 173.9 (C=O). MS (ES, pos. mode): *m/z* (%): 482.24 (M + H$^+$, 100), purity: 95%.

Methyl 3-(1-methoxy-7-((7-nitrobenzo[*c*][1,2,5]oxadiazol-4-yl)amino)-1-oxoheptan-2-yl)-1*H*-indole-1-carboxylate 9c
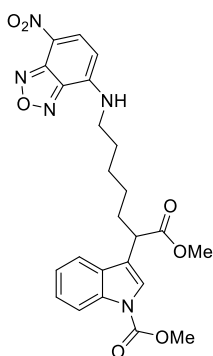
Red oil, yield 70.5%, R$_f$ = 0.68 (PE/EtOAc 1/1). ^{1}H NMR (500 MHz, CDCl$_3$): δ 1.39-1.45 (2H, m, CH$_2$), 1.48-1.54 (2H, m, CH$_2$), 1.74-1.83 (2H, m, CH$_2$), 1.92-1.96 and 2.09-2.16 (2H, m, CH$_2$), 3.42-3.51 (2H, m, CH$_2$), 3.67 (3H, s, OCH$_3$), 3.80 (1H, t, *J* = 7.0 Hz, CH), 4.02 (3H, s, OCH$_3$) 6.10 (1H, d, *J* = 8.4 Hz, CH), 6.30-6.43 (1H, br s, NH), 7.22-7.25 (1H, m, CH), 7.31 (1H, t, *J* = 7.6 Hz, CH), 7.54 (1H, s, CH), 7.58 (1H, d, *J* = 7.6, CH), 8.14 (1H, s, CH), 8.43 (1H, d, *J* = 8.6 Hz, CH). ^{13}C NMR (126 MHz, CDCl$_3$): δ 26.7 (CH$_2$), 27.3 (CH$_2$), 28.3 (CH$_2$), 31.9 (CH$_2$), 42.6 (CH), 43.9 (CH$_2$), 52.3 (OCH$_3$), 54.0 (OCH$_3$), 98.6 (CH), 115.4 (CH), 119.1 (C), 119.3 (CH), 123.1 (C), 123.2 (CH), 123.9 (CH), 125.0 (CH), 129.4 (C), 135.5 (C), 136.7 (CH), 143.9 (C), 144.1 (C), 144.3 (C), 151.4 (C=O), 174.1 (C=O). MS (ES, pos. mode): *m/z* (%): 496.24 (M + H$^+$, 100), purity: 100%.

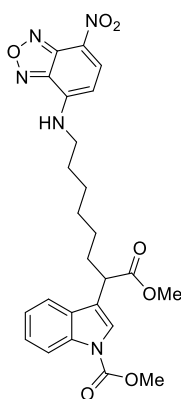**Methyl 3-(1-methoxy-8-((7-nitrobenzo[c][1,2,5]oxadiazol-4-yl)amino)-1-oxooctan-2-yl)-1H-indole-1-carboxylate 9d**

Red oil, yield 77%, R_f = 0.80 (PE/EtOAc 1/1). ^{1}H NMR (500 MHz, CDCl$_3$): δ 1.36-1.44 (6H, m, 3 × CH$_2$), 1.73-1.79 (2H, m, CH$_2$), 1.87-1.95 and 2.09-2.13 (2H, m, CH$_2$), 3.42-3.43 (2H, m, CH$_2$), 3.66 (3H, s, OCH$_3$), 3.79 (1H, t, J = 7.5 Hz, CH), 4.01 (3H, s, OCH$_3$) 6.10 (1H, d, J = 8.6 Hz, CH), 6.43-6.53 (1H, br s, NH), 7.23 (1H, t, J = 7.6 Hz, CH), 7.31 (1H, t, J = 7.8 Hz, CH), 7.53 (1H, s, CH), 7.58 (1H, d, J = 7.9, CH), 8.12 (1H, s, CH), 8.42 (1H, d, J = 8.6 Hz, CH). ^{13}C NMR (126 MHz, CDCl$_3$): δ 26.7 (CH$_2$), 27.5 (CH$_2$), 28.4 (CH$_2$), 29.1 (CH$_2$), 32.0 (CH$_2$), 42.7 (CH), 44.0 (CH$_2$), 52.3 (OCH$_3$), 54.0 (OCH$_3$), 98.6 (CH), 115.3 (CH), 119.3 (C), 119.4 (CH), 123.1 (C), 123.2 (CH), 123.7 (CH), 124.9 (CH), 129.5 (C), 135.5 (C), 136.7 (CH), 143.9 (C), 144.1 (C), 144.3 (C), 151.4 (C=O), 174.2 (C=O). MS (ES, pos. mode): m/z (%): 510.32 (M + H$^+$, 100), purity: 100%.

Methyl 2-(1H-indol-3-yl)-8-((7-nitrobenzo[c][1,2,5]oxadiazol-4-yl)amino)octanoate 10d
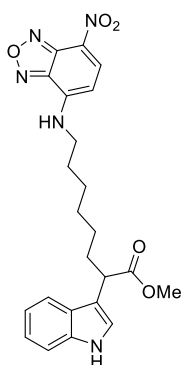
Red oil, yield 81%, R_f = 0.86 (CH$_2$Cl$_2$/Ac 4.5/0.5). ^{1}H NMR (500 MHz, acetone-d_6): δ 1.33-1.51 (6H, m, 3 × CH$_2$), 1.78 (2H, m, CH$_2$), 1.84-1.97 and 2.08-2.14 (2H, m, CH$_2$), 3.57 (5H, m, CH$_2$, OCH$_3$), 3.85 (1H, t, J = 6.9 Hz, CH), 6.38 (1H, d, J = 8.6 Hz, CH), 6.98 (1H, t, J = 6.9 Hz, CH), 7.06 (1H, t, J = 7.0 Hz, CH), 7.22 (1H, s, CH), 7.36 (1H, d, J = 7.9 Hz, CH), 7.61 (1H, d, J = 7.6, CH), 8.18-8.34 (1H, br s, NH), 8.46 (1H, d, J = 8.3 Hz, CH), 10.05-10.21 (1H, br s, NH). ^{13}C NMR (126 MHz, acetone-d_6): δ 26.6 (CH$_2$), 27.5 (CH$_2$), 28.0 (CH$_2$), 29.8 (CH$_2$), 32.7 (CH$_2$), 42.8 (CH), 43.7 (CH$_2$), 50.9 (OCH$_3$), 98.6 (CH), 111.5 (CH), 113.3 (C), 118.7 (CH), 118.9 (CH), 121.5 (CH), 122.5 (CH), 122.7 (CH), 126.8 (C), 136.8 (C), 137.1 (CH), 144.4 (C), 144.7 (C), 144.9 (C), 174.6 (C=O). MS (ES, pos. mode): m/z (%): 452.29 (M + H$^+$, 100), purity: 97%.

2-(1*H*-Indol-3-yl)-5-((7-nitrobenzo[*c*][1,2,5]oxadiazol-4-yl)amino)pentanoic acid 11a
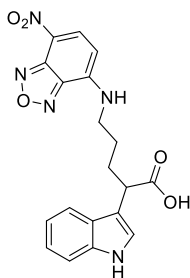
Red crystals, yield 52%, R$_f$ = 0.19 (CH$_2$Cl$_2$/Ac 4/0.5). ^{1}H NMR (500 MHz, acetone-d_6): δ 1.81-1.91 (2H, m, CH$_2$), 2.07-2.15 and 2.22-2.30 (2H, m, CH$_2$), 3.55-3.72 (2H, m, CH$_2$), 3.94 (1H, t, *J* = 7.8 Hz, CH), 6.31 (1H, d, *J* = 7.9 Hz, CH), 6.95 (1H, t, *J* = 7.5 Hz, CH), 7.05 (1H, t, *J* = 7.6 Hz, CH), 7.27 (1H, s, CH), 7.34 (1H, d, *J* = 8.3 Hz, CH), 7.64 (1H, d, *J* = 8.3 Hz, CH), 8.23-8.35 (1H, br s, NH), 8.41 (1H, d, *J* = 8.9 Hz, CH), 10.06-10.23

(1H, br s, NH). ^{13}C NMR (126 MHz, acetone-d_6): δ 26.1 (CH$_2$), 29.8 (CH$_2$), 42.3 (CH), 43.7 (CH$_2$), 98.6 (CH), 111.5 (CH), 113.0 (C), 118.8 (CH), 119.1 (CH), 121.5 (CH), 122.8 (CH), 123.0 (C), 126.8 (C), 136.8 (C), 137.0 (CH), 144.3 (C), 144.7 (C), 144.9 (C), 174.8 (C=O). MS (ES, neg. mode): *m/z* (%): 394.33 (M - H$^+$, 100), purity: 87%.

2-(1*H*-Indol-3-yl)-6-((7-nitrobenzo[*c*][1,2,5]oxadiazol-4-yl)amino)hexanoic acid 11b
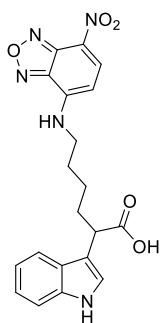
Red crystals, yield 28%, R$_f$ = 0.14 (CH$_2$Cl$_2$/Ac 5/0.2). ^{1}H NMR (500 MHz, acetone-d_6): 1.49-1.57 (2H, m, CH$_2$), 1.83-1.90 (2H, m, CH$_2$), 1.95-1.99 and 2.15-2.21 (2H, m, CH$_2$), 3.52-3.69 (2H, m, CH$_2$), 3.86 (1H, t, *J* = 7.6 Hz, CH), 6.39 (1H, d, *J* = 8.9 Hz, CH), 6.96 (1H, t, *J* = 7.5 Hz, CH), 7.05 (1H, t, *J* = 8.1 Hz, CH), 7.25 (1H, s, CH), 7.34 (1H, d, *J* = 8.3 Hz, CH), 7.63 (1H, d, *J* = 7.6 Hz, CH), 8.22-8.35 (1H, br s, NH), 8.46 (1H, d, *J* = 8.6 Hz, CH), 10.07-10.21

(1H, br s, NH). ^{13}C NMR (126 MHz, acetone-d_6): 25.0 (CH$_2$), 27.9 (CH$_2$), 32.3 (CH$_2$), 42.6 (CH), 43.6 (CH$_2$), 98.6 (CH), 111.4 (CH), 113.3 (C), 118.8 (CH), 119.0 (CH), 121.4 (CH), 122.4 (C), 122.8 (CH), 126.9 (C), 136.8 (C), 137.1 (CH), 144.4 (C), 144.7 (C), 145.0 (C), 174.9 (C=O). MS (ES, neg. mode): *m/z* (%): 408.35 (M - H$^+$, 100), purity: 100%.

2-(1*H*-Indol-3-yl)-7-((7-nitrobenzo[c][1,2,5]oxadiazol-4-yl)amino)heptanoic acid 11c
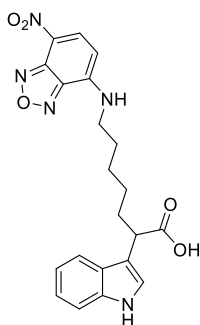
Red crystals, yield 49%, R$_f$ = 0.33 (CH$_2$Cl$_2$/Ac 4/0.5). ^{1}H NMR (500 MHz, acetone-d_6): 1.40-1.47 (2H, m, CH$_2$), 1.49-1.55 (2H, m, CH$_2$), 1.78-1.84 (2H, m, CH$_2$), 1.87-1.94 and 2.09-2.17 (2H, m, CH$_2$), 3.49-3.68 (2H, m, CH$_2$), 3.85 (1H, t, *J* = 7.6 Hz, CH), 6.40 (1H, d, *J* = 8.9 Hz, CH), 6.97 (1H, t, *J* = 7.0 Hz, CH), 7.06 (1H, t, *J* = 7.6 Hz, CH), 7.25 (1H, s, CH), 7.35 (1H, d, *J* = 8.3 Hz, CH), 7.64 (1H, d, *J* = 7.9 Hz, CH), 8.24-8.35 (1H, br s, NH), 8.48 (1H, d, *J* = 8.9 Hz, CH), 10.08-10.18 (1H, br s, NH). ^{13}C NMR (126 MHz, acetone-d_6): 26.6 (CH$_2$), 27.3 (CH$_2$), 27.9 (CH$_2$), 32.6 (CH$_2$), 42.6 (CH), 43.5 (CH$_2$), 98.5

(CH), 111.5 (CH), 113.5 (C), 118.7 (CH), 119.0 (CH), 121.4 (CH), 122.5 (CH), 122.7 (C), 126.9 (C), 136.7 (C), 137.2 (CH), 144.4 (C), 144.7 (C), 144.9 (C), 174.9 (C=O). MS (ES, neg. mode): m/z (%): 422.38 (M - H$^+$, 100), purity: 98%.

2-(1H-Indol-3-yl)-8-((7-nitrobenzo[c][1,2,5]oxadiazol-4-yl)amino)octanoic acid 11d
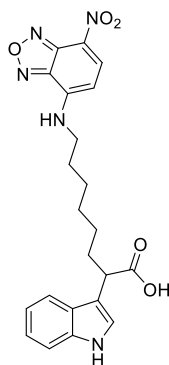
Red crystals, yield 35%, R$_f$ = 0.52 (CH$_2$Cl$_2$/Ac 4/0.5). ^{1}H NMR (500 MHz, acetone-d_6): δ 1.35-1.47 (6H, m, 3 × CH$_2$), 1.77-1.82 (2H, m, CH$_2$), 1.85-1.93 and 2.08-2.13 (2H, m, CH$_2$), 3.51-3.68 (2H, m, CH$_2$), 3.83 (1H, t, J = 7.6 Hz, CH), 6.42 (1H, d, J = 8.9 Hz, CH), 6.98 (1H, t, J = 7.5 Hz, CH), 7.06 (1H, t, J = 7.5 Hz, CH), 7.24 (1H, s, CH), 7.36 (1H, d, J = 7.9 Hz, CH), 7.65 (1H, d, J = 7.0 Hz, CH), 8.22-8.36 (1H, br s, NH), 8.49 (1H, d, J = 8.9 Hz, CH), 10.03-10.21 (1H, br s, NH). ^{13}C NMR (126 MHz, acetone-d_6): δ 26.6 (CH$_2$), 27.6 (CH$_2$), 27.9 (CH$_2$), 29.9 (CH$_2$), 32.7 (CH$_2$), 42.7 (CH), 43.7 (CH$_2$), 98.6 (CH), 111.4 (CH), 113.6 (C), 118.8 (CH), 119.1 (CH), 121.4 (CH), 122.5 (C), 122.6 (CH), 126.9 (C), 136.8 (C), 137.2 (CH), 144.8 (C), 145.0 (C), 145.2 (C), 174.9 (C=O). MS (ES, neg. mode): m/z (%): 436.31 (M - H$^+$, 100), purity: 96%.

4.3. Biological testing

4.3.1. Preliminary testing and selection of the lead compounds

First of all, in order to select the lead compounds from fluorescently labelled auxin derivatives with fluorescent label attached at NH-position **I-IV** (Bieleszova 2017) or at α-position **V-VIII** (Figure 13), the ability of these compounds to inhibit the primary root growth in *Arabidopsis thaliana* ecotype Col-0 seedlings, to promote GUS expression in DR5::GUS transgenic plant line of *Arabidopsis thaliana* and their ability to be uptaken and distributed in *Arabidopsis thaliana* (Col-0) roots was evaluated.
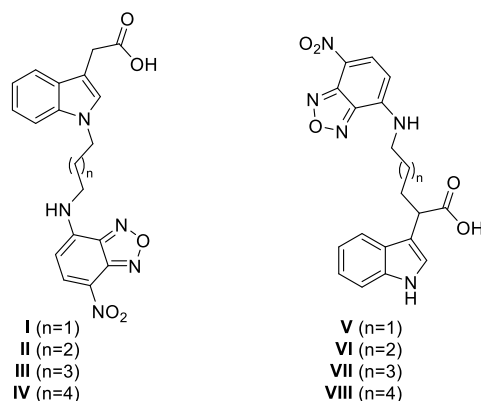
Figure 13 Auxin derivatives with fluorescent label attached at NH- or at α-position

4.3.1.1. Effect of the compounds on the phenotype of *Arabidopsis thaliana* (Col-0) roots

Typically, auxins inhibit primary root growth already at nanomolar concentrations and promote root hair formation (Woodward and Bartel 2005). *Arabidopsis thaliana* Col-0 seedlings were grown on medium with IAA as a positive control, and fluorescently labelled auxins **I-VIII** at 1, 5, 10 and 20 μM concentrations. Despite being IAA derivatives, fluorescently labelled compounds **I-VIII** did not inhibit primary root growth (Figure 14, A and B). Only mild root growth inhibition could be observed at the highest concentrations of compound **V**, however the roots of the plants lacked root hair suggesting that observed effect is not auxin-induced.

Subsequently, the ability of **I-VIII** to block auxin-induced primary root growth inhibition was evaluated. Precisely, *Arabidopsis thaliana* Col-0 seedlings were grown on medium with fluorescently labelled auxins **I-VIII** at 1, 5, 10 and 20 μM concentrations in the presence of 1 μM IAA for 5 days. All compounds, to a lesser or greater extent, were able to revert such auxin-induced effect in a dose-dependent manner (Figure 14 C and D). The activity of the compounds was highly related to the length of the linker between IAA and NBD label. While derivatives **I** and **V** with the shortest linker had barely any noticeable effect, compounds **IV** and **VIII**, bearing the longest linkers, at 10 or 20 μM concentration were able to almost completely overcome IAA-induced primary root growth inhibition, suggesting their activity as anti-auxins.
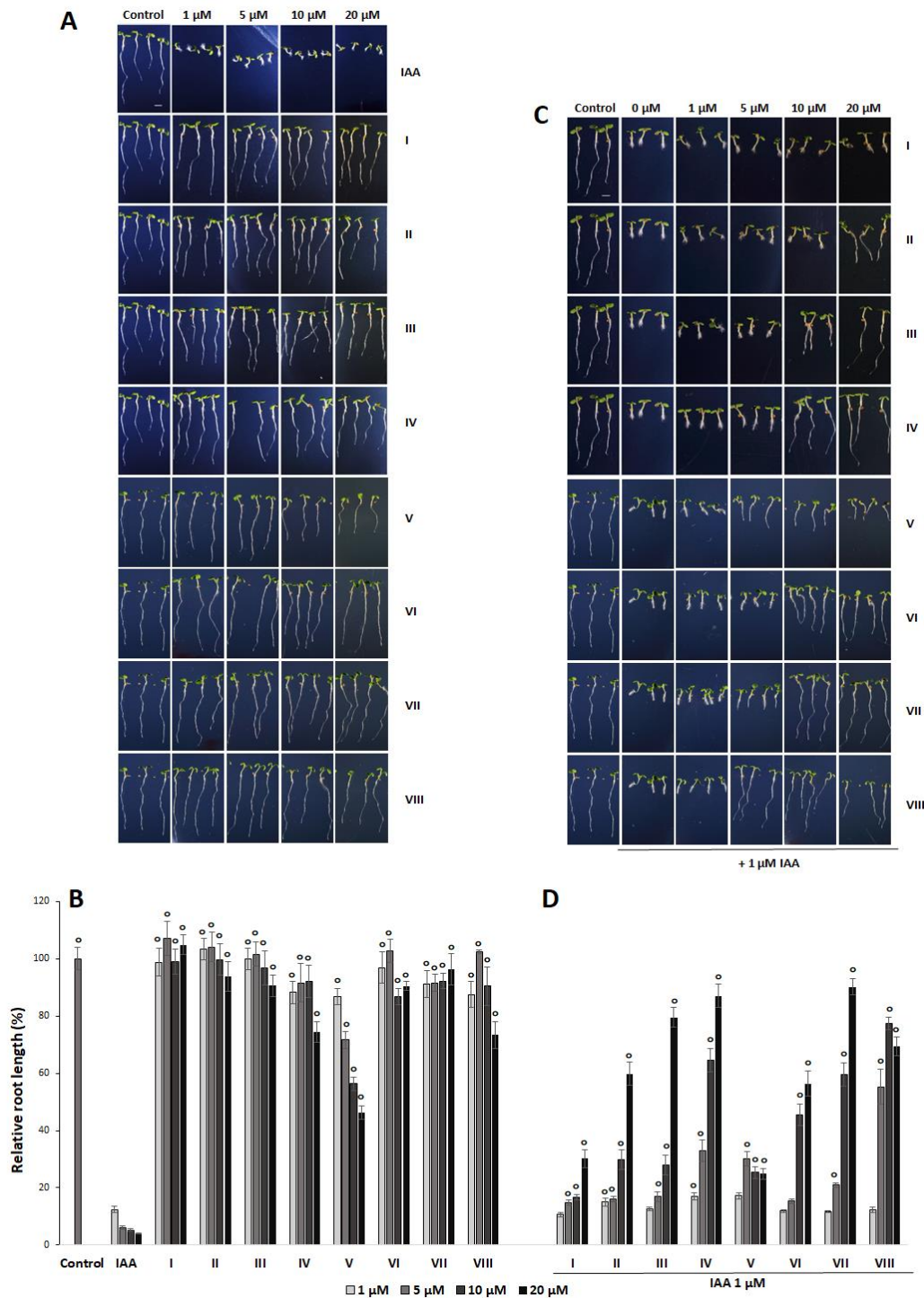
Figure 14 The effect of derivatives **I-VIII** on *Arabidopsis thaliana* (Col-0) primary root growth. Phenotype of primary root was determined on seedlings (5 DAG) grown on 1, 5, 10, 20 µM **I-VIII** in the absence (A, B) or presence (C, D) of 1 µM IAA. The length of primary root normalized to DMSO treatment was quantified. 1 µM IAA was used as control. Statistical analyses were performed using the t-test, values are means ± S.E. White circles (○) indicate statistically significant differences between the effect of **I-VIII** compared to 1 µM IAA treatment, ○ corresponds to $P < 0.01$. Scale bar represents 1 mm.

Moreover, it was observed that the most active derivatives **IV** and **VIII** effectively inhibited auxin-induced (1 µM IAA) root hair formation, **IV** from 10 µM concentration and **VIII** from 5 µM concentration (Figure 15), further suggesting their anti-auxin activity.
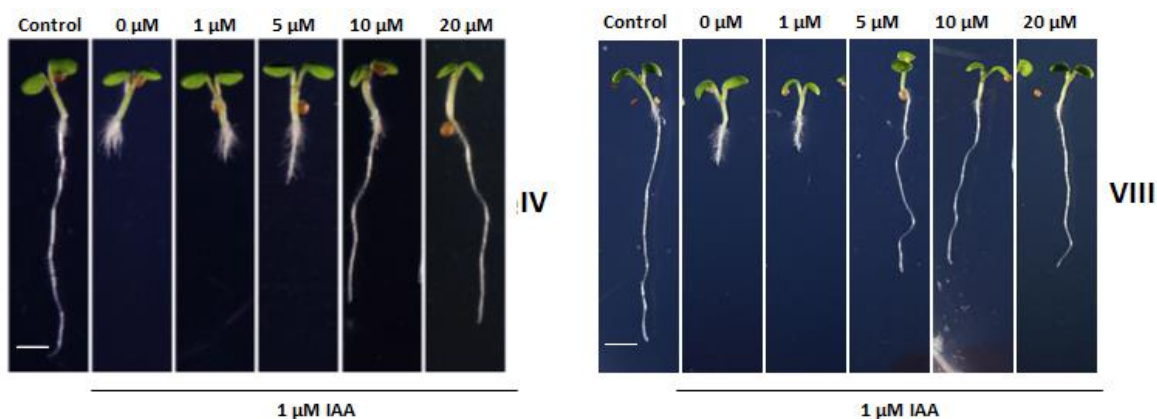
Figure 15 Inhibitory effect of **IV** and **VIII** on auxin-induced root hair formation in *Arabidopsis thaliana* (Col-0) roots. Root hair formation was evaluated in seedlings (5 DAG) grown on 1, 5, 10, 20 μM **IV** and **VIII** in the presence of 1 μM IAA. Scale bar represents 1 mm.

4.3.1.2. The effect of compounds in the DR5::GUS transgenic plants of *Arabidopsis thaliana*

Further, ability of fluorescently labelled auxin derivatives **I-VIII** to promote GUS expression was evaluated. For this, *Arabidopsis* transgenic line pDR5::GUS, which has β-glucuronidase (GUS) reporter gene under the control of the synthetic auxin-inducible DR5 promoter (Ulmasov, Murfett *et al.* 1997) was used. The regulation of GUS expression in this line is directly related to the capacity of auxin. As anticipated, compounds **I-VIII** did not induce GUS expression even at 50 μM concentration, confirming the absence of auxin activity (Figure 16, A and B). In contrast, co-applied with 2 μM IAA, some of the fluorescently labelled compounds blocked auxin-induced GUS expression in a dose-dependent manner. Analogously to the previous experiment, the strength of the auxin antagonist effect of **I-VIII** was also linker-dependent. The most potent compounds **IV** and **VIII** completely inhibited DR5::GUS expression induced by 2 μM IAA at 20 and 25 μM concentration, respectively (Figure 16, C and D).
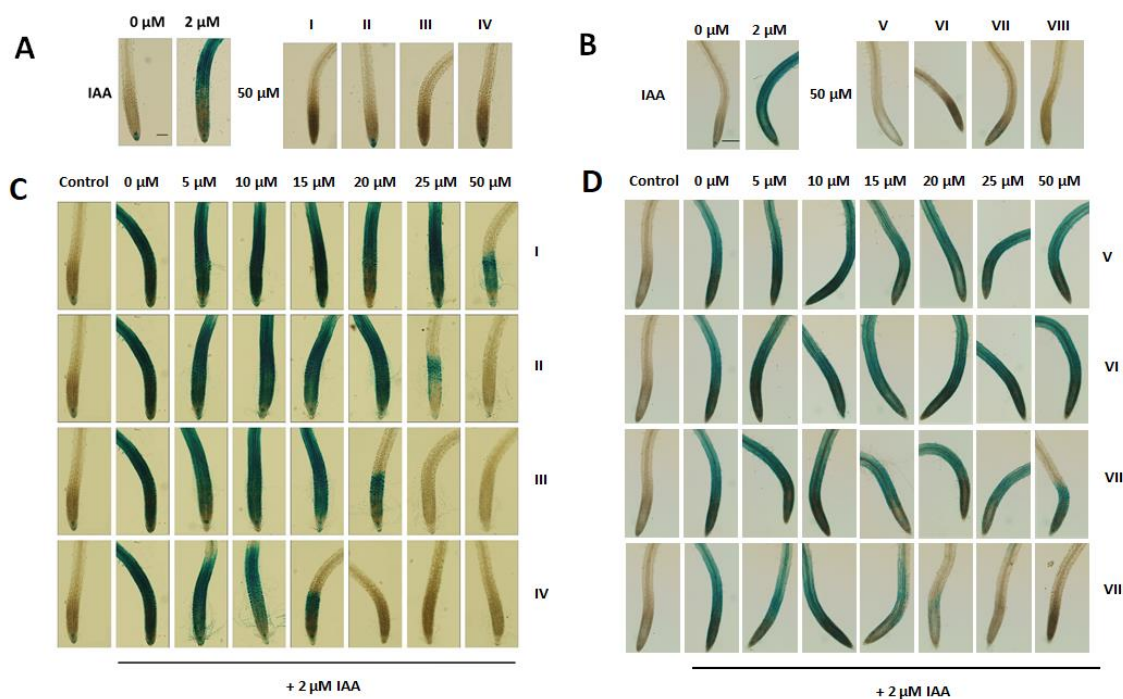
Figure 16 Effect of compounds **I-VIII** on GUS expression in the DR5::GUS transgenic plants of *Arabidopsis thaliana*. (A, B) Seedlings (5 DAG) were treated with IAA at 2 μM and compounds **I-VIII** at 50 μM concentration for 5 h. Derivatives **I-VIII** showed no GUS expression pattern. (C, D) Seedlings (5 DAG) were treated with **I-VIII** at given concentrations (5, 10, 15, 20, 25 and 50 μM) for 2 h followed by wash-out and treatment with 2 μM IAA for 3 h. Some compounds were able to inhibit DR5::GUS expression induced by 2 μM IAA. Figures were chosen as representatives from two independent repetitions. Scale bars represent 200 μm.

4.3.1.3. Uptake of fluorescently labelled IAA derivatives in *Arabidopsis thaliana* wild-type Col-0 roots

Subsequently, the uptake of fluorescently labelled compounds **I-VIII** in the roots of *Arabidopsis* was observed by confocal microscopy, in order to assess their applicability to be used as auxin tracers. Analogously to the previous experiments, the uptake of the fluorescently labelled compounds **I-VIII** in *Arabidopsis thaliana* wild-type roots had a strong positive correlation with the length of the linker (Figure 17). Namely, from the group of the compounds with the linker attached at the N1 position, compound **IV** had the best uptake and subsequent fluorescent signal in the roots, while among the compounds with the linker attached at the α-position of IAA molecule, compound **VIII** was the one with the best uptake and fluorescence.
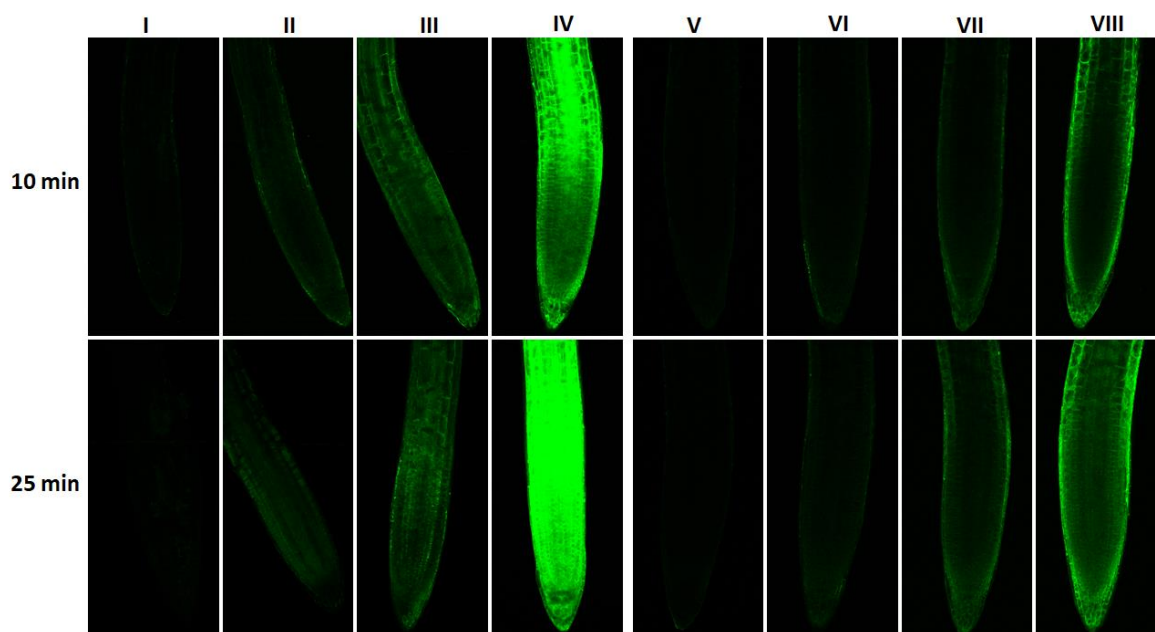
Figure 17 Uptake of fluorescently labelled IAA derivatives **I-VIII** in *Arabidopsis thaliana* roots. Seedlings (5 DAG) were treated with **I-VIII** at 10 µM concentration for 10 min and 25 min. Experimental set up involved 10× objective. Results are from 2 different experiments. For compounds **I-IV** conditions of confocal microscope were set for compound **I**, while for compounds **V**-**VIII** conditions were optimized for compound **VIII**.

Based on the latter results two the most active compounds which also had the best uptake and fluorescence in the *Arabidopsis thaliana* roots, namely, compounds **IV** and **VIII**, were chosen as lead compounds for the further experiments (Figure 18).
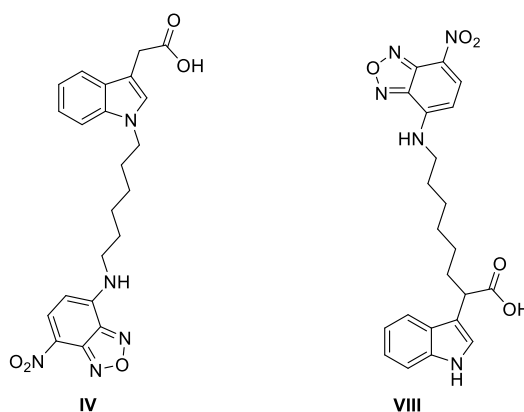
Figure 18 Lead fluorescently labelled compounds **IV** and **VIII**

4.3.2. Elucidation of the biological activity of the lead compounds IV and VIII

With the lead compounds **IV** and **VIII** in hand, their biological activity was further investigated. This included rapid root growth assay, lateral root formation, apical hook development, auxin distribution in gravistimulated roots of DR5$_{rev}$::RFP, effect of

compounds in the DR5::LUC transgenic plants of *Arabidopsis thaliana*, PIN1 subcellular localization and BFA body formation of PIN2.

4.3.2.1. The effect of the compounds on the primary root growth of *Arabidopsis thaliana* (Col-0) roots in short term

Roots of *Arabidopsis thaliana* in response to the natural auxin indole-3-acetic acid (IAA) inhibit their growth very rapidly, in less than 30 s after auxin reaches the root surface (Fendrych, Akhmanova *et al*. 2018). Growth inhibition is triggered by nanomolar concentrations of IAA. Thus, the effect of the compounds **IV** and **VIII** in a range of concentrations (1, 5, 10, 20, 50 µM) on the primary root growth in the first 12 h was evaluated. Interestingly, both fluorescently labelled compounds **IV** and **VIII** showed weak auxin-like activity, which was dose dependent and both compounds at 20 µM concentrations inhibited root growth similarly like 50 nM IAA. Moreover, the compounds at the highest tested concentration (50 µM) almost completely inhibited primary root growth (Figure 19 A and B). These findings appear to be contrary to the long-term effect of the compounds **IV** and **VIII** on the root growth, in which the primary root growth was not inhibited by the compounds, but on the contrary – root growth inhibition induced by IAA was antagonized by compounds treatment.
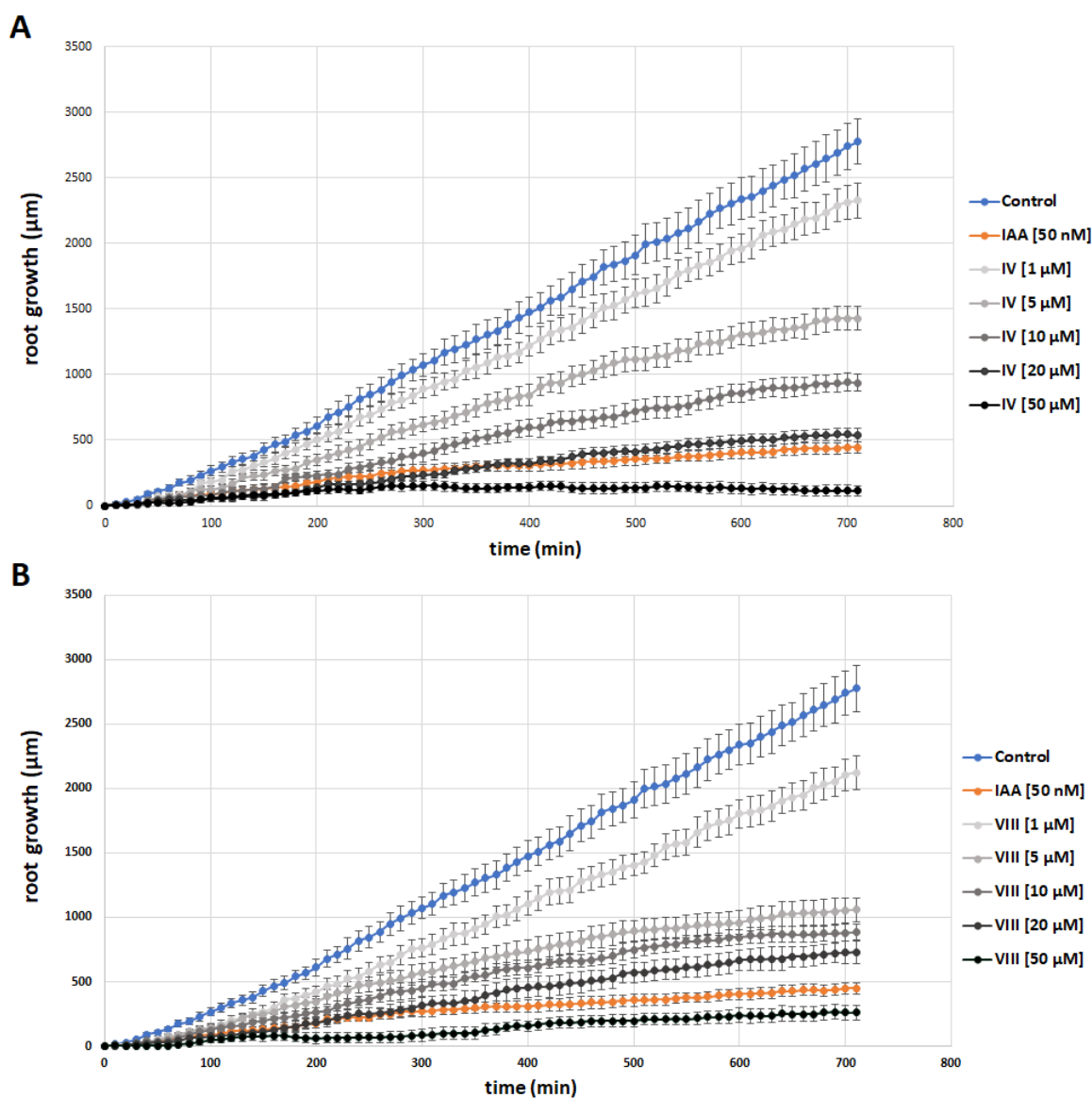
Figure 19 The effect of derivatives **IV** and **VIII** on *Arabidopsis thaliana* (Col-0) root growth. Seedlings (5 DAG) were transfered to plates with media containing **IV** (graph A) and **VIII** (graph B) at 1, 5, 10, 20 and 50 μM concentrations for 12 hours. 50 nM IAA was used as a positive control. Results are averages from two independent repetitions. Values are means ± S.E.

4.3.2.2. The effect of compounds in the DR5::LUC transgenic plants of *Arabidopsis thaliana*

Due to observed discrepancies in the effect of the compounds on the root growth, to compare the anti-auxin activity of fluorescently labelled compounds **IV** and **VIII** which was established on the basis of DR5::GUS assay, we also used the synthetic auxin-responsive promoter DR5 driving the firefly luciferase enzyme DR5::LUC (Moreno-Risueno, Van Norman *et al.* 2010; Fendrych, Akhmanova *et al.* 2018). In this case, auxin response is determined by the luminescence intensity of luciferase. The experiment was performed with

derivatives **IV** and **VIII** at 20 µM concentration for 1 and 3 h. In comparison with the control, luciferase response was only slightly higher after 1 h of treatment, while after 3 h of treatment, luciferase response was strongly increased once again indicating weak auxin activity of compounds **IV** and **VIII** (Figure 20).
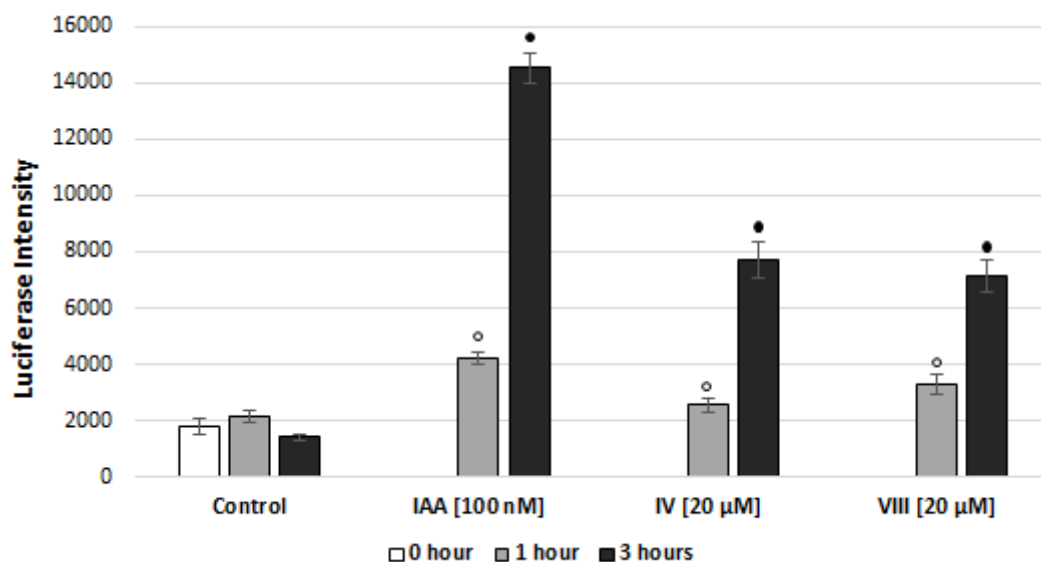
Figure 20 The effect of compounds **IV** and **VIII** in the DR5::LUC transgenic plants of *Arabidopsis thaliana.* Five-day-old *Arabidopsis thaliana* seedlings of transgenic plant line DR5::LUC were transferred to control, tested fluorescent auxin analogues **IV** and **VIII** in final concentration of 20 µM or 100 nM IAA for 1 or 3 h. The luminiscence intensity in the roots was measured. Results are averages from three independent repetitions. Statistical analyses were performed using the t-test, values are means ± S.E. White and black circles (○), (●) indicate statistically significant differences between the effect of **IV** and **VIII** compared to control, ○,● correspond to $P < 0.01$.

4.3.2.3. The effect of compounds on lateral root formation in *Arabidopsis thaliana*

Auxin, among other numerous effects, also promotes lateral root (LR) formation (Fukaki, Okushima *et al*. 2007). Thus, the effect of compounds on LR formation in *Arabidopsis thaliana* (Col-0) was evaluated. Both compounds **IV** and **VIII** at 10 µM and 20 µM concentration did not promote lateral root formation. Moreover, **IV** and **VIII** at 20 µM concentration effectively inhibited auxin-induced (100 nM IAA) lateral root formation (Figure 21), once again implying their activity as anti-auxins.
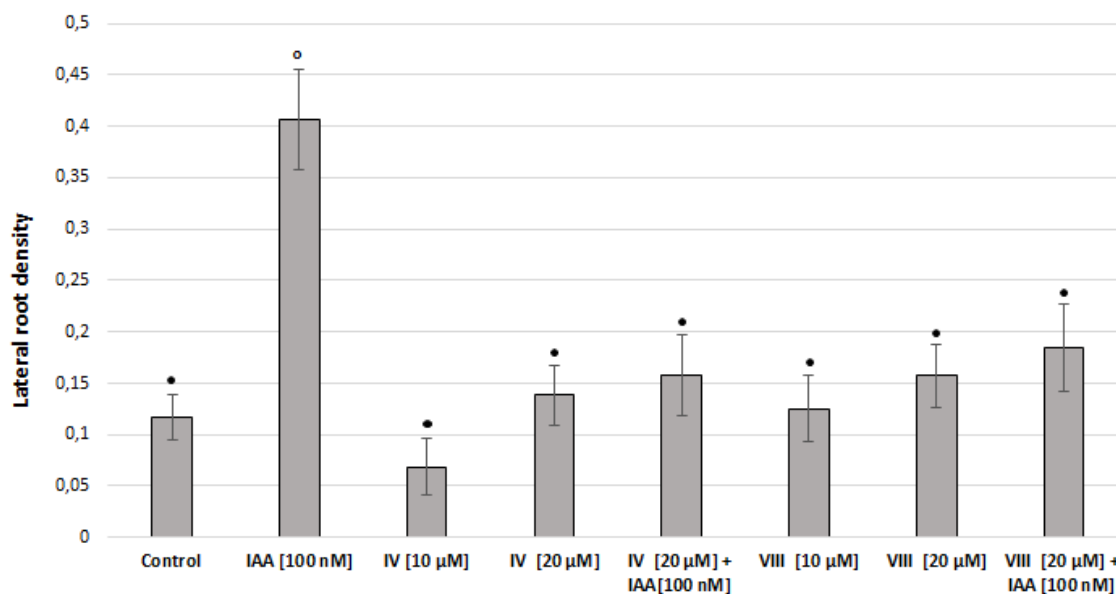
Figure 21 Effect of compounds **IV** and **VIII** on lateral root formation. IAA (100 nM) was used as control. 5 DAG seedlings were transferred to plates with media containing **IV** and **VIII** at 10 and 20 µM concentration in presence or absence of IAA (100 nM) and grown for 5 days. The number of lateral roots was counted and the density of lateral roots was calculated. Results are averages from two independent repetitions. Statistical analyses were performed using the t-test, values are means ± S.E. White circles (○) indicate statistically significant differences between the effect of IAA, **IV** and **VIII** compared to control, while black circles (●) indicate statistically significant differences between the effect of control, **IV** and **VIII** compared to 100 nM IAA, ○,● correspond to $P < 0.01$.

4.3.2.4. The effect of compounds in apical hook development

Plant growth and development is regulated by dynamic formation of auxin gradients, one of such processes is apical hook development. Apical hook development proceeds through three phases, i.e. formation, maintenance and opening (Raz and Ecker 1999). The formation phase starts when the seedling emerges from the seed coat and lasts until the hook reaches roughly 180°. In maintenance phase seedling actively keeps its hook closed while the hypocotyl rapidly elongates. Finally, in opening phase the hook starts to open, reaching angle zero. Thus, the effect of compounds **IV** and **VIII** in apical hook development was evaluated in dark-grown *Arabidopsis* seedlings, which was recorded continuously from synchronized germination (Zadnikova, Petrasek *et al.* 2010). Compound **VIII** at 20 µM concentration showed similar effect to 1 µM IAA, that is the maintenance phase was shorter than in control, implying its activity as an auxin. However, compound **IV** at 20 µM concentration showed opposite effect, with the maintenance phase being longer (Figure 22).
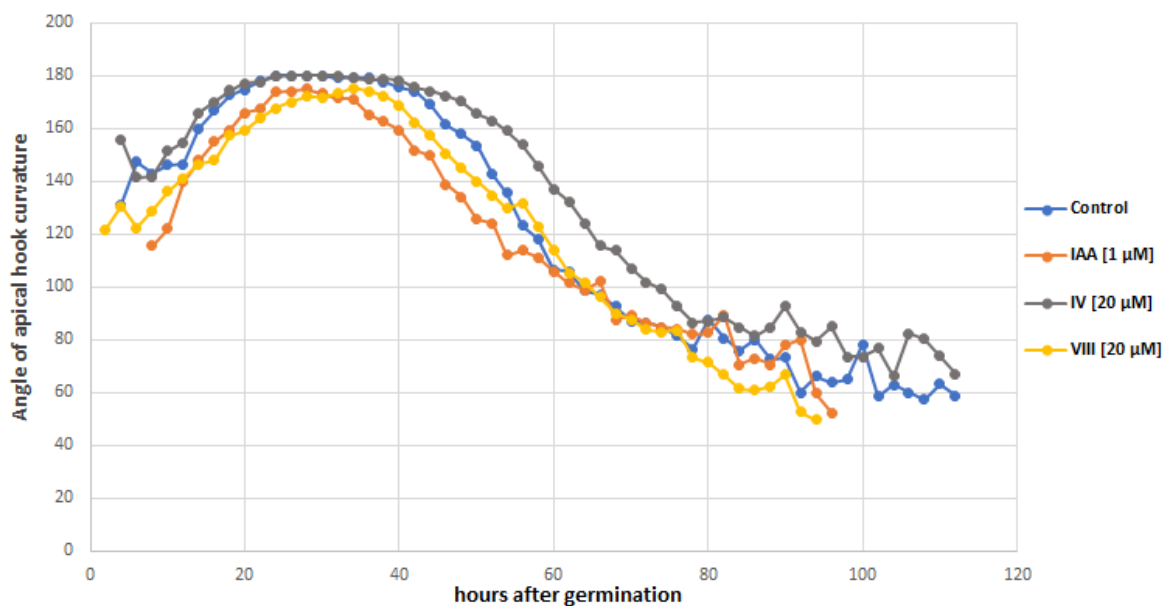
Figure 22 The effect of compounds **IV** and **VIII** in apical hook development. *Arabidopsis thaliana* wild-type Col-0 seedlings were grown in square plates containing sterile ½ MS medium supplemented with a blank control, 1 µM IAA as a positive control or tested fluorescent auxin analogues **IV** and **VIII** in final concentration of 20 µM. Seedling development was recorded at 1-hour intervals for 7 days. Results are averages from three independent repetitions.

4.3.2.5. The effect of compounds on asymmetric auxin distribution in gravistimulated roots of transgenic plant line DR5$_{rev}$::RFP

Subsequently, the effect of compounds **IV** and **VIII** on asymmetric auxin distribution during gravistimulation in the roots of DR5$_{rev}$::RFP seedlings was tested. In control plants, gravistimulation induces auxin accumulation at the lower side of the root tip leading to the root bending according to gravity vector. DR5$_{rev}$::RFP fluorescence signal intensity increases at the lower side of the root (Figure 23 A) as a result of auxin accumulation, making the ratio of the signal intensity of upper/lower half of the root lower than one (Figure 23 B). However, if auxin is applied exogenously the asymmetric distribution of auxin is not established, root is not bending and the upper (U)/lower (L) ratio of the signal intensity is around one. Similarly to exogenously applied auxin (500 nM IAA), treatment with compounds **IV** and **VIII** resulted in symmetric auxin distribution in the gravistimulated roots of transgenic plant line DR5$_{rev}$::RFP, suggesting the auxin activity of compounds **IV** and **VIII**. Moreover, RFP signal was stronger with compounds **IV** and **VIII** at tested concentrations, in comparison to control or 500 nM IAA (Figure 23 C).
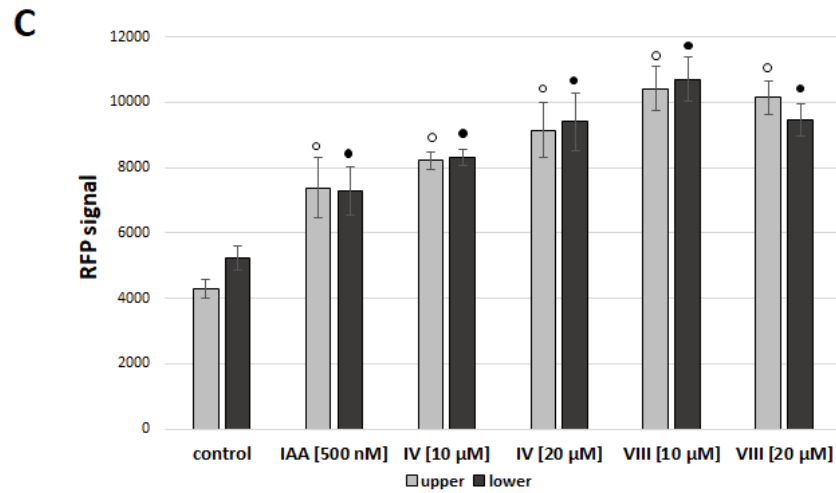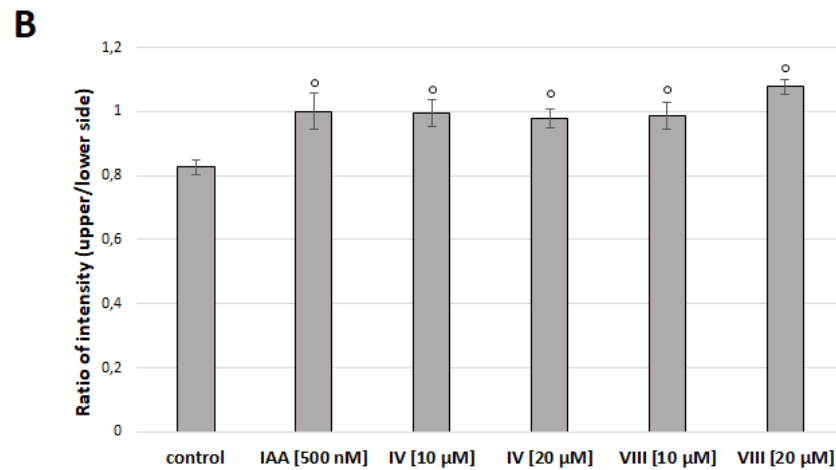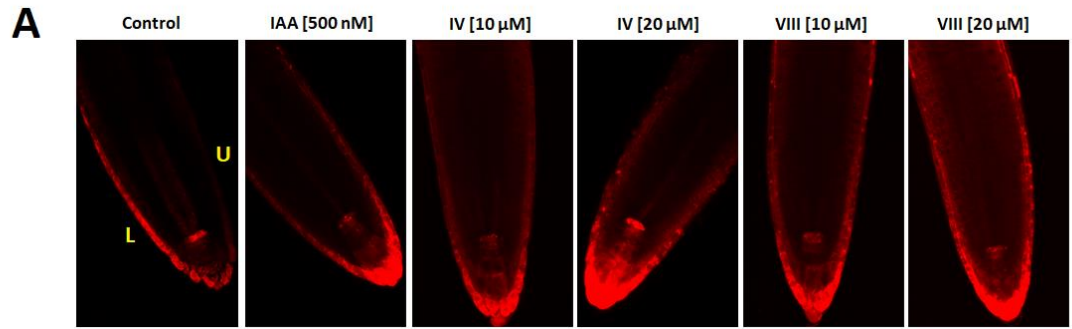
Figure 23 The effect of compounds **IV** and **VIII** on asymmetric auxin distribution in gravistimulated roots. Four-day-old *Arabidopsis thaliana* seedlings of transgenic plant line DR5rev::RFP were transferred to control, tested fluorescent auxin analogues **IV** and **VIII** in final concentration of 10 and 20 µM or 500 nM IAA for 30 min and subsequently gravistimulated for 4 h and imaged (A). Intensity in both sides (epidermis) of the roots was measured (C) and the ratio of the intensities was calculated (B). Results are averages from two independent repetitions. Statistical analyses were performed using the t-test, values are means ± S.E. White and black circles (○), (●) indicate statistically significant differences between the effect of **IV** and **VIII** compared to control, ○,● correspond to P < 0.01.

4.3.2.6. The effect of compounds on the subcellular localization of PIN1

Under standard conditions, PIN1 is localized at the basal sides of endodermal and pericycle cells and cells of the vascular tissue (Friml, Benkova *et al.* 2002). Auxin induces PIN1 relocalization from basal to the inner lateral plasma membrane (PM) of root endodermal and pericycle cells (Prat, Hajny *et al.* 2018). The effect of fluorescently labelled compounds **IV** and **VIII** on lateralization of PIN1 was tested in four-day-old *Arabidopsis thaliana* (Col 0) seedlings. Seedlings were treated with 10 μM NAA or compounds **IV** and **VIII** at 20 or 50 μM concentrations for 4 h. Then, immunolocalizaton *in situ* of PIN1 was performed using primary antibody anti-PIN1 and secondary antibody anti-Cy3. Derivatives similarly like 10 μM NAA, which was used as a positive control, promoted the accumulation of PIN1 at the lateral side of PM, suggesting their auxin-like activity (Figure 24 A and B).
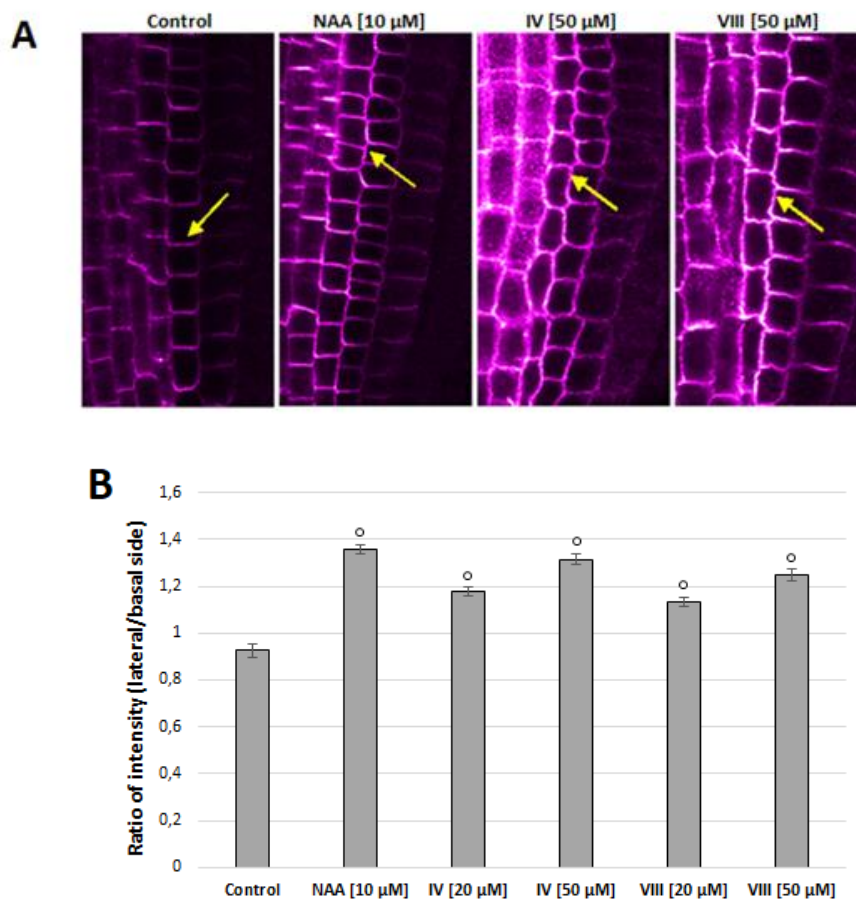
Figure 24 Effect of fluorescently labelled compounds **IV** and **VIII** on lateralization of PIN1. Four-day-old *Arabidopsis thaliana* (Col 0) seedlings were treated with 10 μM NAA or compounds **IV** and **VIII** at 20 or 50 μM concentrations for 4 h. Then, immunolocalizaton analysis of PIN1 was performed. Ratio intensity of lateral/basal side of endodermal cells was calculated. Results of compounds **IV** and **VIII** at 20 μM concentration, 10 μM NAA and control are averages from two independent repetitions, while results of compounds **IV** and **VIII** at 50 μM concentration are from one repetition. Statistical analyses were performed using the t-test, values are means ± S.E. White circles (○) indicate statistically significant differences between the effect of **IV** and **VIII** compared to control, ○ correspond to P < 0.01. Arrows show accumulation of PIN1 in endodermal cells.

4.3.2.7. The effect of compounds on the BFA body formation of PIN2

Brefeldin A (BFA) is a fungal lactone metabolite which interrupts continuous cycling of PINs between the PM and endosomes by inhibiting resecretion of the endocytic PIN populations back to the cell surface (Kleine-Vehn and Friml 2008). Therefore upon treatment with BFA, PINs are accumulated in distinct large multivesicular structures called BFA bodies (G Robinson, Langhans *et al.* 2008). Auxins suppress the accumulation of BFA bodies by blocking the endocytosis (Jasik, Bokor *et al.* 2016). Therefore, the effect of compounds **IV** and **VIII** on the BFA body formation of PIN2 was evaluated. Firstly, the experiment was performed using transgenic plant line PIN2::PIN2-mCherry (Figure 25 A). The seedlings were treated with NAA at 10 µM concentration and compounds **IV** and **VIII** at 50 µM concentration for 30 min and co-treated with 50 µM BFA for additional 1 h. Expectedly, NAA efficiently suppressed the accumulation of BFA bodies. Surprisingly, in case of compounds **IV** and **VIII** strong vacuolization could be observed in cells, making the assessment of the effect of the compounds **IV** and **VIII** on the BFA body formation impossible. Thus, an alternative experimental design was attempted. Namely, *Arabidopsis thaliana* (Col 0) seedlings were treated with 10 µM NAA or compounds **IV** and **VIII** at 50 µM concentration for 30 min and co-treated with 50 µM BFA for additional 1 h, while control seedlings were left without BFA treatment. Then, immunolocalization *in situ* of PIN2 was performed using primary antibody anti-PIN2 and secondary antibody anti-Cy3. (Figure 25 B). Interestingly, it had to be concluded that compounds **IV** and **VIII** did not affect BFA body formation.
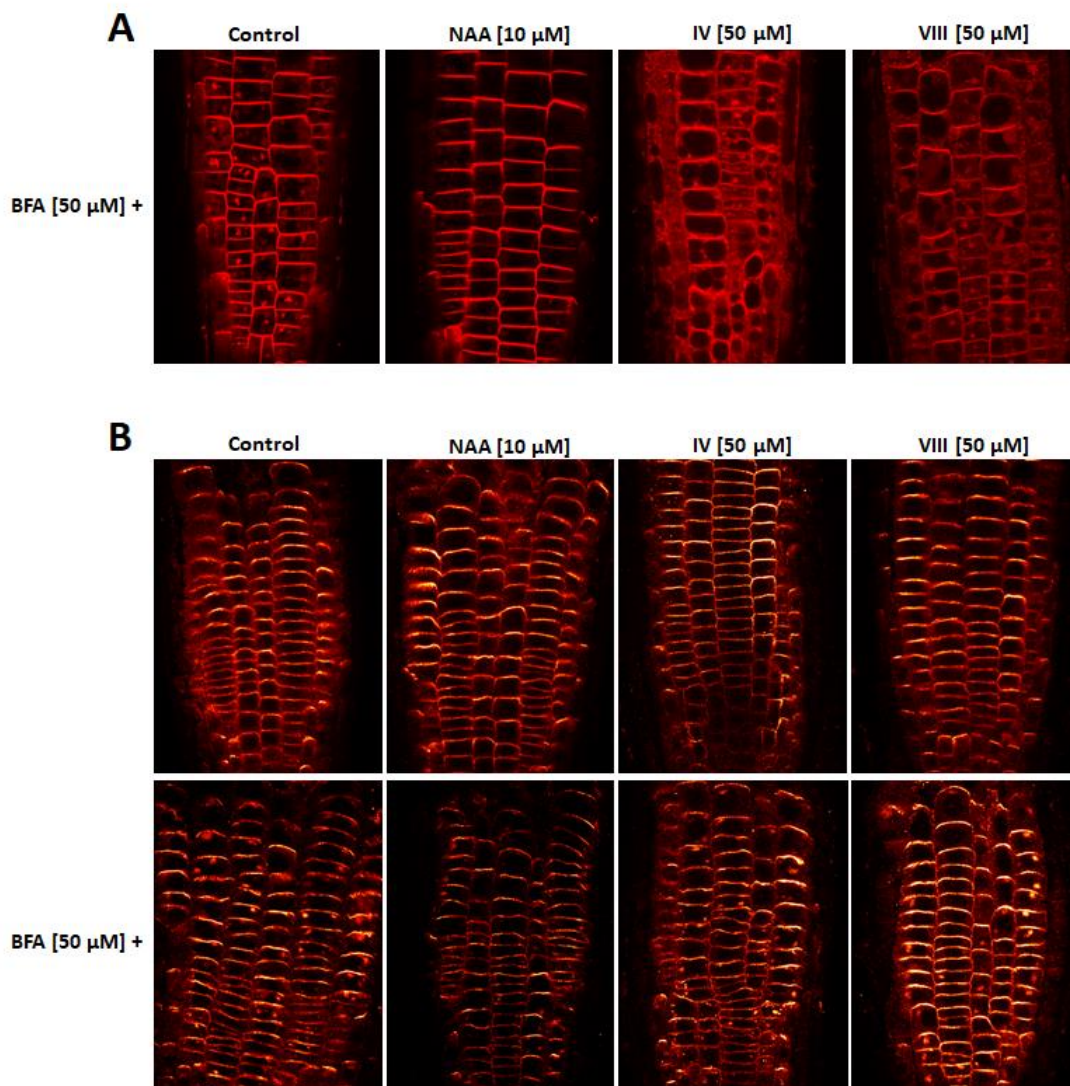
Figure 25 The effect of compounds **IV** and **VIII** on the BFA body formation of PIN2. (A) Five-day-old *Arabidopsis thaliana* seedlings of transgenic plant line PIN2::PIN2-mCherry were pre-treated with 10 µM NAA or compounds at 50 µM concentration for 30 minutes and co-treated with 50 µM BFA for additional 1 hour and imaged. (B) Four-day-old *Arabidopsis thaliana* (Col 0) seedlings were pre-treated with 10 µM NAA or compounds **IV** and **VIII** at 50 µM concentration for 30 minutes and co-treated with 50 µM BFA or left without BFA for additional 1 hour. Then, immunolocalization analysis of PIN2 was performed. One biological replicate.

5. Discussion

Fluorescently labelled plant hormones are powerful molecules that can allow monitoring of the phytohormone transport and cell/tissue specific localization in plants (Lace and Prandi 2016). Development of such tools has great potential for answering questions concerning plant growth and development (Rigal, Ma *et al.* 2014). Even though auxin is one of the most important plant hormones, up to date only few fluorescently labelled auxins have been developed, all of which have certain limitations.

In this work, new fluorescently labelled IAA derivatives, which bear fluorescent NBD label attached *via* aliphatic linkers at *α*-position of the molecule, were prepared. Synthesis of these derivatives was done by step-wise strategy. Firstly, readily available IAA-dimethyl ester was alkylated at the *α*-position with various Boc-protected iodoalkylamines. Subsequently, Boc protecting group was cleaved and resulting primary amine was fluorescently labelled with NBD-Cl. Finally, hydrolysis of the fluorescently labelled IAA dimethyl esters was performed giving rise to four fluorescently labelled IAA analogues **V-VIII**.

Subsequently, preliminary assessment of the biological activity of these newly prepared fluorescently labelled IAA derivatives **V-VIII**, in parallel with the fluorescently labelled NH-tagged auxins **I-IV**, which were prepared during bachelor thesis (Bieleszova 2017) , was undertaken in order to select the lead molecules of the study.

Firstly, effect of compounds **I-VIII** on the primary root growth was evaluated. Growth inhibition is normally triggered by nanomolar concentrations of IAA (Woodward and Bartel 2005). Surprisingly, despite being IAA derivatives, fluorescently labelled compounds **I-VIII** did not inhibit primary root growth. On the contrary, in co-treatment with 1 μM IAA, the ability of compounds **I-VIII** to revert auxin-induced primary root growth inhibition was found, effect similar to that of known anti-auxins (Hayashi, Neve *et al.* 2012). The extent of the anti-auxin activity was highly depended on the length of the linker. Namely, while compounds with the shorter linker had barely any noticeable effect; compounds **IV** and **VIII** bearing the longest 6C linkers, at 10 or 20 μM concentration were able to almost completely overcome IAA-induced (1 μM) primary root growth inhibition. Such activity dependency on the size of the substituent was also noticed in other known anti-auxins (Hayashi, Neve *et al.* 2012). Additionally, it was observed that the most active derivatives **IV** and **VIII** effectively inhibited auxin-induced (1 μM IAA) root hair formation. Subsequently, ability of fluorescently labelled auxin derivatives **I-VIII** to promote GUS expression in DR5::GUS

transgenic line was tested. Expectedly, compounds **I-VIII** did not induce GUS expression even at 50 μM concentration. On the other hand, some of the fluorescently labelled compounds blocked auxin-induced GUS expression in a dose-dependent manner. Analogously with previous experiment, the most potent compounds **IV** and **VIII** completely inhibited DR5::GUS expression induced by 2 μM IAA at 20-25 μM concentration. Moreover, we observed the uptake of fluorescently labelled compounds **I-VIII** in the roots of *Arabidopsis thaliana* (Col-0) by confocal microscopy. Once again, the positive correlation between the length of the linker and the fluorescence of the compounds **I-VIII** in *Arabidopsis* roots was observed, with the compounds **IV** and **VIII** being the most fluorescent in their respective groups.

Based on these results, two the most active compounds **IV** and **VIII**, which also had the best fluorescence in *Arabidopsis thaliana* roots, were chosen for further experiments. Firstly, effect of the compounds **IV** and **VIII** on rapid root growth was assayed. Roots of *Arabidopsis thaliana* in response to IAA inhibit their growth very rapidly, in less than 30 s after auxin reaches the root surface (Fendrych, Akhmanova *et al*. 2018). Fluorescently labelled compounds **IV** and **VIII** inhibited primary root growth and the effect was dose dependent. These results are contrary to the long-term effect of the compounds **IV** and **VIII** on the root growth, in which the primary root growth was not inhibited by the compounds, but rather reverted by them. Dynamic formation of auxin gradients is important for plant growth and development, one of such processes being apical hook development. In apical hook development assay, compound **VIII** at 20 μM concentration showed similar effect to positive control IAA (1 μM), that is the maintenance phase of apical hook development was shorter than in the negative control. However, compound **IV** at 20 μM concentration showed opposite effect, with the maintenance phase being longer, suggesting either anti-auxin activity or no-activity of compound **IV** on apical hook development. Further, in contrary to findings from DR5::GUS assay, compounds **IV** and **VIII** showed weak auxin activity in the luciferase assay in DR5::LUC transgenic plants. Also, compounds **IV** and **VIII** showed symmetric auxin-like distribution in the gravistimulated roots of transgenic plant line DR5$_{rev}$::RFP which is typical for exogenously applied auxin. Moreover, RFP signal was stronger with compounds **IV** and **VIII** at tested concentrations, in comparison to control or 500 nM IAA. Compounds **IV** and **VIII** also promoted relocalization of PIN1 proteins from basal to the inner lateral plasma membrane (PM) of root endodermal and pericycle cells, suggesting their auxin-like activity. On the other hand, in agreement with preliminary observations, **IV** and **VIII** did not promote lateral root formation; moreover, they inhibited

lateral root formation induced by 100 nM IAA. Additionally, compounds **IV** and **VIII** did not inhibit formation of BFA bodies of PIN2. In standard conditions, upon treatment with BFA, PINs are accumulated in distinct large multivesicular structures called BFA bodies (G Robinson, Langhans *et al*. 2008) and auxins inhibit the accumulation of BFA bodies by blocking the endocytosis (Jasik, Bokor *et al*. 2016), but none of these effects were noticed with compound **IV** and **VIII**.

Despite the potential of the compound **IV** and **VIII** to be used as auxin tracers, due to the discrepancies between the obtained results, both, suggesting auxin and anti-auxin activity of the compounds depending on the assay, exact biological activity of these compounds currently cannot be concluded. However, certain steps could be taken to try to shed some light on the actual biological activity of the compounds.

First of all*, in vitro* auxin co-receptor based assays, for instance surface plasmon resonance (SPR) analysis (Lee, Sundaram *et al*. 2014) or yeast two-hybrid (Y2H) assays would allow to validate if the auxin signalling co-receptor interaction between TIR1/AFBs and Aux/IAA proteins is being promoted or antagonized by the compounds, (Villalobos, Lee *et al.* 2012) also allowing to compare the affinity of the compounds to different auxin co-receptor systems (Quareshy, Prusinska *et al*. 2018). Most importantly, this would allow to establish the biological activity of the compounds without being influenced by various *in vivo* effects.

Even though sometimes use of racemates is inevitable or even preferred in agricultural applications, it has to be kept in mind that the enantiomers often possess opposite or different extent of biological activities (Katayama, Kato *et al.* 1995; Katayama, Kato *et al.* 2004). Thus, in case of the compound **VIII**, its chiral resolution and assessment of the biological activity of its enantiomerically pure forms would be particularly interesting to ascribe the biological activity to the respective enantiomers.

Stability of the compounds is important for their use in different analyses (Sokolowska, Kizinska *et al.* 2014). Even though the compounds **IV** and **VIII** are stable in their pure forms as well as in solution, at this point it cannot be ruled out that the compounds may not be stable *in planta* compromising the obtained data. Possible sensitivity of the compounds to hydrolytic enzymes, which are present in plant tissues, could prevent or limit their application *in vivo*. To elucidate the possible degradation of the compounds *in planta*, isotopically labelled standards of the compounds **IV** and **VIII** and their possible metabolites should be prepared, and the levels of the compounds and their metabolites quantified post treatment in defined time points. This would allow to establish a timeframe in which the

compounds can be used in *in vivo* applications. Moreover, it is likely, that treatment with the compounds results in substantial changes of endogenous auxin or other phytohormone levels, which may have played an important role in resulting data. Therefore, quantification of endogenous phytohormone levels could be performed in compound-treated plants.

Finally, as the behaviour of anti-auxins in some of the performer assays is not known, for instance the effect of anti-auxins on subcellular PIN localization, their accumulation pattern in gravistimulated DR5$_{rev}$::RFP transgenic plant line, etc., it would be useful to repeat these experiments including appropriate anti-auxin controls (i.e., auxinole, BH-IAA).

6. Conclusions

Fluorescently labelled auxins could serve as valuable tools to monitor auxin distribution and transport in plants. However, up to now, only few fluorescently labelled auxins have been published; none of which being able to promote auxin signalling and at the same time being stable *in planta* (Hayashi, Nakamura *et al*. 2014; Sokolowska, Kizinska *et al*. 2014).

This master thesis is aimed at the synthesis and biological evaluation of fluorescently labelled indole-3-acetic acid derivatives. Herein, we report four novel fluorescently labelled IAA derivatives **V-VIII**, with NBD attached at α-position *via* different length of aliphatic linkers. Subsequently, biological activity of these newly prepared fluorescently labelled auxins **V-VIII** and fluorescently labelled auxins prepared during bachelor thesis **I-IV** was elusidated. Preliminary assessment of their biological activity, based on root growth experiments and DR5::GUS expression, suggested that they act as anti-auxins. The strength of the auxin antagonist effect, uptake and fluorescence in *Arabidopsis* roots of **I-VIII** was linker-dependent. Compounds with the longest linker **IV** and **VIII** were the ones the most active.

Based on the preliminary data, compounds **IV** and **VIII** were chosen as lead compounds for further experiments. More detailed experiments included rapid effect of the compounds on the primary root growth, lateral root formation, apical hook development, auxin distribution in gravistimulated roots of DR5$_{rev}$::RFP, effect of compounds in the DR5::LUC transgenic plants of *Arabidopsis thaliana*, PIN1 lateralization and BFA body formation of PIN2. Compounds **IV** and **VIII** showed auxin-like activity in the rapid root growth assay, increased luciferase response in DR5::LUC transgenic line and lateralization of PIN1. Moreover, they showed symmetric auxin distribution in the gravistimulated roots of transgenic plant line DR5$_{rev}$::RFP which is typical for exogenously applied auxin. On the other hand, compounds **IV** and **VIII** showed anti-auxin activity in lateral root formation and did not influence BFA body formation of PIN2.

Even though compounds **IV** and **VIII** have potential to be used as auxin tracers as demonstrated by their uptake and fluorescence in *Arabidopsis thaliana* (Col-0) roots, discrepancies among obtained biological data makes the full understanding of the biological activity of these compounds difficult at this stage. For this reason, additional experiments should be performed to fully unravel biological activity of the compounds. For example, SPR analysis or yeast two-hybrid (Y2H) assays would allow defining the auxin/anti-auxin activity of the compounds *in vivo*. Stability studies of the compounds *in planta* and

assessment of the effect of the compounds to influence endogenous auxin or other phytohormone levels would enable to elucidate whether the compounds themselves or the decomposition products and/or altered phytohormone levels are responsible for the observed biological activities. Finally, additional anti-auxin controls should be included to make the evaluation of the obtained data easier.

7. List of literature

Abas, L., R. Benjamins, *et al*. (2006). "Intracellular trafficking and proteolysis of the Arabidopsis auxin-efflux facilitator PIN2 are involved in root gravitropism." <u>Nature Cell Biology</u> **8**(3): 249-256.

Adamowski, M. and J. Friml (2015). "PIN-Dependent Auxin Transport: Action, Regulation, and Evolution." <u>Plant Cell</u> **27**(1): 20-32.

Bainbridge, K., S. Guyomarc'h, *et al*. (2008). "Auxin influx carriers stabilize phyllotactic patterning." <u>Genes & Development</u> **22**(6): 810-823.

Bandyopadhyay, A., J. J. Blakeslee, *et al*. (2007). "Interactions of PIN and PGP auxin transport mechanisms." <u>Biochemical Society Transactions</u> **35**: 137-141.

Bartel, B. and G. R. Fink (1994). "DIFFERENTIAL REGULATION OF AN AUXIN-PRODUCING NITRILASE GENE FAMILY IN ARABIDOPSIS-THALILANA." <u>Proceedings of the National Academy of Sciences of the United States of America</u> **91**(14): 6649-6653.

Bender, J. and J. L. Celenza (2009). "Indolic glucosinolates at the crossroads of tryptophan metabolism." <u>Phytochemistry Reviews</u> **8**(1): 25-37.

Bender, R. L., M. L. Fekete, *et al*. (2013). "PIN6 is required for nectary auxin response and short stamen development." <u>Plant Journal</u> **74**(6): 893-904.

Benkova, E., M. Michniewicz, *et al*. (2003). "Local, efflux-dependent auxin gradients as a common module for plant organ formation." <u>Cell</u> **115**(5): 591-602.

Bennett, M. J., A. Marchant, *et al*. (1996). "Arabidopsis AUX1 gene: A permease-like regulator of root gravitropism." <u>Science</u> **273**(5277): 948-950.

Bieleszova, K. (2017). Bachelor thesis „Synthesis of fluorescently labelled indole-3-acetic acid."

Bieleszova, K., B. Parizkova, *et al*. (2019). "New fluorescently labelled auxins exhibit promising anti-auxin activity." <u>New Biotechnology</u> **48**: 44-52.

Blakeslee, J. J., A. Bandyopadhyay, *et al*. (2007). "Interactions among PIN-FORMED and P-glycoprotein auxin transporters in Arabidopsis." <u>Plant Cell</u> **19**(1): 131-147.

Blilou, I., J. Xu, *et al*. (2005). "The PIN auxin efflux facilitator network controls growth and patterning in Arabidopsis roots." <u>Nature</u> **433**(7021): 39-44.

Bradley, D., G. Williams, *et al*. (2010). "Drying of Organic Solvents: Quantitative Evaluation of the Efficiency of Several Desiccants." <u>Journal of Organic Chemistry</u> **75**(24): 8351-8354.

Brumos, J., J. M. Alonso, *et al*. (2014). "Genetic aspects of auxin biosynthesis and its regulation." <u>Physiologia Plantarum</u> **151**(1): 3-12.

Burstrom, H. (1950). "STUDIES ON GROWTH AND METABOLISM OF ROOTS .4. POSITIVE AND NEGATIVE AUXIN EFFECTS ON CELL ELONGATION." <u>Physiologia Plantarum</u> **3**(3): 277-292.

Busi, R., D. E. Goggin, *et al*. (2018). "Weed resistance to synthetic auxin herbicides." <u>Pest Management Science</u> **74**(10): 2265-2276.

Dal Bosco, C., A. Dovzhenko, *et al*. (2012). "The endoplasmic reticulum localized PIN8 is a pollen-specific auxin carrier involved in intracellular auxin homeostasis." <u>Plant Journal</u> **71**(5): 860-870.

Dharmasiri, N., S. Dharmasiri, *et al*. (2005). "Plant development is regulated by a family of auxin receptor F box proteins." <u>Developmental Cell</u> **9**(1): 109-119.

Dhonukshe, P., I. Grigoriev, *et al*. (2008). "Auxin transport inhibitors impair vesicle motility and actin cytoskeleton dynamics in diverse eukaryotes." <u>Proceedings of the National Academy of Sciences of the United States of America</u> **105**(11): 4489-4494.

Dindas, J., S. Scherzer, *et al*. (2018). "AUX1-mediated root hair auxin influx governs SCFTIR1/AFB-type Ca2+ signaling." <u>Nature Communications</u> **9**.

Eklund, D. M., K. Ishizaki, *et al*. (2015). "Auxin Produced by the Indole-3-Pyruvic Acid Pathway Regulates Development and Gemmae Dormancy in the Liverwort Marchantia polymorph." <u>Plant Cell</u> **27**(6): 1650-1669.

Ensch, C. and M. Hesse (2002). "Total syntheses of the spermine alkaloids (-)-(R,R)-hopromine and (+/-)-homaline." <u>Helvetica Chimica Acta</u> **85**(6): 1659-1673.

Fendrych, M., M. Akhmanova, *et al*. (2018). "Rapid and reversible root growth inhibition by TIR1 auxin signalling." <u>Nature Plants</u> **4**(7): 453-459.

Friml, J., E. Benkova, *et al*. (2002). "AtPIN4 mediates sink-driven auxin gradients and root patterning in Arabidopsis." <u>Cell</u> **108**(5): 661-673.

Friml, J. and K. Palme (2002). "Polar auxin transport - old questions and new concepts?" <u>Plant Molecular Biology</u> **49**(3-4): 273-284.

Friml, J., A. Vieten, *et al*. (2003). "Efflux-dependent auxin gradients establish the apical-basal axis of Arabidopsis." <u>Nature</u> **426**(6963): 147-153.

Friml, J., J. Wisniewska, *et al*. (2002). "Lateral relocation of auxin efflux regulator PIN3 mediates tropism in Arabidopsis." <u>Nature</u> **415**(6873): 806-809.

Fukaki, H., Y. Okushima, *et al*. (2007). Auxin-mediated lateral root formation in higher plants. <u>International Review of Cytology - a Survey of Cell Biology, Vol 256</u>. K. W. Jeon. San Diego, Elsevier Academic Press Inc. **256:** 111-137.

G Robinson, D., M. Langhans, *et al*. (2008). <u>BFA effects are tissue and not just plant specific</u>.

Galweiler, L., C. H. Guan, *et al*. (1998). "Regulation of polar auxin transport by AtPIN1 in Arabidopsis vascular tissue." <u>Science</u> **282**(5397): 2226-2230.

Goldsmith, M. H. M. (1977). "The Polar Transport of Auxin." <u>Annual Review of Plant Physiology</u> **28**(1): 439-478.

Grossmann, K. (2003). "Mediation of herbicide effects by hormone interactions." <u>Journal of Plant Growth Regulation</u> **22**(1): 109-122.

Grossmann, K. (2010). "Auxin herbicides: current status of mechanism and mode of action." <u>Pest Management Science</u> **66**(2): 113-120.

Grunewald, W. and J. Friml (2010). "The march of the PINs: developmental plasticity by dynamic polar targeting in plant cells." <u>EMBO Journal</u> **29**(16): 2700-2714.

Guilfoyle, T. J. and G. Hagen (2007). "Auxin response factors." <u>Current Opinion in Plant Biology</u> **10**(5): 453-460.

Hasegawa, J., T. Sakamoto, *et al*. (2018). "Auxin decreases chromatin accessibility through the TIRl/AFBs auxin signaling pathway in proliferative cells." <u>Scientific Reports</u> **8**.

Hayashi, K., J. Neve, *et al*. (2012). "Rational Design of an Auxin Antagonist of the SCFTIR1 Auxin Receptor Complex." ACS Chemical Biology **7**(3): 590-598.

Hayashi, K., X. Tan, *et al*. (2008). "Small-molecule agonists and antagonists of F-box protein-substrate interactions in auxin perception and signaling." Proceedings of the National Academy of Sciences of the United States of America **105**(14): 5632-5637.

Hayashi, K. I., S. Nakamura, *et al*. (2014). "Auxin transport sites are visualized in planta using fluorescent auxin analogues." Proceedings of the National Academy of Sciences of the United States of America **111**(31): 11557-11562.

He, W. R., J. Brumos, *et al*. (2011). "A Small-Molecule Screen Identifies L-Kynurenine as a Competitive Inhibitor of TAA1/TAR Activity in Ethylene-Directed Auxin Biosynthesis and Root Growth in Arabidopsis." Plant Cell **23**(11): 3944-3960.

Hull, A. K., R. Vij, *et al*. (2000). "Arabidopsis cytochrome P450s that catalyze the first step of tryptophan-dependent indole-3-acetic acid biosynthesis." Proceedings of the National Academy of Sciences of the United States of America **97**(5): 2379-2384.

Chen, J. J., A. Kassenbrock, *et al*. (2013). "Discovery of a potent anti-tumor agent through regioselective mono-N-acylation of 7H-pyrrolo 3,2-f quinazoline-1,3-diamine." Medchemcomm **4**(9): 1275-1282.

Cho, M., S. H. Lee, *et al*. (2007). "P-glycoprotein4 displays auxin efflux transporter-like action in Arabidopsis root hair cells and tobacco cells." Plant Cell **19**(12): 3930-3943.

Jasik, J., B. Bokor, *et al*. (2016). "Effects of Auxins on PIN-FORMED2 (PIN2) Dynamics Are Not Mediated by Inhibiting PIN2 Endocytosis." Plant Physiology **172**(2): 1019-1031.

Jian, O. Y., X. Shao, *et al*. (2000). "Indole-3-glycerol phosphate, a branchpoint of indole-3-acetic acid biosynthesis from the tryptophan biosynthetic pathway in Arabidopsis thaliana." Plant Journal **24**(3): 327-333.

Jiang, K. and T. Asami (2018). "Chemical regulators of plant hormones and their applications in basic research and agriculture." Bioscience Biotechnology and Biochemistry **82**(8): 1265-1300.

Jones, A. R., E. M. Kramer, *et al*. (2009). "Auxin transport through non-hair cells sustains root-hair development." Nature Cell Biology **11**(1): 78-U156.

Kakei, Y., C. Yamazaki, *et al*. (2015). "Small-molecule auxin inhibitors that target YUCCA are powerful tools for studying auxin function." Plant Journal **84**(4): 827-837.

Kasahara, H. (2016). "Current aspects of auxin biosynthesis in plants." Bioscience Biotechnology and Biochemistry **80**(1): 34-42.

Katayama, M., K. Kato, *et al*. (1995). "(S)-(+)-4,4,4-TRIFLUORO-3-(INDOLE-3-)BUTYRIC ACID, A NOVEL FLUORINATED PLANT-GROWTH REGULATOR." Experientia **51**(7): 721-724.

Katayama, M., Y. Kato, *et al*. (2004). "Synthesis, absolute configuration and biological activities of both enantiomers of 2-(5,7-dichloro-3-indolyl)propionic acid: a novel dichloroindole auxin and antiauxin." Bioscience Biotechnology and Biochemistry **68**(6): 1287-1292.

Katekar, G. F. and A. E. Geissler (1977). "AUXIN TRANSPORT INHIBITORS .3. CHEMICAL REQUIREMENTS OF A CLASS OF AUXIN TRANSPORT INHIBITORS." Plant Physiology **60**(6): 826-829.

Kimura, T., K. Haga, *et al*. (2018). "Asymmetric Auxin Distribution is Not Required to Establish Root Phototropism in Arabidopsis." <u>Plant and Cell Physiology</u> **59**(4): 828-840.

Kleine-Vehn, J. and J. Friml (2008). Polar Targeting and Endocytic Recycling in Auxin-Dependent Plant Development. <u>Annual Review of Cell and Developmental Biology</u>. Palo Alto, Annual Reviews. **24:** 447-473.

Krecek, P., P. Skupa, *et al*. (2009). "The PIN-FORMED (PIN) protein family of auxin transporters." <u>Genome Biology</u> **10**(12).

Kriechbaumer, V., W. J. Park, *et al*. (2007). "Maize nitrilases have a dual role in auxin homeostasis and beta-cyanoalanine hydrolysis." <u>Journal of Experimental Botany</u> **58**(15-16): 4225-4233.

Kubes, M., H. B. Yang, *et al*. (2012). "The Arabidopsis concentration-dependent influx/efflux transporter ABCB4 regulates cellular auxin levels in the root epidermis." <u>Plant Journal</u> **69**(4): 640-654.

Lace, B. and C. Prandi (2016). "Shaping Small Bioactive Molecules to Untangle Their Biological Function: A Focus on Fluorescent Plant Hormones." <u>Molecular Plant</u> **9**(8): 1099-1118.

Lankova, M., R. S. Smith, *et al*. (2010). "Auxin influx inhibitors 1-NOA, 2-NOA, and CHPAA interfere with membrane dynamics in tobacco cells." <u>Journal of Experimental Botany</u> **61**(13): 3589-3598.

Last, R. L., P. H. Bissinger, *et al*. (1991). "TRYPTOPHAN MUTANTS IN ARABIDOPSIS - THE CONSEQUENCES OF DUPLICATED TRYPTOPHAN SYNTHASE BETA GENES." <u>Plant Cell</u> **3**(4): 345-358.

Lee, S., S. Sundaram, *et al*. (2014). "Defining Binding Efficiency and Specificity of Auxins for SCFTIR1/AFB-Aux/IAA Co-receptor Complex Formation." <u>ACS Chemical Biology</u> **9**(3): 673-682.

Li, J. and R. L. Last (1996). "The Arabidopsis thaliana trp5 mutant has a feedback-resistant anthranilate synthase and elevated soluble tryptophan." <u>Plant Physiology</u> **110**(1): 51-59.

Mano, Y. and K. Nemoto (2012). "The pathway of auxin biosynthesis in plants." <u>Journal of Experimental Botany</u> **63**(8): 2853-2872.

Marchant, A., R. Bhalerao, *et al*. (2002). "AUX1 promotes lateral root formation by facilitating indole-3-acetic acid distribution between sink and source tissues in the Arabidopsis seedling." <u>Plant Cell</u> **14**(3): 589-597.

Marin, E., V. Jouannet, *et al*. (2010). "miR390, Arabidopsis TAS3 tasiRNAs, and Their AUXIN RESPONSE FACTOR Targets Define an Autoregulatory Network Quantitatively Regulating Lateral Root Growth." <u>Plant Cell</u> **22**(4): 1104-1117.

Mashiguchi, K., K. Tanaka, *et al*. (2011). "The main auxin biosynthesis pathway in Arabidopsis." <u>Proceedings of the National Academy of Sciences of the United States of America</u> **108**(45): 18512-18517.

Mikkelsen, M. D., C. H. Hansen, *et al*. (2000). "Cytochrome P450CYP79B2 from Arabidopsis catalyzes the conversion of tryptophan to indole-3-acetaldoxime, a precursor of indole glucosinolates and indole-3-acetic acid." <u>Journal of Biological Chemistry</u> **275**(43): 33712-33717.

Miles, E. W. (1991). "STRUCTURAL BASIS FOR CATALYSIS BY TRYPTOPHAN SYNTHASE." Advances in Enzymology and Related Areas of Molecular Biology **64**: 93-+.

Mockaitis, K. and M. Estelle (2008). Auxin Receptors and Plant Development: A New Signaling Paradigm. Annual Review of Cell and Developmental Biology. Palo Alto, Annual Reviews. **24:** 55-80.

Moreno-Risueno, M. A., J. M. Van Norman, *et al*. (2010). "Oscillating Gene Expression Determines Competence for Periodic Arabidopsis Root Branching." Science **329**(5997): 1306-1311.

Mravec, J., S. K. Kracun, *et al*. (2017). "Click chemistry-based tracking reveals putative cell wall-located auxin binding sites in expanding cells." Scientific Reports **7**.

Mravec, J., P. Skupa, *et al*. (2009). "Subcellular homeostasis of phytohormone auxin is mediated by the ER-localized PIN5 transporter." Nature **459**(7250): 1136-U1127.

Muller, A. and E. W. Weiler (2000). "Indolic constituents and indole-3-acetic acid biosynthesis in the wild-type and a tryptophan auxotroph mutant of Arabidopsis thaliana." Planta **211**(6): 855-863.

Murofushi, N., H. Yamane, *et al*. (1999). 8.02 - Plant Hormones A2 - Barton, Sir Derek. Comprehensive Natural Products Chemistry. K. Nakanishi and O. Meth-Cohn. Oxford, Pergamon**:** 19-136.

Nafisi, M., S. Goregaoker, *et al*. (2007). "Arabidopsis cytochrome P450 monooxygenase 71A13 catalyzes the conversion of indole-3-acetaldoxime in camalexin synthesis." Plant Cell **19**(6): 2039-2052.

Nishimura, T., K. Hayashi, *et al*. (2014). "Yucasin is a potent inhibitor of YUCCA, a key enzyme in auxin biosynthesis." Plant Journal **77**(3): 352-366.

Noh, B., A. Bandyopadhyay, *et al*. (2003). "Enhanced gravi- and phototropism in plant mdr mutants mislocalizing the auxin efflux protein PIN1." Nature **423**(6943): 999-1002.

Normanly, J., J. D. Cohen, *et al*. (1993). "ARABIDOPSIS-THALIANA AUXOTROPHS REVEAL A TRYPTOPHAN-INDEPENDENT BIOSYNTHETIC-PATHWAY FOR INDOLE-3-ACETIC-ACID." Proceedings of the National Academy of Sciences of the United States of America **90**(21): 10355-10359.

Okushima, Y., P. J. Overvoorde, *et al*. (2005). "Functional genomic analysis of the AUXIN RESPONSE FACTOR gene family members in Arabidopsis thaliana: Unique and overlapping functions of ARF7 and ARF19." Plant Cell **17**(2): 444-463.

Oono, Y., C. Ooura, *et al*. (2003). "p-chlorophenoxyisobutyric acid impairs auxin response in Arabidopsis root." Plant Physiology **133**(3): 1135-1147.

Overvoorde, P. J., Y. Okushima, *et al*. (2005). "Functional genomic analysis of the AUXIN/INDOLE-3-ACETIC ACID gene family members in Arabidopsis thaliana." Plant Cell **17**(12): 3282-3300.

Paciorek, T., E. Zazimalova, *et al*. (2005). "Auxin inhibits endocytosis and promotes its own efflux from cells." Nature **435**(7046): 1251-1256.

Parizkova, B., M. Pernisova, *et al*. (2017). "What Has Been Seen Cannot Be Unseen-Detecting Auxin In Vivo." International Journal of Molecular Sciences **18**(12).

Park, W. J., V. Kriechbaumer, *et al*. (2003). "The nitrilase ZmNIT2 converts indole-3-acetonitrile to indole-3-acetic acid." Plant Physiology **133**(2): 794-802.

Parry, G., L. I. Calderon-Villalobos, *et al*. (2009). "Complex regulation of the TIR1/AFB family of auxin receptors." Proceedings of the National Academy of Sciences of the United States of America **106**(52): 22540-22545.

Patten, C. L. and B. R. Glick (1996). "Bacterial biosynthesis on indole-3-acetic acid." Canadian Journal of Microbiology **42**(3): 207-220.

Peret, B., K. Swarup, *et al*. (2012). "AUX/LAX Genes Encode a Family of Auxin Influx Transporters That Perform Distinct Functions during Arabidopsis Development." Plant Cell **24**(7): 2874-2885.

Prat, T., J. Hajny, *et al*. (2018). "WRKY23 is a component of the transcriptional network mediating auxin feedback on PIN polarity." PLoS Genetics **14**(1).

Quareshy, M., J. Prusinska, *et al*. (2018). "The Tetrazole Analogue of the Auxin Indole-3-acetic Acid Binds Preferentially to TIR1 and Not AFB5." ACS Chemical Biology **13**(9): 2585-2594.

Radwanski, E. R., A. J. Barczak, *et al*. (1996). "Characterization of tryptophan synthase alpha subunit mutants of Arabidopsis thaliana." Molecular and General Genetics **253**(3): 353-361.

Radwanski, E. R., J. M. Zhao, *et al*. (1995). "ARABIDOPSIS-THALIANA TRYPTOPHAN SYNTHASE-ALPHA - GENE CLONING, EXPRESSION, AND SUBUNIT INTERACTION." Molecular and General Genetics **248**(6): 657-667.

Rahman, A., M. Takahashi, *et al*. (2010). "Gravitropism of Arabidopsis thaliana Roots Requires the Polarization of PIN2 toward the Root Tip in Meristematic Cortical Cells." Plant Cell **22**(6): 1762-1776.

Remington, D. L., T. J. Vision, *et al*. (2004). "Contrasting modes of diversification in the Aux/IAA and ARF gene families." Plant Physiology **135**(3): 1738-1752.

Rigal, A., Q. Ma, *et al*. (2014). "Unraveling plant hormone signaling through the use of small molecules." Frontiers in Plant Science **5**.

Robert, H. S. and J. Friml (2009). "Auxin and other signals on the move in plants." Nature Chemical Biology **5**(5): 325-332.

Ruegger, M., E. Dewey, *et al*. (1998). "The TIR1 protein of Arabidopsis functions in auxin response and is related to human SKP2 and yeast Grr1p." Genes & Development **12**(2): 198-207.

Salanenka, Y., I. Verstraeten, *et al*. (2018). "Gibberellin DELLA signaling targets the retromer complex to redirect protein trafficking to the plasma membrane." Proceedings of the National Academy of Sciences of the United States of America **115**(14): 3716-3721.

Santner, A., L. I. A. Calderon-Villalobos, *et al*. (2009). "Plant hormones are versatile chemical regulators of plant growth." Nature Chemical Biology **5**(5): 301-307.

Sauer, M., T. Paciorek, *et al*. (2006). "Immunocytochemical techniques for whole-mount in situ protein localization in plants." Nature Protocols **1**(1): 98-103.

Sauer, M., S. Robert, *et al*. (2013). "Auxin: simply complicated." Journal of Experimental Botany **64**(9): 2565-2577.

Sekimoto, H., M. Seo, *et al*. (1997). "Cloning and molecular characterization of plant aldehyde oxidase." Journal of Biological Chemistry **272**(24): 15280-15285.

Seo, M., S. Akaba, *et al*. (1998). "Higher activity of an aldehyde oxidase in the auxin-overproducing superroot1 mutant of Arabidopsis thaliana." Plant Physiology **116**(2): 687-693.

Scheuring, D., C. Lofke, *et al*. (2016). "Actin-dependent vacuolar occupancy of the cell determines auxin-induced growth repression." Proceedings of the National Academy of Sciences of the United States of America **113**(2): 452-457.

Sieburth, L. E. and M. K. Deyholos (2006). "Vascular development: the long and winding road." Current Opinion in Plant Biology **9**(1): 48-54.

Soeno, K., H. Goda, *et al*. (2010). "Auxin Biosynthesis Inhibitors, Identified by a Genomics-Based Approach, Provide Insights into Auxin Biosynthesis." Plant and Cell Physiology **51**(4): 524-536.

Sokolowska, K., J. Kizinska, *et al*. (2014). "Auxin conjugated to fluorescent dyes - a tool for the analysis of auxin transport pathways." Plant Biology **16**(5): 866-877.

Steenackers, W., P. Klima, *et al*. (2017). "cis-Cinnamic Acid Is a Novel, Natural Auxin Efflux Inhibitor That Promotes Lateral Root Formation." Plant Physiology **173**(1): 552-565.

Stepanova, A. N., J. Yun, *et al*. (2011). "The Arabidopsis YUCCA1 Flavin Monooxygenase Functions in the Indole-3-Pyruvic Acid Branch of Auxin Biosynthesis." Plant Cell **23**(11): 3961-3973.

Su, T. B., J. A. Xu, *et al*. (2011). "Glutathione-Indole-3-Acetonitrile Is Required for Camalexin Biosynthesis in Arabidopsis thaliana." Plant Cell **23**(1): 364-380.

Sugawara, S., S. Hishiyama, *et al*. (2009). "Biochemical analyses of indole-3-acetaldoximedependent auxin biosynthesis in Arabidopsis." Proceedings of the National Academy of Sciences of the United States of America **106**(13): 5430-5435.

Swarup, K., E. Benkova, *et al*. (2008). "The auxin influx carrier LAX3 promotes lateral root emergence." Nature Cell Biology **10**(8): 946-954.

Swarup, R. and B. Peret (2012). "AUX/LAX family of auxin influx carriers-an overview." Frontiers in Plant Science **3**.

Tamaki, H., M. Reguera, *et al*. (2015). "Targeting Hormone-Related Pathways to Improve Grain Yield in Rice: A Chemical Approach." PLoS One **10**(6).

Tan, X., L. I. A. Calderon-Villalobos, *et al*. (2007). "Mechanism of auxin perception by the TIR1 ubiquitin ligase." Nature **446**(7136): 640-645.

Teale, W. D., I. A. Paponov, *et al*. (2006). "Auxin in action: signalling, transport and the control of plant growth and development." Nature Reviews Molecular Cell Biology **7**(11): 847-859.

Terasaka, K., J. J. Blakeslee, *et al*. (2005). "PGP4, an ATP binding cassette P-glycoprotein, catalyzes auxin transport in Arabidopsis thaliana roots." Plant Cell **17**(11): 2922-2939.

Torii, K. U., S. Hagihara, *et al*. (2018). "Harnessing synthetic chemistry to probe and hijack auxin signaling." New Phytologist **220**(2): 417-424.

Uchida, N., K. Takahashi, *et al*. (2018). "Chemical hijacking of auxin signaling with an engineered auxin-TIR1 pair." Nature Chemical Biology **14**(3): 299-+.

Ulmasov, T., J. Murfett, *et al.* (1997). "Aux/IAA proteins repress expression of reporter genes containing natural and highly active synthetic auxin response elements." Plant Cell **9**(11): 1963-1971.

Vandenbussche, F., J. Petrasek, *et al.* (2010). "The auxin influx carriers AUX1 and LAX3 are involved in auxin-ethylene interactions during apical hook development in Arabidopsis thaliana seedlings." Development **137**(4): 597-606.

Vanneste, S. and J. Friml (2009). "Auxin: A Trigger for Change in Plant Development." Cell **136**(6): 1005-1016.

Villalobos, L., S. Lee, *et al.* (2012). "A combinatorial TIR1/AFB-Aux/IAA co-receptor system for differential sensing of auxin." Nature Chemical Biology **8**(5): 477-485.

Vorwerk, S., S. Biernacki, *et al.* (2001). "Enzymatic characterization of the recombinant Arabidopsis thaliana nitrilase subfamily encoded by the NIT2/NIT1/NIT3-gene cluster." Planta **212**(4): 508-516.

Wabnik, K., W. Govaerts, *et al.* (2011). "Feedback models for polarized auxin transport: an emerging trend." Molecular BioSystems **7**(8): 2352-2359.

Walsh, T. A., R. Neal, *et al.* (2006). "Mutations in an auxin receptor homolog AFB5 and in SGT1b confer resistance to synthetic picolinate auxins and not to 2,4-dichlorophenoxyacetic acid or indole-3-acetic acid in arabidopsis." Plant Physiology **142**(2): 542-552.

Wang, B., J. F. Chu, *et al.* (2015). "Tryptophan-independent auxin biosynthesis contributes to early embryogenesis in Arabidopsis." Proceedings of the National Academy of Sciences of the United States of America **112**(15): 4821-4826.

Wisniewska, J., J. Xu, *et al.* (2006). "Polar PIN localization directs auxin flow in plants." Science **312**(5775): 883-883.

Won, C., X. L. Shen, *et al.* (2011). "Conversion of tryptophan to indole-3-acetic acid by TRYPTOPHAN AMINOTRANSFERASES OF ARABIDOPSIS and YUCCAs in Arabidopsis." Proceedings of the National Academy of Sciences of the United States of America **108**(45): 18518-18523.

Woodward, A. W. and B. Bartel (2005). "Auxin: Regulation, action, and interaction." Annals of Botany **95**(5): 707-735.

Yamada, R., K. Murai, *et al.* (2018). "A Super Strong Engineered Auxin-TIR1 Pair." Plant and Cell Physiology **59**(8): 1538-1544.

Yang, H. B. and A. S. Murphy (2009). "Functional expression and characterization of Arabidopsis ABCB, AUX 1 and PIN auxin transporters in Schizosaccharomyces pombe." Plant Journal **59**(1): 179-191.

Yang, Y. D., U. Z. Hammes, *et al.* (2006). "High-affinity auxin transport by the AUX1 influx carrier protein." Current Biology **16**(11): 1123-1127.

Young, G. B., D. L. Jack, *et al.* (1999). "The amino acid/auxin : proton symport permease family." Biochimica Et Biophysica Acta-Biomembranes **1415**(2): 306-322.

Zadnikova, P., J. Petrasek, *et al.* (2010). "Role of PIN-mediated auxin efflux in apical hook development of Arabidopsis thaliana." Development **137**(4): 607-617.

Zazimalova, E., A. S. Murphy, *et al.* (2010). "Auxin Transporters - Why So Many?" Cold Spring Harbor Perspectives in Biology **2**(3).

Zhao, Y. D., A. K. Hull, *et al*. (2002). "Trp-dependent auxin biosynthesis in Arabidopsis: involvement of cytochrome P450s CYP79B2 and CYP79B3." <u>Genes & Development</u> **16**(23): 3100-3112.